FACTORS THAT MODULATE INSECT DEVELOPMENTAL, METABOLIC, AND REPRODUCTIVE PHYSIOLOGY IN TWO VECTORS OF HUMAN AND ANIMAL DISEASE

by

NIA IMANI KEYES-SCOTT

(Under the Direction of Kevin J. Vogel)

ABSTRACT

Mosquitoes and kissing bugs are blood feeding insects and principal contributors to the annual global public health burden. Vector management strategies that limit insect populations have aided the reduction of human and animal disease. Moreover, vector management strategies are informed through investigation of pest-insect behavior, ecology, and physiology. The work presented in this dissertation seeks to explore the basic biology of mosquitoes and kissing bugs through examination of biochemical and microbial factors that contribute to insect reproduction, molting, development, and metabolism in hopes to inform future pest management strategies. Insect reproduction is regulated by the coordination of several hormones that are released from the brain or associated endocrine tissues after a blood meal. The first two studies delve into the role of several G protein-coupled receptors (GPCRs) and a peptide hormone (CNMamide) in *Aedes aegypti* mosquito reproductive physiology. We found that the CNMa receptor underwent a gene duplication event in Culicidae, resulting in two copies of the CNMa receptor, CNMaR_1a and CNMaR_1b. Only CNMa and CNMaR_1b were expressed in females, and CNMaR_1a was only expressed in male antennae. We found a reduction in fecundity of mated blood fed female

mosquitoes after injection of exogenous CNMa peptide. Next, I established that both AAEL003647 and AAEL019988 were highly expressed in the ovaries. Knockdown of both orphan receptors reduced egg laying in adult females. Until this point, the roles of CNMa, AAEL003647, and AAEL019988 in *Ae. aegypti* had not yet been explored. The current studies identified a role of CNMa, AAEL003647, and AAEL019988 in the reproductive physiology of female mosquitoes. In addition to hormones, gut bacteria also contribute reproductive and metabolic physiology in insects, primarily through nutrient supplementation. Thus, the final studies of this dissertation explore the role of the kissing bug microbiome in lipid metabolism and modulation of genes in *de novo* lipogenesis. I demonstrate that in *Rhodnius prolixus*, the microbiome differentially affects expression of acetyl-CoA carboxylase and downstream genes. Further, I demonstrate that the microbiome promotes blood meal digestion which may subsequently influence the synthesis of lipids involved in triglyceride energy stores, development, and desiccation resistance.

INDEX WORDS: mosquito, *Aedes aegypti*, kissing bug, *Rhodnius prolixus*, insects, physiology, biochemistry, microbiome, symbiont

FACTORS THAT MODULATE INSECT DEVELOPMENTAL, METABOLIC, AND REPRODUCTIVE PHYSIOLOGY IN TWO VECTORS OF HUMAN AND ANIMAL DISEASE

by

NIA IMANI KEYES-SCOTT

BA, Valdosta State University, 2018

BS, Valdosta State University, 2018

A Dissertation Submitted to the Graduate Faculty of The University of Georgia in Partial Fulfillment of the Requirements for the Degree

DOCTOR OF PHILOSOPHY

ATHENS, GEORGIA

2024

FACTORS THAT MODULATE INSECT DEVELOPMENTAL, METABOLIC, AND REPRODUCTIVE PHYSIOLOGY IN TWO VECTORS OF HUMAN AND ANIMAL DISEASE

by

NIA IMANI KEYES-SCOTT

Major Professor:	Kevin J. Vogel
Committee:	Mark R. Brown
	Patricia J. Moore
	Michael R. Strand

Electronic Version Approved:

Ron Walcott
Vice Provost for Graduate Education and Dean of the Graduate School
The University of Georgia
May 2024

DEDICATION

I would like to dedicate this dissertation to all current and future students of underrepresented backgrounds. May you be confident in yourselves, your ideas, and your plans. May you stand firm in your morals, values, and beliefs. May you remain true to who you are. May you be your strongest, loudest advocates and trust your intuitions. May you emanate kindness to all those around you. May you propel your friends and colleagues forward on your paths to greatness. May you take advantage of every opportunity offered to you. May you own your mistakes and learn from them. May you prevail throughout every challenge encountered throughout your journey. May you create a seat at the table when one is not provided for you. May you remember those who inspired you and strive to trailblaze for those who will succeed you. May you flourish in all of your endeavors.

ACKNOWLEDGEMENTS

As I write this acknowledgements section, I cannot help but be overwhelmed with emotion and gratitude for all of the individuals I have encountered over the years. I first would like to express my gratitude to my husband, Christopher. He has offered endless support and understanding throughout this entire six-year program. From the days that he came with me to the lab on the weekends to sort pupae, to the days he watched me inoculate bacterial cultures, I cannot thank him enough for how patient he has been with me. Secondly, I would like to thank my parents, Rodney, and Vicki, who have called me "Dr. Nia" since I was just a little girl. I know were expecting a different type of doctor, but they very frequently articulate to me how proud they are to have an entomologist daughter. I would also like to thank my sister, Ashley, who has also come with me to the lab on several occasions. I am so very proud of her recent master's degree completion, and she has offered me so much emotional support, as we commiserated together many times about our graduate school experiences. I would be remiss to not express gratitude to my in-laws Arthur and Evelyn Scott, who have also been very supportive of me along my journey.

I could not imagine how my experience would have gone without the many members of the Vogel lab that I worked with over the years. I would like to first thank Logan Harrell, whom is now a forever friend. Logan made my transition from working on mosquitoes to kissing bugs one to remember. From our kickboxing workouts together to our outbursts of laughter recording training videos, I will be forever grateful for the time we had together in the Vogel lab. I would like to acknowledge Carissa Gilliland, whom I drudged through the Insect Taxonomy collection

and Insect Physiology exams with. Through the years, we bounced so many research ideas off each other, cried many tears over bugs, and overcame many challenges. Next, I would like to thank Ashley McCormick, whom I held onto for dear life for the final year of graduate school. I have been so grateful for Ashley's positivity and upbeat personality. We have had lots of laughs together in the lab, and in our last years, we supported each other during our respective military officer selection processes. I would like to also thank all of the undergraduate students I have been able to mentor over the years: Kyle Swade, Lena Allen, and Ashley Lomax. I am unspeakably grateful for the opportunity that I had to teach these bright students, and I am so appreciative of their contributions to my work. Finally, I would like to thank all of the Vogel lab technicians that have helped with rearing throughout the years.

I would also like to thank the many friends I have made in my time here, especially Katherine Hagan, Gabriela Cardona-Rivera, Kelly Tims, and Yelena Pacheco. Next, I would like to thank some individuals that have inspired and mentored me throughout my journey, including my former advisor, Dr. Mark Blackmore, Major Jareé Johnson, Dr. Ruby Harrison, and especially Dr. Mark Brown. Next, I would like to acknowledge the US Navy and the Navy HSCP Program for funding me for my final year and a half of graduate school. I also am grateful for my recruiter Lieutenant Nicholas Gilmore for investing so much time into helping me throughout the HSCP selection process and through onboarding as a sailor. I would also like to thank CrossFit Liberate, Georgia Strength, Creed Fitness, and Slow Girl Run Club for helping me stay fit and balanced throughout graduate school.

Lastly, I would like to sincerely thank my advisor, Dr. Kevin Vogel, for allowing me to pursue a doctorate degree in his lab. I was delighted to be one of the first students chosen to be a Vogel lab member. I know this journey has been far from easy, and we have all experienced

some growing pains. Throughout each bump in the road Kevin has offered support and has always believed in me. I am very thankful for the kindness and patience that Kevin has shown me over the years. We have also had many moments of celebration including my selection to the Navy HSCP program, the papers our lab published, and Kevin earning tenure and the NSF CAREER award. I will forever appreciate these experiences and my time in the Vogel lab. I have great respect for Kevin as a person and scientist, and I am honored to be the first PhD student to graduate from his lab.

TABLE OF CONTENTS

Page

LIST OF TABLES

Page

LIST OF FIGURES

Page

CHAPTER 1

INTRODUCTION AND LITERATURE REVIEW

1.1 Impacts of model organisms on human and animal health

Mosquitoes (Order: Diptera, Family: Culicidae) are the most dangerous animals in the world, as they create a significant public health burden in human and animal populations globally due to their ability to transmit pathogens among vertebrate hosts. Pathogens transmitted by mosquitoes to human hosts include viruses, such as Dengue, West Nile, Chikungunya, Yellow Fever, and protozoan pathogens, including *Plasmodium spp*, which are the causative agents of malaria (CDC 2020). In addition to pathogen transmission to human hosts, mosquitoes also transmit numerous pathogens to animal hosts, including and Eastern Equine Encephalitis, Western Equine Encephalitis, and filarial nematodes (CDC 2020). Transmission of these pathogens results in increased morbidity and mortality of animal populations which can also result in significant loss of livestock populations and severely impact the agricultural industry (USDA 2024).

Similar to mosquitoes, kissing bugs (Order: Hemiptera, Family: Reduviidae, Subfamily: Triatominae) also contribute to the global human public health burden. The name “kissing bug” was coined as a result of the propensity of these insects to feed near the mouth or otherwise on the face. Kissing bugs consume a blood meal up to ten times their body size (Ayub et al. 2020). Due this massive incurrence of blood volume in the midgut, kissing bugs begin diuresis during blood feeding in order to expel fluid mass (Martini et al. 2007). Diuresis and defecation during

the blood meal facilitates transmission of *Trypanosoma cruzi*, a protozoan parasite, which is the causative parasite of Chagas disease (Vallejo et al. 2009; CDC 2023). The CDC estimates that hundreds of thousands of individuals worldwide are infected with *T. cruzi*, thus having Chagas disease. Currently there is no treatment available for latent infection stage of Chagas disease.

Together, mosquitoes and kissing bugs affect the health of millions of people and animals annually. These insects impact human health because of the evolved behavior of hematophagy, or blood-feeding. Only female mosquitoes are hematophagous, meaning only females have the ability to transmit pathogens, and this occurs through blood feeding on multiple different vertebrate hosts (Tedrow et al. 2019). The blood meal is a requirement for most female mosquito species to produce eggs. Female mosquitoes can also undergo multiple gonotrophic, or reproductive, cycles throughout their lifetime, and can feed multiple times during a single gonotrophic cycle (Brackney et al. 2021; Scott and Takken 2012). Dissimilar to mosquitoes, kissing bugs are obligately hematophagous insects, requiring a blood meal at every developmental stage for both sexes, and for adult females to produce eggs.

Hematophagy has independently evolved multiple times within the class Insecta, including multiple times within orders, such as Diptera and Hemiptera (Freitas and Nery 2020). Blood feeding behavior evolved twice in Hemiptera (bed bugs and kissing bugs) and several times in Diptera, including multiple times in both telmophagous and solenophagous flies (Freitas and Nery 2020). Hematophagy has also independently evolved in the Siphonaptera, Lepidoptera, and Psocodea. These independent hematophagous insect lineages have all convergently evolved mechanisms that aid host-seeking and blood feeding behavior, blood meal digestion, and heme detoxification, to promote survival of the insect (Arcà and Ribeiro 2018; Francis et al. 1997; Oliveira et al. 1999; Oliveira et al. 2005; Oliveira et al. 2007; Freitas and Nery 2020).

This body of work seeks to further explore the biochemical and microbial factors that promote reproductive, developmental, and lipid metabolic physiology in the mosquito, *Aedes aegypti,* and the kissing bug, *Rhodnius prolixus*. The basic biology and physiology of these disease vectors may be useful for informing future vector management strategies, which could reduce the global health disease burden posed by these blood feeding insects. Therefore, the first section of the current literature review will provide a brief overview of mechanisms that drive mosquito reproductive physiology.

1.2 Brief overview mosquito reproductive physiology

Pre-vitellogenesis, nutrition, and juvenile hormone

After the adult female mosquito has eclosed from a pupa, she begins the pre-vitellogenic, non-reproductive state. During this phase the ovaries undergo growth and development. Mosquitoes and many other holometabolous insects have polytrophic meroistic ovarioles, which are supplemented with nutritional components such as proteins, RNA, and ribosomes by trophocytes or nurse cells to promote development (Klowden 2013). Two days after adult eclosion, growth of the oocytes is arrested and ready to enter the vitellogenic state following a blood meal (Valzania et al. 2019). Pre-vitellogenic nutrition plays a major role in reproductive success in animals (Gu et al. 2015). Limited nutrient availability results in lower teneral reserves, which are stored energy sources from the larval stage. Lower teneral reserves in mosquitoes can impact body size and subsequently the reproductive output of females (Reyes-Villanueva 2004).

Pre-vitellogenic nutrition, such as sugar feeding, during the adult stage also influences reproductive output. Female *Ae. aegypti* given a 3% sucrose solution post-eclosion consumed significantly larger blood meals yet laid significantly fewer eggs than those provided with 20% sucrose solution (Clifton and Noriega 2012). Furthermore, mosquitoes fed water only or 3%

sucrose exhibited significantly higher oocyte yolk resorption after blood feeding than those provided with 20% sucrose (Clifton and Noriega 2012). This oocyte resorption and pre-vitellogenic nutrient sensing was found to be mediated by juvenile hormone (JH) (Clifton and Noriega 2011; 2012). Altogether, this demonstrates that pre-vitellogenic nutrition strongly influences mosquito reproductive physiology and that this process is modulated by the mosquito endocrine system.

Mating behavior and reproductive physiology

Within the first one to two days of adult eclosion, the female mosquito will engage in mating with one male mosquito, however, males will generally mate with more than one female (Cator et al. 2021; Dahalan et al. 2019; Helinski et al. 2012; Degner and Harrington 2016). These mating events often occur within mating swarms that can occur within close proximity to a vertebrate host (Cator et al. 2011; Hartberg 1971). Once in copula, males transfer sperm into the female oviduct, and the sperm then travels to the spermatheca where it is stored and nourished until fertilization. When the oocytes are mature, forming what will become the egg, fertilization will occur by the female utilizing stored sperm from the spermatheca. This process of female fertilization will transpire as the mature oocytes travel down the oviduct just prior to oviposition (Klowden 2013; Pascini et al. 2020).

In addition to sperm, male accessory gland (MAG) secretions are transferred from males to females in copula. MAG secretions consist of proteins and hormones that induce physiological changes in females. In *Anopheles* mosquitoes, proteins in MAG secretions induce monogamy behavior in females, reducing multiple mating behavior (Shutt et al. 2010). MAG secretions stimulate oviposition and promote survival in females (Villarreal et al. 2018; Klowden and Chambers 1991; Hiss and Fuchs 1972). After injection of isolated MAG proteins, virgin female

Ae. aegypti laid significantly more eggs and lived significantly longer than those injected with saline (Villarreal et al. 2018). Other studies have shown that male derived hormones in MAG secretions stimulate egg production in female *Anopheles* mosquitoes (Baldini et al. 2013).

Mosquito host-seeking and feeding behavior

Pathogen-vectoring mosquito species are primarily anautogenous and require a blood meal for the production of eggs. These anautogenous mosquitoes utilize many cues to locate a human host, including CO_2, temperature, skin odors, and moisture (Coutinho-Abreu et al. 2022; Cardé 2015). Mosquitoes can sense CO_2 from about ten meters away, which draws them closer to the host. When they are within one to two meters, they begin to also rely on skin odors and volatiles produced by skin bacteria and are detected by chemoreceptors (Coutinho-Abreu et al. 2022; Duvall 2019). Chemosensory signals are detected by olfactory neurons which elicit the response of the mosquito drawing closer to the host (Cardé 2015; Coutinho-Abreu et al. 2022). In *Anopheles* mosquitoes, the absence CO_2 even with the presence of attractive volatile chemicals such as ammonia and L-(+)-lactic acid does not result in attraction (Smallegange 2005). This demonstrates that CO_2 is an important signal for host-attraction. After being drawn to within one meter of a human host, female mosquitoes rely on heat and humidity cues to land themselves on the host to begin feeding (Cardé 2015).

Upon reaching the vertebrate host, the female mosquito inserts her solenophagous mouthparts into host capillaries, and releases salivary proteins consisting of anticoagulants, vasodilators, and antihemostatics (Champagne 2004). These proteins assist with evading the host immune system, allowing for the female mosquito to complete ingestion of a blood meal under five minutes (Jones and Pilitt 1973). Following blood meal consumption, female mosquitoes undergo suppressed host-seeking to allow for blood meal digestion, diuresis, and egg production

(Duvall 2019). During this time, neuropeptides that are involved in satiation are released from the brain (Duvall 2019; Duvall et al. 2019; Maguire and Potter 2019).

Vitellogenesis and oviposition

Within hours following the blood meal, ovary ecdysteroidogenic hormone (OEH) and insulin-like peptide 3 (ILP3) are released from the brain and bind to their respective receptor tyrosine kinases (Vogel et al. 2015; Brown et al. 2008; Nuss and Brown 2018). Release of OEH from the brain leads to the production of 20-hydroxyecdysone (20E) from the ovaries, directing the fat body to produce vitellogenin yolk protein which is then taken up by the ovaries (Mane-Padros et al. 2012; Roy et al. 2007). The release of ILP3 from brain neurosecretory cells promotes metabolism, blood meal digestion, and 20E synthesis independently of OEH (Dhara et al. 2013; Brown et al. 2008). ILP3 and OEH both promote egg formation, contributing to female mosquitoes producing up to 125 mature oocytes three days following a blood meal (Clements 1992; Klowden 2013).

After formation of the eggs, gravid female mosquitoes search for a semiaquatic or aquatic environment to oviposit. Gravid females select oviposition sites after assimilation of environmental criteria such as the presence of predators or conspecifics and the availability of nutritional resources which are assessed via visual and chemosensory cues (Mwingira et al. 2020; Sivagnaname et al. 2001; Vonesh and Blaustein 2010; Blaustein and Kotler 1993). For example, gravid female *Culex* mosquitoes are attracted to water sources with Bermuda grass due to the production of volatiles from Bermuda grass fermentation (Millar et al. 1992). Similarly, in *Aedes* mosquitoes, water inoculated with fungal powder was more attractive for oviposition than both tap water and water from larval rearing (Sivgnaname et al. 2001). These studies support that

the presence of volatiles produced by microbes attract gravid females for oviposition, and this is likely an indication of resource availability for developing larvae (Souza et al. 2019).

Following site selection, oviposition occurs by the movement of mature eggs through the ovariole and oviduct via contractions which are induced by the release of myotropin hormones from brain neurosecretory cells (Klowden 2013). Biogenic amines released from the central nervous system including octopamine and dopamine modulate oviposition in mosquitoes (Fuchs et al. 2014). These neurotransmitters are derived from tyramine and bind to GPCRs after release. Injection of exogenous octopamine into gravid females resulted in a significant reduction of oviposition where females withheld the mature oocytes in the ovary (Fuchs et al. 2014). Comparably, injection of exogenous tyramine into gravid females resulted in premature melanization of mature oocytes and a complete arrest of oviposition (Fuchs et al. 2014).

1.3 Study objectives and overview of Chapter 2 and Chapter 3

Endocrine signaling cascades are activated via hormones binding to target tissue cell membrane receptors, which include receptor tyrosine kinases (RTKs), receptor guanylyl cyclases (RGCs), and G-protein coupled receptors (GPCRs). Many GPCRs are so called "orphans," which are receptors that bind unidentified ligands. Correspondingly, many orphan and characterized GPCRs do not have known physiological functions. Vogel et al. 2013 conducted a phylogenetic investigation in efforts to categorize the evolutionary relationships of GPCRs across the genomes of five dipteran species. This framework was used to identify orphan GPCRs that might be involved in mosquito reproductive physiology. In mosquitoes, the CNMa receptor and its hormone ligand CNMa were shown to be highly expressed in the ovaries, suggesting they may hold a reproductive function (Akbari et al. 2013). This receptor and peptide were found to be highly conserved across many other insect orders and non-insect arthropods, though no

function had been ascribed to it. Analysis of the *Drosophila* genome led to identification of the CNMa peptide, the ligand for a recently characterized GPCR, the CNMa receptor (CNMaR) (Jung et al. 2014). Subsequent work identified that CNMa regulates feeding and appetite in *D. melanogaster*, but its role in mosquito reproductive physiology remained unexplored (Christie and Hull 2019; Peng et al. 2021; Kim et al. 2021).

In chapter 2, I assessed the function of CNMa in *Ae. aegypti* in the reproductive physiology of female mosquitoes. In this work, I show that a gene duplication event in mosquitoes resulted in two copies of the CNMa receptor, CNMaR_1a and CNMaR_1b. Next, I confirmed the tissue trophism of CNMa and its receptors, finding that only CNMaR_1b was expressed in female tissues, and that CNMaR_1a was only expressed in male antennae. I also found that both CNMa and CNMaR_1b were significantly more highly expressed in mated females compared to virgin female mosquitoes. Upon exogenous injection of CNMa into mated, blood-fed females, I found that females laid significantly fewer eggs than controls. Altogether, this work shed light on the underpinnings of factors that contribute to mosquito reproductive physiology.

In chapter 3, I determined the function of two orphan GPCRs, AAEL003647 and AAEL019988, in *Ae. aegypti* fecundity and oviposition. Both orphan receptors were also found to be highly expressed in female *Ae. aegypti* ovaries before and after a blood meal (Akbari et al. 2013). Through a phylogenetic analysis, I found that AAEL003647 is sister to the SIFamide receptor and AAEL019988 is sister to the trapped in endoderm (Tre1) receptor. With quantitative PCR, I found that expression AAEL003647 was highest in the ovaries of unfed and recently blood fed adult females. Similarly, AAEL019988 was most highly expressed in the ovaries of unfed females, and 48- and 72-hour post blood fed females. I found that knockdown of

AAEL003647 and AAEL019988 in adult female mosquitoes resulted in a significant reduction of eggs laid. In AAEL019988 knockdown females, there were significantly more mature oocytes withheld in the ovary compared to controls. The purpose of this research was to determine if AAEL003647 and AAEL019988 are important for *Ae. aegypti* female reproductive physiology. The second half of the dissertation focused on impacts of the kissing bug microbiome on developmental and lipid metabolic physiology.

1.4 Brief overview of kissing bug molting, development, and metabolism

Evolution of hematophagy in Triatomines and biochemical adaptations

The emergence of Reduviid bugs occurred around 230 million years ago (Otálora-Luna et al. 2015). Predatory Reduviid bugs in the family Triatominae were primarily entomaphagous, feeding on the hemolymph of insects, especially cockroaches (Cohen 1990; Sandoval et al. 2010). Reduviid insect predators and gave rise to hematophagous triatomines around 30 million years ago, following the evolution of birds and mammals (Otálora-Luna et al. 2015). Triatomines evolved behaviors that allowed for colonization of niches like vertebrate nests that were abundant with invertebrate prey. It is hypothesized that through inadvertent feeding of vertebrate hosts and prolonged association between Triatomines and vertebrates in nests that hematophagy arose (Lehane 2005; Otálora-Luna et al. 2015). Further, the abundance of nutrients in a blood meal made for an advantageous full diet transition (Lehane 2005).

Additional adaptations to accommodate hematophagy include the emergence of host-anticoagulant, anti-inflammatory, and vasodilatory salivary proteins to evade vertebrate host immunity and defense and to maximize blood meal volume (Andersen et al. 2005; Otálora-Luna et al. 2015). The protein richness of a blood meal is starkly different from that of plant-sap, which is consumed by most hemipterans. Hematophagous triatomines co-opted proteases,

including carboxypeptidases, aminopeptidases, and cathepsins because digestive trypsin serine proteases, are absent in Hemiptera (Lehane 2005; Waniek et al. 2012). It is thought that loss of digestive serine proteases in hemipterans occurred over time due to most Hemipterans feeding on protein poor diets. Finally, hematophagous triatomines adapted the ability to detoxify heme through the formation of hemozoin. Hemozoin is crystallized heme, which is formed by the posterior midgut perimicrovillar membrane. Hemozoin formation protects triatomines from heme toxicity after consumption of blood (Oliveira et al. 2000; 1999; 2005; 2007; Silva et al. 2007).

Kissing bug lipid synthesis, transport, and mobilization

Insects and mammals have a conserved *de novo* lipogenesis pathway, and acetyl-CoA carboxylase (ACC) is the rate limiting enzyme for *de novo* lipid synthesis (Goldring and Read 1994; Wang et al. 2022). This is especially beneficial for obligately hematophagous insects because although vertebrate blood contains lipids and carbohydrates, these macromolecules are in low relative abundance compared to protein (Lynch et al. 2017; Gorbatov 1988; Sorapukdee and Narunatsopanon 2017). Thus, hematophagous insects rely on the ACC *de novo* lipogenesis pathway in order to convert diet derived amino acids and carbohydrates to fatty acids. Blood meal digestion begins one day following ingestion of a blood meal, and blood meal derived fatty acids and phospholipids are endocytosed by midgut epithelial cells (Gondim et al. 2018; Grillo et al. 2003; Bittencourt-Cunha et al. 2013). During digestion, triglycerides from the blood meal are hydrolyzed by midgut lipases to release free fatty acids (Grillo et al. 2007). Some blood meal derived fatty acids and phospholipids that are endocytosed remain in the midgut epithelial cells and are incorporated into the perimicrovillar membrane (Roberto Silva et al. 2006; Lane and Harrison 1979). Alternatively, in the midgut epithelial cells, fatty acids are used for the synthesis of diacylglycerol. Diacylglycerol is released from midgut epithelial cells and transported from

the midgut to peripheral tissues by lipophorins in the hemolymph (Gondim et al. 2018). After reaching the target tissue, such as the fat body or ovary, diacylglycerol is used for synthesis of triacylglycerol (Entringer et al. 2013; Pontes et al. 2008).

The insect fat body, analogous to the human liver, is the primary lipid storage site in the insect. Following a blood meal and transport by lipophorins, monoacylglycerol, diacylglycerol, and fatty acids are synthesized into triacylglycerol by the glycerol-3-phosphate pathway (Canavoso et al. 2001; Gondim et al. 2018). Triglycerides are the largest resource of stored energy within the insect (Arrese and Soulages 2010; Saraiva et al. 2020; Pontes et al. 2008). ACC is the rate limiting enzyme, and it is upstream of many other lipogenesis genes. *Acc* is expressed in the midgut and the fat body (Moraes et al. 2022). Knockdown of *acc* in *R. prolixus* results in a reduction of phospholipids, diacylglycerol, monoacylglycerol, hydrocarbons, and triacylglycerol in the fat body (Moraes et al. 2022). ACC converts acetyl-CoA to malonyl-CoA, which can then be acted on by fatty acid synthase (FAS) for production of long chain fatty acids (Gondim et al. 2018). Knockdown of fatty acid synthase 3 (RPRC000123) in *R. prolixus* results in a significant reduction of long chain fatty acids and hydrocarbons in the integument (Moriconi et al. 2019). In the mosquito *Ae. aegypti*, knockdown of fatty acid synthase 1 resulted in impaired blood meal digestion and reduced fat body phospholipid and triglycerides (Alabaster et al. 2011). Although three fatty acid synthase genes have been identified in the *R. prolixus* genome, the roles of fatty acid synthase 1 and fatty acid synthase 2 in lipogenesis have not yet been determined (Majerowicz et al. 2017).

Following triglyceride synthesis and storage in the fat body, lipases hydrolyze triglycerides for ß-oxidation and mobilization (Aredes et al. 2024). Brummer lipase (*bmm*) is the primary lipase that modulates triglyceride mobilization in *R. prolixus*. Knockdown of *bmm*

results in reduced mobilization of triacylglycerol and its accumulation in the fat body even three weeks following a blood meal in *R. prolixus* (Aredes et al. 2024). Similarly, lipid mobilization is also controlled by adipokinetic hormone (AKH) which binds its associated G protein-coupled receptor, the adipokinetic hormone receptor (AKHR) (Zandawala et al. 2015; Alves-Bezerra et al. 2016). Knockdown of the AKHR resulted in significant accumulation of triacylglycerol in the fat body *R. prolixus* adults (Zandawala et al. 2015). Additional hormones that modulate lipid metabolism in hematophagous insects are insulin-like peptides (ILPs), JH, and ecdysone (Gondim et al. 2018).

Kissing bug molting and synthesis of the integument

The kissing bug, *Rhodnius prolixus,* was a primary insect model for the establishment of foundational knowledge in insect physiology. This research was spearheaded by Sir Vincent Wigglesworth, the father of insect physiology, in the early 1900's. Wigglesworth's research led to uncovering the roles of juvenile hormone and ecdysone in kissing bug molting and ecdysis. Molting and ecdysis are mainly controlled by JH and ecdysone in the kissing bug. JH is synthesized by the corpora allatum, an organ proximal to the insect brain, and is released following a blood meal (Wigglesworth 1934; Nabert 1913). The juvenile hormone III skipped bisepoxide homolog (JHSB3), initially identified in the stink bug *Plautia stali*, has been identified to be the physiologically active form of JH in *R. prolixus* (Villalobos-Sambucaro et al. 2020; Kotaki et al. 2011). In *R. prolixus,* hemolymph JH titer increases within one day after blood feeding but is highest between six and seven days following a blood meal in fourth instars, roughly three days preceding the fifth instar molt (Villalobos-Sambucaro et al. 2020).

In addition to JH, ecdysteroids are released from the prothoracic glands post blood feeding and coordinate with JH to initiate molting (Garcia et al. 1987b; Steel et al. 1982; Marchal

et al. 2010). The synthesis and release of ecdysteroids is stimulated by the release of prothoracicotropic hormone (PTTH) from the prothoracic glands (Wigglesworth 1952; Vafopoulou and Steel 1991; Vafopoulou and Steel 2002). In *R. prolixus*, interruption of JH and ecdysone signaling during the "head critical period" (HCP) and the "juvenile hormone sensitivity period" (JHSP) following a blood meal is known to cause molt arrest and a precocious or premature molt, respectively (Wigglesworth 1934; Villalobos-Sambucaro et al. 2020; de Azambuja et al. 1984; Garcia et al. 1987a). Thus, the activity of these hormones is critical for the insect to undergo successful development.

Induction of JH and ecdysone release after a blood meal stimulates nymphal growth and the synthesis of the new cuticle, by the epidermis (Wigglesworth 1933). The basal lamina, an extracellular matrix, is the innermost layer of the integument and serves as the barrier between the body cavity and the integument (Klowden 2013). Beyond the basement membrane lies the epidermis, which is made up of dermal gland cells, sensory receptors, and oenocytes (Klowden 2013). The dermal cells and oenocytes are secretory cells that secrete lipids, waxes, and polyphenols (once known as "sclerotins"), through pore canals and wax channels that coat the outermost layer of the integument (Wigglesworth 1985a; 1985b; 1988). The secretion of these waxes is dependent on stimuli from the environment that are sensed and relayed by sensory receptors (Klowden 2013; Rajpurohit et al. 2020; Wang et al. 2022).

Beyond the epidermis is the procuticle which is composed of the endocuticle, mesocuticle, and exocuticle, all of which have chitin. The endocuticle is a soft and permeable layer of the integument consisting mainly of proteins and chitin. This layer allows for insect flexibility. During the process of molting and development, this layer is completely digested by enzymes and recycled for the synthesis of the new integument. The mesocuticle is similar to the

endocuticle in that it does not consist of cross-linked proteins, allowing for flexibility. The mesocuticle is also primarily made up of lipids and proteins. The exocuticle, unlike the endocuticle and the mesocuticle, is made up of cross-linked proteins, providing the insect with structural integrity (Wigglesworth 1970; Klowden 2013). Finally, the epicuticle and envelope (or outer epicuticle) are the outermost regions of the insect integument, and cuticular lipids, waxes, and polyphenols are secreted by oenocytes to coat the epicuticle, just prior to molting (Wigglesworth 1970; 1975; 1985a; 1985b; 1988). Epicuticular lipids are comprised of cuticular hydrocarbons, fatty alcohols, and fatty acid esters, and polyphenols promote tanning, sclerotization and melanization of the cuticle (Lockey 1988; Dennell 1947; Wigglesworth 1985; 1988).

Cuticular lipids confer desiccation and thermal tolerance, and some are also implicated in mediating airway clearance and waterproofing the trachea (Wigglesworth 1970; Wigglesworth 1985a; 1985b; 1986; Jaspers et al. 2014; Ferveur et al. 2018; Wang et al. 2022; Krupp et al. 2020). Knockdown of fatty acyl-CoA reductase (*facr*) genes in the brown rice planthopper resulted in ecdysis arrest events in which planthopper nymphs were unable to shed their exuviae, which resulted in mortality (Li et al. 2020). In *R. prolixus*, knockdown of *FASN3* resulted in an inability of nymphs to melanize and sclerotize the cuticle after molting, resulting in immediate mortality and desiccation after a molt (Moriconi et al. 2019). The immediate desiccation phenotype observed in *FASN3* knockdown nymphs was in part due to reduced levels of epicuticular hydrocarbons as a consequence of *FASN3* knockdown (Moriconi et al. 2019). In addition to FACRs and FASNs, the insect microbiome also promotes both formation of the cuticle and desiccation tolerance. In the saw-tooth grain beetle *Oryzaephilus surinamensis*, removal of symbiotic bacteria results in increased desiccation sensitivity, malformation of the

cuticle, and reduced cuticle sclerotization (Engl et al. 2017). Contributions of the kissing bug microbiome to desiccation tolerance and cuticle formation have yet to be investigated.

The kissing bug gut microbiome

T. cruzi is part of the kissing bug microbiome, and it is hypothesized that these parasites were acquired first through the acquisition of *Phytomonas* trypanosomatids, prior to the evolution of hematophagy (Jaskowska et al. 2015). *Phytomonas* are a type of single-celled parasite that invade plants (Jaskowska et al. 2015). Fungi are not known to be commonly found within the kissing bug gut microbiome. The kissing bug microbiome has a limited bacterial diversity, and often a single genera becomes dominant in older instar and adult stage bugs (Rodríguez-Ruano et al. 2018; Brown et al. 2020; Eberhard et al. 2022; Arias-Giraldo et al. 2020). Kissing bug gut communities also differ by species, location, and developmental stage (Brown et al. 2020; Rodriguez-Ruano et al. 2018).

In *Rhodnius prolixus*, bacteria from the orders *Enterobacterales, Corynebacteriales, Lactobacillales, Clostridiales, Chlamydiales* are dominant in the gut (Rodríguez-Ruano et al. 2018). Additional bacteria found to be abundant within the *R. prolixus* gut are *Kocuria koreensis, Candidatus Symbiopectobacterium, Serratia marcescens, and Rhodococcus rhodnii* (Eberhard et al. 2022; Novakova et al., unpublished). *Rhodococcus rhodnii* (formerly *Nocardia rhodnii and Actinomyces rhodnii*) was first identified in the gut of *Rhodnius prolixus* nymphs in the 1930's, by Wigglesworth (Wigglesworth 1936). Wigglesworth found that *R. rhodnii* was acquired by nymphs through consumption of feces from conspecifics. He found that these bacteria were symbiotic in *R. prolixus* because removal of the bacteria through egg surface sterilization resulted in impaired development and developmental arrest at the fifth instar (Brecher and Wigglesworth 1944).

R. rhodnii alone is able to rescue development in *R. prolixus* and also in other germ-free kissing bug species, including *Triatoma protracta* and *Triatoma rubida* (Gilliland et al. 2023; Nyirady 1973). In *R. prolixus* supplementation of B vitamins was able to partially rescue *R. prolixus* development, suggesting that B vitamin supplementation was a function of *R. rhodnii* in *R. prolixus* (Baines 1956). Additional studies utilizing bacteria that are auxotrophic for B vitamin synthesis further supported the role of symbionts in provisioning essential B vitamins (Lake and Friend 1968). B vitamin supplementation is a well-established benefit of microbial symbionts in obligately hematophagous insects due to the inability of the host to synthesize or otherwise acquire these nutrients through diet (Rio et al. 2016; Bing et al. 2017; Hosokawa et al. 2010; Hickin et al. 2022; Douglas 2017; Tobias et al. 2020). Our lab has established that *R. rhodnii* can biosynthesize all eight essential B vitamins through *de novo* or salvage pathways (Gilliland et al. 2023). B vitamins are also essential cofactors for many metabolic pathways in insects, especially lipid metabolic pathways (Douglas et al. 2017). For example, the conversion of acetyl-CoA to malonyl-CoA by ACC is biotin (vitamin B_7) dependent. Due to the role of the microbiome in B vitamin supplementation in hematophagous insects, and the requirement of B vitamins for lipid synthesis and metabolism, I sought to investigate the role of the microbiome in lipid metabolic physiology in the kissing bug, *R. prolixus*. The goal of this body of work is to explore the contributions of the microbiome to lipid synthesis and metabolism through the ACC *de novo* lipogenesis pathway.

1.5 Study objectives and overview of Chapter 4 and Chapter 5

Because ACC is the rate limiting enzyme for *de novo* lipogenesis (Gondim et al. 2018), I first examined expression of *acc* in axenic (germ-free), conventional (complete microbiome), and gnotobiotic (*R. rhodnii* monoculture) bugs. I found that axenic bugs differentially express

acc in the whole gut, fat body, and integument tissues compared to conventional and gnotobiotic bugs. To further elucidate the role of the microbiome in lipogenesis, I selected four genes downstream of ACC (one fatty acid synthase ortholog: RPRC011289 and three fatty acyl-CoA reductases: RPRC000873, RPRC000223, and RPRC011813) that were differentially expressed in axenic and gnotobiotic bugs based on transcriptomic data. The primary objectives of this work are to understand the contributions of the microbiome to lipid synthesis and metabolism in the kissing bug *R. prolixus* and to determine the lipogenic function of genes downstream of ACC.

In chapter 4, I first explore the role of the microbiome in lipogenesis through generation of a fat body triglyceride profile comparing triglyceride levels in fourth instar unfed fourth instar axenic, conventional, and gnotobiotic bugs and fed bugs at multiple times post blood meal. I found that axenic bugs exhibited a significant delay in triglyceride synthesis relative to conventional and gnotobiotic bugs. I discovered that axenic bugs retained undigested blood in the anterior midgut after molting, which could be a contributing factor to differences in lipid abundance. It has been established that knockdown of *FAS1* in *Ae. aegypti* females impairs blood meal digestion (Alabaster et al. 2011). Thus, I wanted to determine the potential role of fatty acid synthase ortholog (FAS289) in blood meal digestion in *R. prolixus*. I found that knockdown of *fas289* did not impair blood meal digestion but did decrease fat body triglyceride stores in fed bugs. Finally, I conducted a whole gut and fat body lipidomics experiment in unfed and fed axenic, conventional, and gnotobiotic bugs to identify the role of the microbiome in lipogenesis of each major class of lipid including free fatty acids, phospholipids, diacylglycerol, and triacylglycerol. Altogether, this work highlighted the role of the microbiome in lipogenesis and provided insights into the function of a novel fatty acid synthase gene in *R. prolixus*.

Lipids are not only important for energy storage and metabolism, but they also are primary components of the insect integument. Cuticular lipids, including cuticular hydrocarbons (CHCs), in the epicuticle are implicated in insect communication and desiccation prevention (Holze et al. 2021). CHCs are synthesized by enzymes in the ACC lipogenesis pathway in the oenocytes (Holze et al. 2021). Thus, in chapter 5, I investigated the role of the microbiome in cuticular hydrocarbon biosynthesis and desiccation tolerance. Further, I examined role of the microbiome in modulation of genes in the cuticular hydrocarbon biosynthetic pathway. Through microscopy, I found that the microbiome differentially affects the formation of the epicuticle. Next, I found that gut bacteria promote the synthesis of cuticular hydrocarbons, and that axenic bugs are more sensitive to desiccation when exposed to low humidity conditions. Similarly, I found that knockdown of *facr873* and *facr813* resulted in malformation of the epicuticle. Moreover, *facr223* and *facr873* knockdowns induced desiccation sensitivity relative to controls. In summary, this study emphasized the role of the microbiome in promoting desiccation tolerance by aiding synthesis of cuticular hydrocarbons, formation of the epicuticle, and through modulation of fatty acyl-CoA reductase genes.

CHAPTER 2

THE PEPTIDE HORMONE CNMA INFLUENCES EGG PRODUCTION IN THE MOSQUITO *AEDES AEGYPTI* [1]

[1]Keyes-Scott NI, Lajevardi A, Swade KR, Brown MR, Paluzzi JP, Vogel KJ. 2022. *Insects*. 3(3):230. Reprinted here with permission of publisher.

2.1 Simple Summary

Hormones are important signaling molecules mediating insect reproduction that require specific receptors to transmit their signal across the plasma membrane of target cells. While the hormones many receptors bind are known, some receptors are “orphans” with unknown ligands. The hormone CNMa was previously found to bind a specific receptor in fruit flies. Two copies of the receptor are found in mosquitoes, but only one gene for the hormone is present. We found that both receptors in the yellow fever mosquito are activated by CNMa. One of the receptors is expressed in mosquito ovaries, which to us implied the hormone and its receptors may be involved in mosquito reproduction. We further found that injecting the peptide into females reduced the number of eggs that were laid. These experiments suggest that CNMa may be an important factor governing mosquito reproduction.

2.2 Abstract

Mosquito reproduction is regulated by a suite of hormones, many acting through membrane-bound receptor proteins. The *Aedes aegypti* G protein-coupled receptors AAEL024199 (AeCNMaR-1a) and AAEL018316 (AeCNMaR-1b) were identified as orthologs of the *Drosophila melanogaster* CNMa receptor (DmCNMaR). The receptor duplicated early in the evolution of insects and subsequently in the Culicidae, into what we refer to as CNMaR-1a and CNMaR-1b. AeCNMaR-1a was only detected in male mosquito antennae while AeCNMaR-1b is expressed at high levels in mosquito ovaries following a blood meal. Using a heterologous cell assay, we determined that AeCNMa activates AeCNMaR-1a with a ~10-fold lower concentration than it does AeCNMaR-1b, though both receptors displayed half maximal

effective concentration of AeCNMa in the low nanomolar range. Finally, we show that injection of AeCNMa into blood fed, mated female Ae. aegypti resulted in fewer eggs laid.

Keywords: GPCR, insect endocrinology, reproduction

2.3 Introduction

Mosquitoes are significant vectors of human pathogens due to their requirement of blood meals to produce successive clutches of eggs. The process of egg production in mosquitoes involves coordination of multiple events from pre-vitellogenic oogenesis (Clifton and Noriega 2012), mating (Duval et al. 2017; Hiss and Fuchs 1972), host-seeking and blood feeding (Matsumoto et al. 1989; Naccarati et al. 2012), blood digestion and yolk production (Gulia-Nuss et al. 2011; Wang et al. 2017), and oocyte maturation and oviposition (Gulia-Nuss et al. 2011; Riehle and Brown 1999; Brown et al. 2008; Vogel et al. 2015). At each stage, endocrine factors play critical roles in regulating these processes. In the pre-vitellogenic stage of development, juvenile hormone (JH) is secreted by the corpora allata shortly after eclosion (Wang et al. 2017) Rivera-Perez et al. 2014). JH ultimately acts upon the fat body and ovaries to induce competency for uptake of yolk proteins (vitellogenin) synthesized from digested blood proteins Gwadz and Spielman 1973). Following a blood meal, insulin-like peptides (ILPs) and ovary ecdysteroidogenic hormone (OEH) are released from the mosquito brain, inducing ecdysteroid production in the ovaries and expression of serine proteases in the midgut (Matsumoto et al. 1989; Gulia-Nuss et al. 2011; Brown et al. 2008). Ecdysteroids then act on the fat body to stimulate expression of yolk protein genes, resulting in the production of vitellogenin, which is taken up by the 100-150 developing oocytes in the ovaries (Matsumoto et al. 1989). Disruption

of any of these signaling pathways blocks development of oocytes, resulting in reproductive failure (Brown et al. 2008; Vogel et al. 2015).

Endocrine factors must transduce their signal across the membranes of target cells. Peptide hormones bind and activate transmembrane receptors including G protein-coupled receptors (GPCRs), protein kinase receptors (PKRs), and receptor guanylyl cyclases (RGCs). The genome of the yellow fever mosquito, *Aedes aegypti*, encodes numerous GPCRs, PKRs, and RGCs, many of which have known functions and characterized ligands (Vogel et al. 2013). Ligands of some *Ae. aegypti* receptors are inferred through their orthology with characterized receptors in other arthropods, while others are true orphans with no known ligands (Vogel et al. 2013). Likewise, several neuropeptides identified in *Ae. aegypti* lack a characterized receptor (Predel et al. 2010).

The peptide CNMamide (CNMa) was initially discovered in Drosophila melanogaster and was named after the conserved carboxyl-terminal cysteine-asparagine-methionine motif that ends with an amide post-translationally modified from a glycine (Jung et al. 2014). Two splice variants of the CNMa gene were predicted to be processed into two similar but distinct propeptides, which are subsequently cleaved into distinct peptides. The authors identified that the peptides were expressed in the brain and ventral nerve cord. The receptor for CNMa in *D. melanogaster* (DmCNMaR) was identified as a GPCR, CG33696, which is expressed in the *D. melanogaster* central nervous system (CNS). With a heterologous cell assay, it was demonstrated that DmCNMaR binds CNMa at nanomolar concentrations (Jung et al. 2014; Kim et al. 2021). Initial studies showed no phenotype following transgenic RNAi knockdown of the receptor in *Drosophila*. Recently, Kim et al. 2021 have reported expression of DmCNMa in other tissues,

including the midgut and fatbody, and demonstrated that CNMa and CNMaR act as a signal of nutritional status and alter behavior in response to low essential amino acid levels in hemolymph.

Phylogenetic analysis of the CNMa gene indicated that it is widely conserved across arthropods, including in the crustacean Daphnia pulex, though it appears absent in Lepidoptera (Jung et al. 2014). CNMaR has undergone multiple duplications, first into the paralogs CNMaR-1 and CNMaR-2, prior to the diversification of Hymenoptera. Paralogs of the receptor were differentially lost among insect orders, with all examined dipteran and lepidopteran genomes retaining the CNMaR-1 paralog but not CNMaR-2, though the red flour beetle, *Tribolium castaneum*, retains only the CNMaR-2 paralog. A second duplication event occurred in the Culicidae as two paralogs of CNMaR-1 are seen in the genomes of the African malaria mosquito, *Anopheles gambiae*; the common house mosquito, *Culex quinquefaciatus*; and *Ae. aegypti*, though the evolutionary timing of the duplication and the biological significance was not addressed (Jung et al. 2014). The subsequent increase in available insect genomes and improved annotation of existing genomes now allows for a more detailed assessment of the evolution of the receptor paralogs, including the extent to which different lineages retain multiple copies of CNMaR.

Using transcriptomic data, we determined that one *Ae. aegypti* paralog of DmCNMaR was highly expressed in reproductive tissues following a bloodmeal (Akbari et al. 2013), suggesting a possible role for the peptide in regulation of reproduction. We assessed the binding of AeCNMa to both paralogs of *Ae. aegypti* CNMaR-1 separately expressed in a mammalian cell line and found that the peptide activated both receptors but at slightly different concentrations. We next sought to identify a function for AeCNMa, by injecting it into blood fed females and assessing whether reproductive processes were altered. Mated, blood fed females injected with

CNMa laid fewer eggs than control mosquitoes, indicating this peptide-receptor system may be involved in the regulation of oviposition by mosquitoes.

3.4 Materials and Methods

Mosquitoes

The UGAL strain of *Ae. aegypti* was used in all experiments. Mosquitoes were kept at 27°C on a 16 h:8 h L:D cycle. Larvae were fed Cichlid Goldfish pellets, and adults were provided with a 8% sucrose solution for 2 days post-eclosion. For virgin female experiments, individual pupae were placed in 0.5 ml of water in the wells of a 48-well polystyrene plate and returned to the environmental chamber to eclose. Following eclosion, adults were sorted by sex and kept in female-only containers prior to bioassays. Females were fed on defibrinated rabbit blood (Hemostat Laboratories, Dixon, CA) provided via a water-jacketed parafilm membrane artificial feeder warmed to 37°C.

Sequence analyses

Orphan peptide hormone receptors identified by Vogel et al. 2013 were queried against a developmental RNAseq dataset (Akbari et al. 2013). Receptors with highly differential expression in female reproductive tracts were selected for further study. *Ae. aegypti* orthologs of the DmCNMaR (CG33696) and DmCNMa peptide (CG13936) were identified through BLAST searches against the NCBI non-redundant database while limiting hits to arthropods (taxid: 6656). While the DmCNMa sequence has two splice forms, we only ever saw evidence of a single band when amplifying the complete AeCNMa sequence with PCR, nor did melting temperature analysis of AeCNMa ever suggest the existence of alternative forms. Furthermore,

no evidence of alternative splice forms was seen in the transcriptomic data supporting the gene model in VectorBase. To obtain sequences for phylogenetic analysis, the AeCNMaR-1b (AAEL018316) was used as a query against the NR database again restricting results to hits within the Arthropoda. Additional sequences were identified through queries of OrthoDB (Kriventseva et al. 2019). Each sequence was assessed for the presence of the characteristic 7 transmembrane domains of canonical GPCRs (Munoz et al. 2017). To identify potentially mis-annotated sequences, the genomic regions surrounding partial CNMaR sequences were aligned against the *Ae. aegypti* CNMaR-1a sequence with Exonerate (Slater 2005) to identify the missing section of the sequence. The identified regions were then appended to the annotated sequences and the merged sequences used for downstream phylogenetic analysis. Only sequences with 6 or more identified transmembrane domains were included in the analysis. CNMaR sequences were aligned using MAFFT with the --linsi option (Katoh et al. 2002). Alignments were trimmed using trimAl with a gap threshold of 0.4 (Capella-Gutiérrez et al. 2009). The alignment was used as input to RAxML (Stamatakis 2014) with the following options: -f a -x 1 -N 100 -p 1. Trees were visualized in Figtree (http://tree.bio.ed.ac.uk/software/figtree/).

Peptide synthesis, receptor cloning, and GPCR activation assays

CNMa peptide was synthesized and HPLC purified (> 90% purity) by Royobiotechs (Shanghai, China) based on the published sequence of AeCNMa peptide sequence (Jung et al. 2014). Both the amidated (YMSLCHFKLCNMa) and the non-amidated (YMSLCHFKLCNM) were produced with a disulfide bridge between cysteines 5 and 10. The complete coding sequence of the two putative *Ae. aegypti* CNMa receptors (VectorBase genes AAEL024199 and AAEL018316, which we henceforth refer to as AeCNMaR-1a and AeCNMaR-1b, respectively)

were commercially synthesized (Integrated DNA Technologies) and subsequently subcloned into pcDNA3.1+ mammalian expression vector (Oryan et al. 2018). A Chinese hamster ovary cell line stably expressing the calcium-dependent bioluminescent protein aequorin (CHO-K1 aeq) (Paluzzi and O'Donnell 2012; Wahedi and Paluzzi 2018) was grown in Dulbecco's modified eagles medium: nutrient F12 (DMEM:F12) media containing 10% heat-inactivated fetal bovine serum (FBS; Wisent, St. Bruno, QC), 200 μg/mL geneticin, and antimycotic-antibiotic mixture as described previously (Sajadi et al. 2020). When cells reached 80-90% confluency, they were transfected using Lipofectamine 3000 transfection reagent following manufacturer recommendations (Life Technologies, Burlington, ON) to transiently express a mammalian construct in pcDNA3.1+ containing either of the two candidate CNMa receptors or mCherry (pcDNA3.1+ mCherry was a gift from Scott Gradia, Addgene plasmid #30125), the latter of which served as a negative control for the receptor functional assay. At 48 h following transfection, CHO-K1 aeq cells were harvested by dislodging from culture flasks using Dulbecco's PBS containing EDTA and subsequently resuspended in receptor assay media [26]. Other *Ae. aegypti* peptides used in this study included "capability" (CAPA)-1 (GPTVGLFAFPRV-NH2), CAPA-2 (pQGLVPFPRV-NH2), AedaeCAPA-pyrokinin (PK) 1 (AGNSGANSGMWFGPRL-NH2), adipokinetic/corazonin like peptide (ACP; pQVTFSRDWNA-NH2), adipokinetic hormone (AKH) (pQLTFTPSW-NH2) and corazonin (CRZ; pQTFQYSRGWTN-NH2) [24,26,27]. Serial dilutions of the peptide stocks were prepared in bovine serum albumin (BSA) assay media (DMEM:F12 media + 0.1% BSA + 1x antibiotic-antimycotic) to test concentrations ranging from 10 pM to 50 μM. Single concentrations of the various peptides were loaded into individual wells of white 96-well luminescence plates (Greiner Bio-One, Germany) with each peptide concentration tested in quadruplicate. CHO-K1 aeq cells

expressing either of the two AeCNMa receptors or mCherry were prepared for the functional assay as described above and injected into each well of 96-well luminescence plates by an automated injector unit integrated with the Synergy 2 Multi-Mode Microplate Reader (BioTek, Winooski, VT, USA). The kinetic luminescent response was measured for 10 sec immediately following application of cells into the wells containing the different peptide treatments or the negative (i.e. BSA media alone) or positive (i.e. 50 μM ATP) controls as described previously (Wahedi and Paluzzi, 2018). Data was assembled in Microsoft Excel and then analyzed in GraphPad Prism 7.02 (GraphPad Software, San Diego, USA) where the dose-response curves from multiple biological replicates were used to determine the half maximal effective concentrations (EC50).

qRT-PCR analysis of target gene expression

Cohorts of female *Ae. aegypti* were sampled 8 to 10 days post-eclosion, pre-blood meal (NBF), then at 2, 4, 6, 8, 12, 24, 48, and 72 h PBM. Four or more females from each timepoint were dissected in cold, RNase-free PBS into head, midgut, ovaries, and abdominal body wall and fat body ("pelt"). Tissue samples were immediately frozen and stored at -80°C. Tissues were thawed on ice, homogenized with a rotor type pestle, then total RNA was extracted using the RNeasy Mini kit (Qiagen) according to the manufacturer's instructions. RNA was treated with DNase using the Turbo DNA-free kit (Ambion). cDNA was synthesized from 100 ng of RNA with the iScript cDNA synthesis kit (BioRad) and used as template in qPCR using the Quantifast SYBR Green PCR kit (Qiagen). Primers for each product are listed in table S1. qPCR was performed on the Qiagen Rotorgene as described in (Vogel et al. 2017). Absolute standard curves were produced by cloning each qPCR product into the pSCA vector using the Strataclone PCR cloning kit (Agilent) and preparing plasmid standards of known copy number. For

comparisons between different genes, copy number of each target was normalized to the copy number of ribosomal protein S7.

Bioassays

Three- to five-day old mated females were blood fed as detailed above, and groups were injected with a range of CNMa in 0.5 µl of saline or saline alone (AS) for a control. Females were allowed to recover and then housed individually in mesh cages. At 3 d PBM, a wet paper towel was provided to the females to facilitate egg laying for up to 48 h then the number of eggs was counted. To assess possible interactions of CNMa with OEH and ILP3, mated females were blood fed then decapitated and injected at 1 h PBM with 150 pmol of CNMa, OEH, or ILP3, or combinations of each hormone (Valzania et al. 2019). Ovaries were dissected at 24 h PBM and yolk deposition was measured along the anterior-posterior axis for 5 oocytes from each individual using an ocular micrometer fitted to a dissecting microscope. For CNMa and JH experiments, pupae were isolated in eclosion chambers for 6 h and females were collected. Females were divided into two groups, one which was immediately injected with 150 pmol of CNMa or saline. The other half of the cohort was held for an additional 8 h then injected with the same solutions. At 3 d post-eclosion, females were blood fed and oviposition was measured for all treatment groups.

Proteomic studies of female and male tissues

To determine if CNMa was transferred from males to females, we examined different male and female tissues before and after mating for the presence of CNMa using HPLC and mass spectrometry. Fifty heads, thoraces, and abdomens from 3-5 day old *Ae. aegypti* females were

collected separately in 200 µl of 80% acetonitrile/0.01% trifluoroacetic acid (TFA) and frozen at -80°C overnight. Samples were thawed and sonicated at low power for 10 s with 100 µl 80% ACN/TFA added. Samples were centrifuged for 5 minutes at 21k RCF, and the supernatant was removed and lyophilized. Samples were resuspended in 500 µl of 10% ACN/TFA for 2 h then centrifuged as before. After a blank run, supernatant was injected into a Jupiter C18 column (300 Å, 4.5 x 200 mm) on a Beckman 126/166 chromatography unit. Samples were run in the following sequence: head extract, thorax extract, abdomen extract, 5 µg of AeCNM and AeCNMa. Sixty male accessory glands were collected from virgin *Aedes* males into 1 ml of 10% ACN/0.1% TFA and frozen at -80. After thawing and sonification, the sample was centrifuged and injected onto the column and eluted as above. Sample material was eluted with a gradient (solvent A, pure water with 0.1%TF; solvent B, 80% ACN/0.1% TFA/pure water: 10%B to 80%B over 40 min; 1 ml/min) monitored at 206 nm and collected in tubes as 1 ml fractions. CNMa and CNM eluted in fraction 25, so fractions 24 and 25 from the body part/tissue HPLC runs were pooled separately, lyophilized and subjected to MALDI-TOF mass spectroscopy (MS), along with synthetic CNMa and CNM.

3.5 Results

CNMaR-1 is duplicated in the Culicidae

Our phylogenetic leveraged additional insect genome sequences to further characterize the timing of CNMaR duplications and retention or loss of orthologous sequences. Our analysis recovered two highly divergent CNMaR sequences in several insect lineages, including the Nevada dampwood termite Zootermopsis nevadensis, milkweed bug Onthophagus taurus, and a large number of hymenopteran species (figure 1). While there is not strong support for two

monophyletic clades in our phylogeny, the distribution of CNMaR1 and CNMaR2 sequences suggests an ancient duplication followed by repeated, frequent losses. Our phylogeny also identifies two robustly supported clades of CNMaR-1 sequences in the Culicidae. Due to limited genomic sequence availability, Jung et al. 2014 were unable to identify the members of each clade from *Ae. aegypti* and *C. quinquefaciatus*, but improvements in genome sequences and annotations for these species have clearly identified two copies of CNMaR-1 in these genomes, which we refer to as CNMaR-1a and CNMa-R1b. Our phylogenetic analysis lacked sufficient power and sampling to determine when the duplication occurred. Either CNMaR-1 duplicated prior to the divergence of the Brachycera, but CNMaR-1b was then lost in the Brachycera, or the duplication occurred after the split of the Culicomorpha from the Psychomorpha, but prior to the divergence of the Anopheline and Culicine lineages (figure 1). The latter is the more parsimonious evolutionary trajectory, but the orthologs of CNMaR-1a group with sequences from Brachycera species, though this branch has very low support (18/100 bootstraps).

Orthologs of AeCNMaR-1a and AeCNMaR-1b were found in species across the family Culicidae. We did not include orthologs from every species with an available genome, as the sequences of CNMaR-1a/b were incomplete in many annotations. However, sequences containing all seven transmembrane domains were found in *Anopheles* spp. from across the phylogeny of sequenced genomes from this genus (Neafsey et al. 2015). In some cases, we were able to identify exonic sequences that were potentially missed during annotation by comparing the full-length sequence of AeCNMaR-1a/b against the genomic regions encoding partial CNMaR sequences. We further interrogated available transcriptomic data for evidence of expression and found many of these sequences lack any evidence for expression. Therefore, it is possible that these are pseudogenes of recent origin.

The most-closely related outgroups to the Culicidae with available genomic sequence data are the phlebotomine sand flies *Lutzomyia longipalpis* and *Phlebotomus papatasi* (Diptera:Psychodomorpha:Psychodidae). BLAST and OrthoDB searches against the genomes of *P. papatasi* found no significant hits against the *Ae. aegypti* CNMaR-1b sequence, while the partial sequence of a single ortholog was found in *L. longipalpis* (figure 1). All other dipteran genomes examined encode a single ortholog of CNMa-1, suggesting that the duplication event occurred after the divergence of the Psychomorpha from the Culicomorpha.

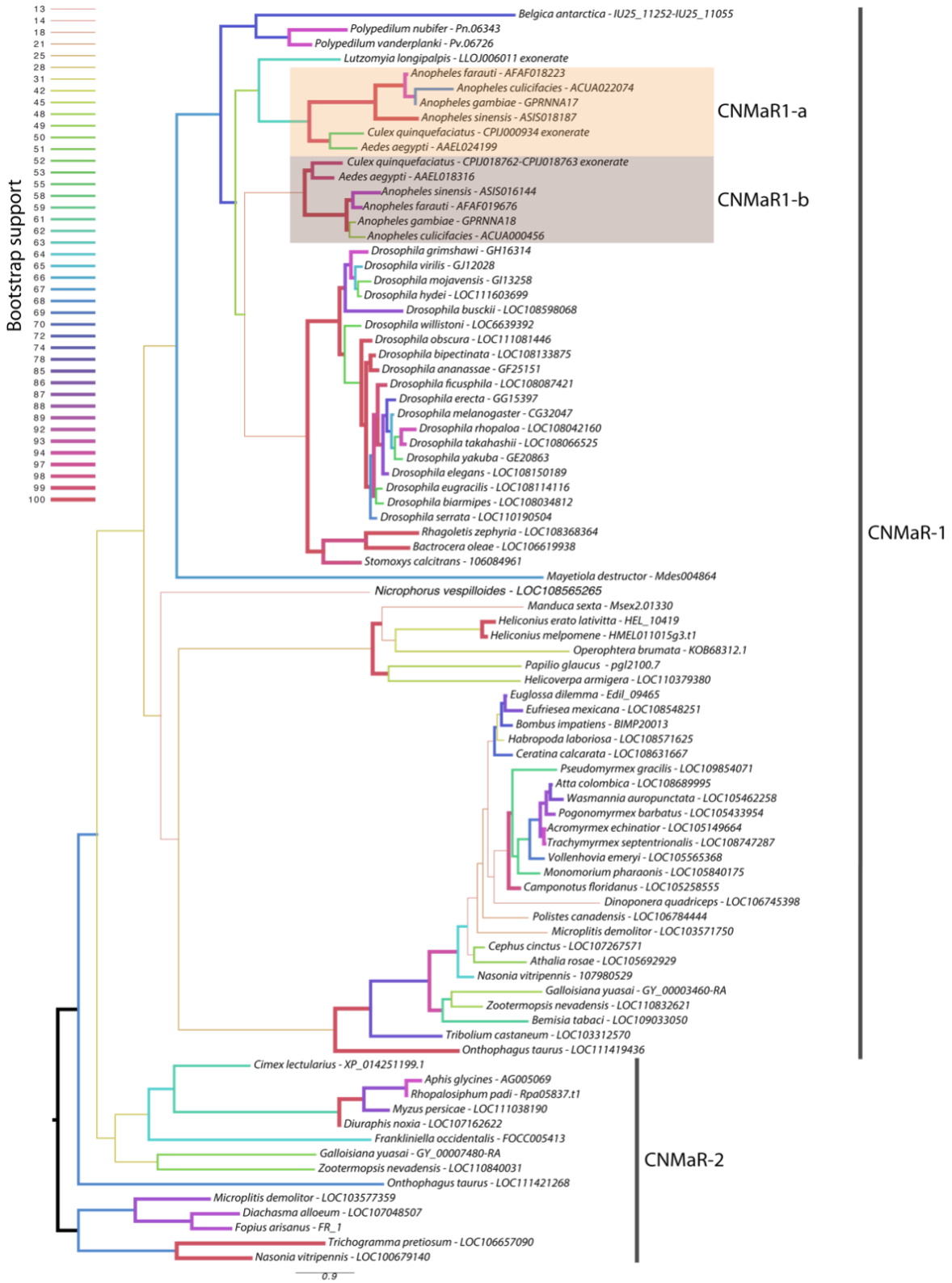

Figure 1: Maximum likelihood phylogenetic tree of CNMaR genes. At least two duplications of CNMaR have occurred in insects. The first duplication of CNMaR occurred prior to the divergence of the holo and hemimetabolous insects as termites retain both CNMaR-1 and CNMaR-2 sequences. Sequences were aligned with MAFFT and phylogenetic tree constructed in RaXML with 100 bootstraps. Bootstrap support is listed at each node and is coded by branch color and weight as indicated by the legend. Sequence accession numbers are listed after each species name. Several sequences were obtained through alignment of coding sequences from closely-related sequences with complete 7 transmembrane domains to genomic regions encoding partial sequences. These are indicated by tips labeled "exonerate."

CNMa receptor binding

We next examined whether the two receptors bound CNMa in a similar manner. Heterologous functional analysis of the Ae. aegypti CNMaRs revealed a dose-dependent selective binding and downstream activation of luminescence signals by the AeCNMa ligand, with an EC50 value of 5.17 nM for AeCNMaR-1a (figure 2A) and 51.8 nM for AeCNMaR-1b (figure 2B). Both receptors were also responsive to the non-amidated AeCNM peptide, although the absence of the C-terminal amidation resulted in lower potency, with EC50 values of 46.29 nM for AeCNMaR-1a (figure 2A) and 125.3 nM for AeCNMaR-1b (figure 2B). AeCNMaR-1a demonstrated a 9-fold increase in sensitivity for the amidated peptide (figure 2A, C), whereas the AeCNMaR-1b receptor isoform displayed greater promiscuity for the two ligands, with only a 2.4-fold greater sensitivity for the amidated peptide (figure 2B, D). Neither of the receptors were responsive to several other Ae. aegypti peptides tested at 1 µM, which yielded luminescent responses similar to background levels when BSA media alone was applied (figure S1). Instead, only AeCNMa and AeCNM were able to elicit a significant response several orders of magnitude over BSA media background luminescent response (figure S1).

To further verify that luminescence was specifically a result of AeCNM receptor binding and activation upon peptide application, cells were also transfected with pcDNA3.1+ encoding mCherry. No luminescence was detected in CHO K1 aeq mCherry-expressing cells in response to 1µM AeCNMa or AeCNM (figure S1) confirming that the AeCNMa or AeCNM-induced luminescent response requires the expression of either of the two AeCNMa receptors.

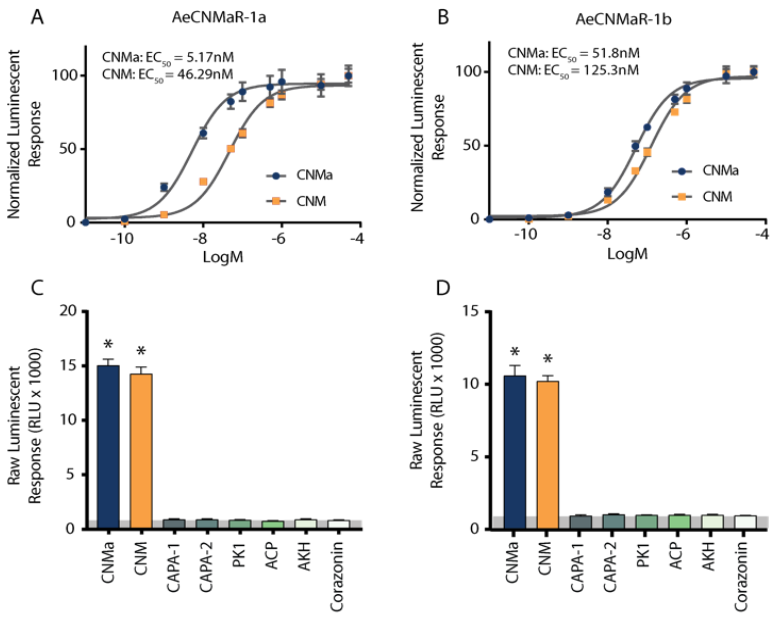

Figure 2: Luminescent response of CHO-K1 aeq cells expressing the *Ae. aegypti* CNMa receptors, AeCNMaR-1a (A, C) and AeCNMaR-1b (B, D). Transient expression of receptors in cells was used to examine functional activation by amidated and non-amidated CNM peptides. Both ligands were able to activate both receptors, with the AeCNMaR-1a receptor displaying higher sensitivity. Luminescence at every dose examined was normalized to the responses obtained following 50µM AeCNMa application (A). Raw luminescent responses were also examined following treatment with various Ae. aegypti peptides tested at 1µM (C, D). Only AeCNMa and AeCNM peptides were able to elicit a response significantly different from background control (BSA media alone in grey shaded area), denoted by an asterisk, as determined by a one-way ANOVA and Dunnett's multiple comparison post-hoc test.

CNMa peptide and receptor expression

We examined expression of AeCNMa, AeCNMaR-1a, and AeCNMaR-1b across life stages and in female tissues taken at various times post blood meal (PBM). Expression of AeCNMaR-1a was never detected in any juvenile-stage or female samples. AeCNMa and AeCNMaR-1b were expressed at varying levels across tissues and development. We found elevated AeCNMa expression at 2-4 h PBM in heads ($F_{9,32} = 3.36$, $p = 0.0052$, ANOVA) and in pelts beginning at 2 h PBM, peaking at 12 h PBM, and returning to low levels by 48 h PBM (figure 3A, $F_{9,36} = 5.19$, $p = 0.0002$, ANOVA). AeCNMaR-1b copy number was highest in the tissues of non-blood fed (NBF) females ($F_{38,119} = 4.28$, $p < 0.0001$, ANOVA, $p < 0.05$, Tukey's HSD) and typically decreased within a few hours after blood feeding and later was more variable or increased in heads, ovaries, and pelts but not guts. We also examined expression of

AeCNMa and AeCMaR-1b in larvae and pupae, finding that both transcripts were at low levels in all juvenile life stages relative to adult expression (figure S2).

We expanded our expression analysis to include males, as previous transcriptomic datasets suggested that AeCNMaR-1a was expressed in male antennae (McBride et al. 2014; Tallon et al. 2019). We confirmed that AeCNMaR-1a is expressed in male antennae and was not detected in other tissues examined (figure 3B). We found that AeCNMa was highly and specifically expressed in male accessory glands, but AeCNMaR-1b was not (figure 4A). We next asked whether expression of AeCNMaR-1b or AeCNMa was influenced by the mating status of females. We found that mated females had a significantly higher abundance of AeCNMa and AeCNMaR-1b than un-mated females (figure 4B, $p = 0.0079$ and $p = 0.009$, Wilcoxon rank-sum test). We attempted to silence expression of AeCNMaR-1a through injection of dsRNA into the thorax of female mosquitoes. While this approach has successfully silenced expression of other peptide hormone receptors in *Ae. aegypti* (Vogel et al. 2015), we were unable to reduce expression of the AeCNMaR-1b or CNMa transcript through traditional RNAi (data not shown).

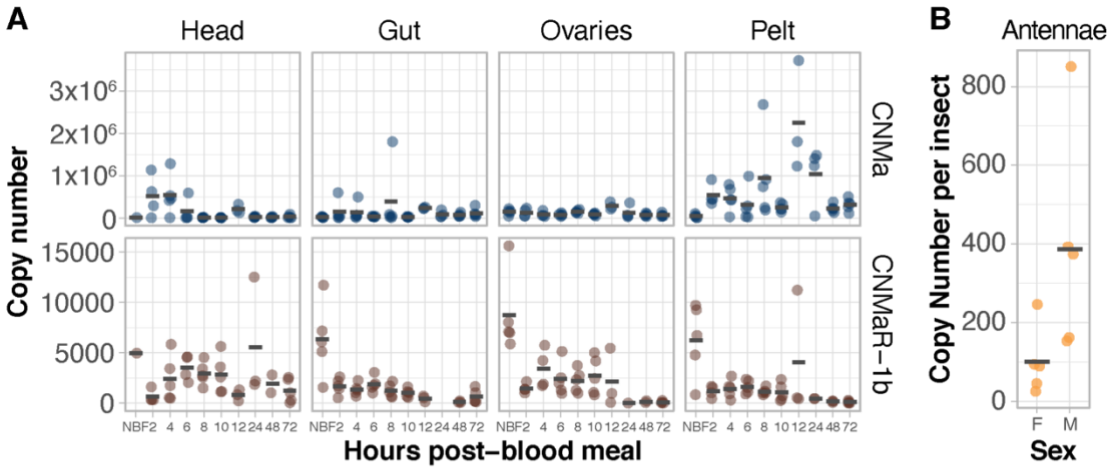

Figure 3: Expression patterns of AeCNMa receptors and peptide. (A) *AeCNMaR-1b* (red), and *AeCNMa* (blue) expression in tissues dissected from adult females at various times post-blood meal. Expression of *AeCNMaR-1b* was highest in ovaries prior to a blood meal (NBF), decreasing steadily until 12h PBM. Expression of the receptor was also high in other tissues prior to a blood meal, and there was moderate expression in female heads 4-10 h PBM. *AeCNMa* was most highly expressed in female pelts 2-24 h post blood meal, peaking at 12h PBM, with secondary expression in the head at 2-4 h PBM. (B) *AeCNMaR-1a* expression was only detected in male antennae. For all plots, points represent individual expression values and bars represent mean.

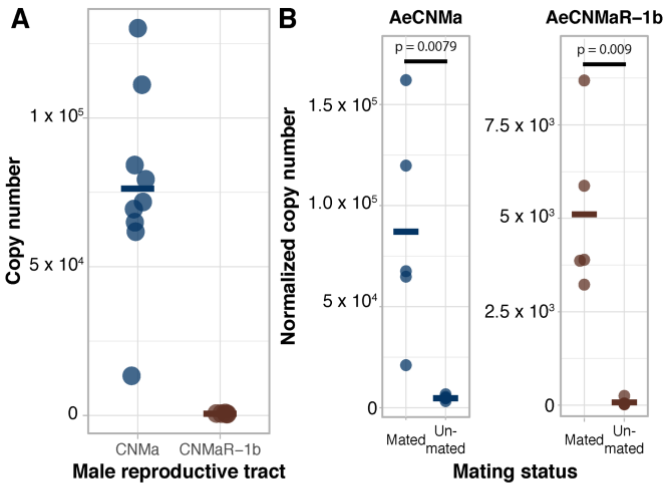

Figure 4: Ligand and receptor expression in male reproductive tissues and induction of *AeCNMa* and *AeCNMaR-1b* in females by mating. (A) *AeCNMa* was expressed at high levels in males reproductive tracts (testes and accessory glands), while expression of the receptor *AeCNMaR-1b* was negligible. (B) Mating of virgin females induced expression of *AeCNMa* (p = 0.0079, Wilcoxon signed-rank test) and *AeCNMaR-1b* (p = 0.009, Wilcoxon signed-rank test).

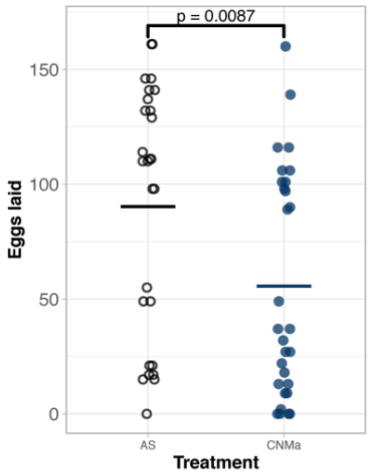

Figure 5: AeCNMa reduces egg clutch size in mated *Ae. aegypti* females. Age-matched females were blood fed on an artificial membrane feeding apparatus and immediately injected with CNMa or *Aedes* saline (AS). After three days females were allowed to oviposit and eggs were counted 48h later. Points represent individuals and bar represents mean. Females injected with AeCNMa produced significantly fewer eggs than controls (p = 0.0087, Wilcoxon rank-sum test).

Effects of AeCNMa injection on *Ae. aegypti* reproduction

Our expression analysis revealed a peak of AeCNMaR-1b in ovarian tissue in non-blood females, followed by a steep decrease in expression following a blood meal. We therefore reasoned that CNMa may regulate some aspect of blood meal digestion or reproduction. To investigate this, we injected mated, blood fed females with 150 pmol of AeCNMa (the optimal dose based on dose-response assay) immediately PBM (figure 5). Mated females injected with AeCNMa laid significantly fewer eggs than controls.

Presence of CNMa in male accessory glands

The reduced oviposition by mated blood fed females injected with AeCNMa, along with the high level of AeCNMa transcript abundance in the male reproductive tract and in mated females suggested AeCNMa may be a negative signal for oviposition during early vitellogenesis. We extracted male accessory glands for HPLC separation. Fractions eluting at the same time as

the AeCNMa and AeCNM standards were subjected to mass spectroscopy. Neither peptide was detected in fractions from the extracts, suggesting that males do not transfer AeCNMa to females during copulation.

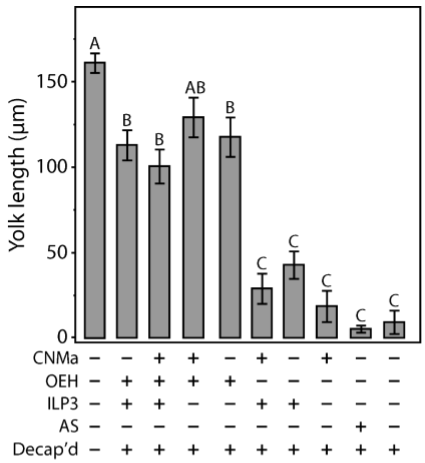

Fig. 6. Injection of CNMa along with ILP3 or OEH does not have a significant effect on yolk uptake in decapitated females. Average amount of yolk per oocyte in mated, blood fed, decapitated females injected with combinations of CNMa (150pmol), ILP3 (20pmol), and OEH (20pmol), Aedes saline (AS), or not injected (intact or decapitation only) at one-hour post blood meal. Error bars show one standard error above and below the mean. Yolk uptake in the CNMa only treatment was not significantly different from decapitated only and AS control treatments. There was no significant difference in yolk uptake in CNMa + OEH + ILP3 injected females compared to ILP3 + OEH injected females. Decapitated females injected with OEH + CNMa demonstrated no significant difference in yolk uptake relative to OEH only or OEH + ILP3 treatments. There was no significant difference in yolk uptake among ILP3 and OEH, ILP3 only, and CNMa and ILP3 treatments. Bars not connected by the same letter are statistically significantly different, $p < 0.05$, Tukey's HSD.

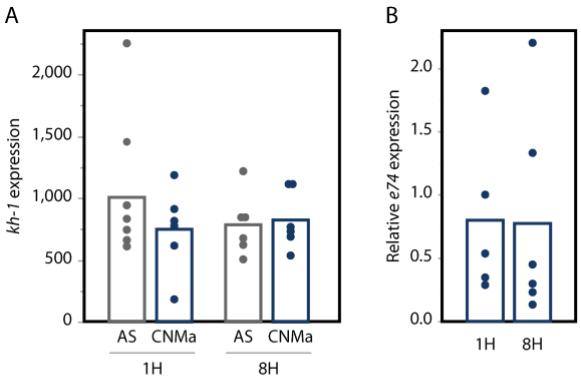

Figure 7: CNMa does not influence expression of A) the JH-responsive gene *kh-1* or B) the 20-hydroxyecdysone gene *e74*. qPCR was performed for *kh-1* as described in the methods. For *e74*, expression is relative to *e74* expression in AS-treated insects. Treatment of insects with CNMa did not significantly impact expression regardless of time administered or gene tested (MANOVA *e74*: $F_{3,19} = 0.8192$, $p = 0.50$; *kh-1*: $F_{1,20} = 0.5141$, $p = 0.68$).

Interaction of CNMa and other reproductive hormones

Given that AeCNMa suppressed egg production by mated female mosquitoes, we next investigated whether the influence of AeCNMa on *Ae. aegypti* egg production was related to interactions with AeOEH or AeILP3 (Vogel et al. 2015; Wu and Brown 2006; Dhara et al. 2013). Decapitation shortly after a blood meal blocks endogenous OEH and ILP3 release from the brain, and injection of AeOEH or AeILP3 restores egg development. We found that AeCNMa did not affect yolk deposition elicited by OEH, ILP3, or both peptides together (figure

6). These results, along with the early window of CNMa action in mated females, suggested that the role of the peptide is independent of OEH and ILP3.

We also tested whether injection of AeCNMa peptide into females resulted in changes in transcript abundance of the JH-responsive gene kruppel-homolog 1 (kh-1) or the ecdysteroid-responsive gene e74. We found no significant difference in their expression between female mosquitoes injected with AeCNMa or saline (figure 7).

3.6 Discussion

The receptor of CNMa has repeatedly duplicated in insects, being differentially lost among lineages. Dipterans retain CNMaR-1, which duplicated prior to the divergence of the Culicomorpha. The retention of both copies of the CNMaR-1 receptors in most mosquito lineages suggests that both genes encode functional proteins that are either redundant or have diverged in their functions. Expression patterns of the two receptors in *Ae. aegypti* differ markedly. AeCNMaR-1a expression was only detected in male antennae, with transcripts never detected in other tissues or timepoints. In contrast, AeCNMaR-1b expression was found primarily in ovary tissues prior to a blood meal, though lower levels of expression were detected in other tissues and life stages.

The gene encoding the peptide does not seem to have been duplicated, with only a single gene encoding a CNMa peptide in *Ae. aegypti* (AAEL010529) and the available *Anopheles* genomes (Neafsey et al. 2015). The *Ae. albopictus* Foshan genome sequence (Palatini et al. 2020) does encode two genes which yield identical CNMa peptides (AALF020855, AALF023040), though given the near identity of the mRNA sequences, their location on different scaffolds, and the incomplete nature of the *Ae. albopictus* genome sequence, it is

possible that the two sequences are an artifact of genome mis-assembly. AeCNMa expression in *Ae. aegypti* females was detected primarily in abdomen pelts, which include the ventral ganglia, and, to a lesser degree, in heads with brains. Neurons or neurosecretory cells in these ganglia are likely sources of CNMa as in *D. melanogaster*, where DmCNMa was localized to tens of cells in the CNS (Jung et al. 2014) and in the gut in response to amino acid starvation (Kim et al. 2021).

Both AeCNMa receptors exhibited specific activation by the AeCNMa peptide, further supporting the hypothesis that both genes encode functional receptors. Surprisingly, AeCNMaR-1a had higher affinity for AeCNMa than AeCNMaR-1b by approximately an order of magnitude, despite the broader transcript distribution and higher abundance of AeCNMaR-1b. Although AeCNMaR-1a had higher affinity for AeCNMa, the EC50 of AeCNMaR-1b was still within physiological range (~50 nM). While AeCNMa induced stronger activation of both receptors than AeCNM, the non-amidated peptide still stimulated both receptors, though the EC50 was 1/10th and 1/5th lower than the amidated form for AeCNMaR-1a and 1b, respectively. Other studies illustrated that activation of the *D. melanogaster* and *Apis mellifera* CNMaRs with D. melanogaster CNMa peptide was comparable to AeCNMaR-1a, while the *Bombyx mori* receptor EC50 was far higher (>1000 nM) than that of either *Aedes* receptor. Differences in AeCNMa binding affinity and in the expression patterns of the two receptors suggest that the peptide and receptors may have distinct functions in male and female mosquitoes. Future studies will examine the role of this peptidergic system in male-specific behaviors.

Given the tissue-specific distribution and timing of AeCNMaR-1b and AeCNMa expression, we suspected that AeCNMa and AeCNMaR-1b played a role in mosquito reproduction. We found that mating induced expression of AeCNMa in female mosquitoes, and so we focused our experiments on determining the role of the peptide in reproduction in female

mosquitoes. By injecting AeCNMa into female mosquitoes, we found that the peptide reduces the number of eggs laid by mated, blood fed females. This effect was independent of the well-characterized effects of other hormones, specifically OEH, ILP3 and 20-hydroxyecdysone (Vogel et al. 2015; Dhara et al. 2013; Roy et al. 2007; Sieglaff et al. 2005). The effects of AeCNMa injection into female mosquitoes suggest that this peptide may play a role in signaling mating status. We examined whether AeCNMa is transferred from males to females during mating but did not detect the peptide in male accessory gland extracts.

CNMa has been shown to affect nutrient sensing in adult *D. melanogaster*. Low levels of amino acids in the gut stimulate DmCNMa expression via target of rapamycin kinase (TOR) signaling. Specific microbes in the gut appear to regulate free amino acid levels, which then stimulate TOR signaling and ultimately CNMa production. The *D. melanogaster* CNMa receptor is predominantly found in the CNS, where binding of CNMa drives preference for diets rich in essential amino acids (Kim et al. 2021). TOR signaling is also critical in the coordination of blood meal digestion and reproduction in *Ae. aegypti* (Roy and Raikhel 2012), and future studies will examine whether nutrient signaling through TOR are important for the action of CNMa.

2.7 Acknowledgments and Funding The authors would like to thank Jena Johnson, Lilith South, Logan Harrell, and Severen Brown for their assistance in mosquito colony maintenance. This work was funded through the support of the National Institutes for Allergy and Infectious Diseases of the National Institutes of Health to KJV (Award #K22AI127849), a Natural Sciences and Engineering Research Council of CanadaDiscovery Grant to J-PP (NSERC #RGPIN-2020-06130), and NSERC Canada Graduate Scholarship to AL.

Table 2.S1. Primers used in this study.

Table S1: Primers used in this study

Target gene	Vectorbase accession	Purpose	Forward primer	Reverse primer
AeCNMa	AAEL010529	qPCR	CTTTTGCAAATTGTGGGAAAC	AAAGTTTTGACAGGGTTCTCT
		RNAi	TAATACGACTCACTATAGGGAGATGATTACACATTGGAGCTGC	TAATACGACTCACTATAGGGAGAAGTTCCAGAAGCTCAAGTAC
AeCNMaR-1a	AAEL024199	qPCR	TATTACACTCCAGCACTGGTC	GCCAGGTAATAAGATGAGGAT
		RNAi	TAATACGACTCACTATAGGGAGAAGTTGGACTTACCTTTCTTGG	TAATACGACTCACTATAGGGAGACTTCCCGTACATCACAGATAG
AeCNMaR-1b	AAEL018316	qPCR	GCCATGAATGAAACCATCTG	GTAAATGGAACCACGAACAC
		RNAi	TAATACGACTCACTATAGGGAGAGTAGTTACGACATCGATCAGC	TAATACGACTCACTATAGGGAGAGCTGATAAACACTCCAATCAG

Underlined sequences denote gene-specific portion of dsRNA synthesis primers

Figure 2.S1

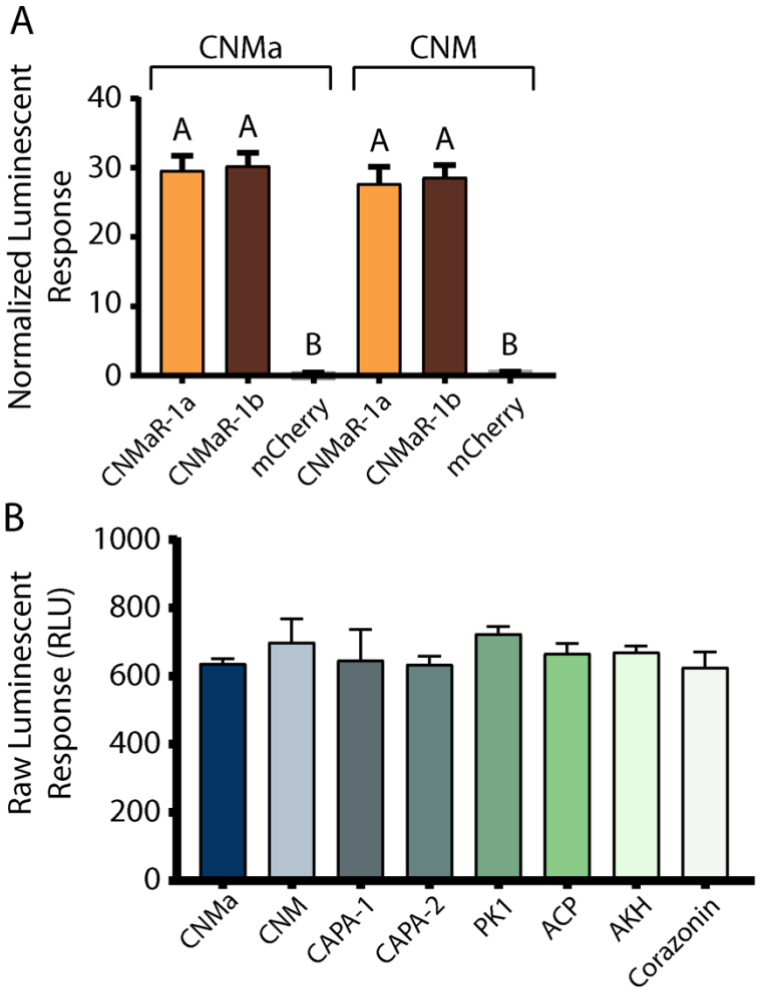

Figure S1. Validation of CNM receptor activation. CHO-K1 aeq cells transfected with only the AedaeCNMaR-1a or AedaeCNMaR-1b receptor are activated in response to 50μM of the amidated or non-amidated peptide when normalized to the ATP response (A), whereas mCherry-transfected cells (B) yield no response to any peptides tested at 1μM compared to background luminescence (BSA media alone denoted in grey shaded area). Statistical tests included a one-way ANOVA with either Tukey's (A) or Dunnett's (B) multiple comparison post-hoc test.

Figure 2.S2

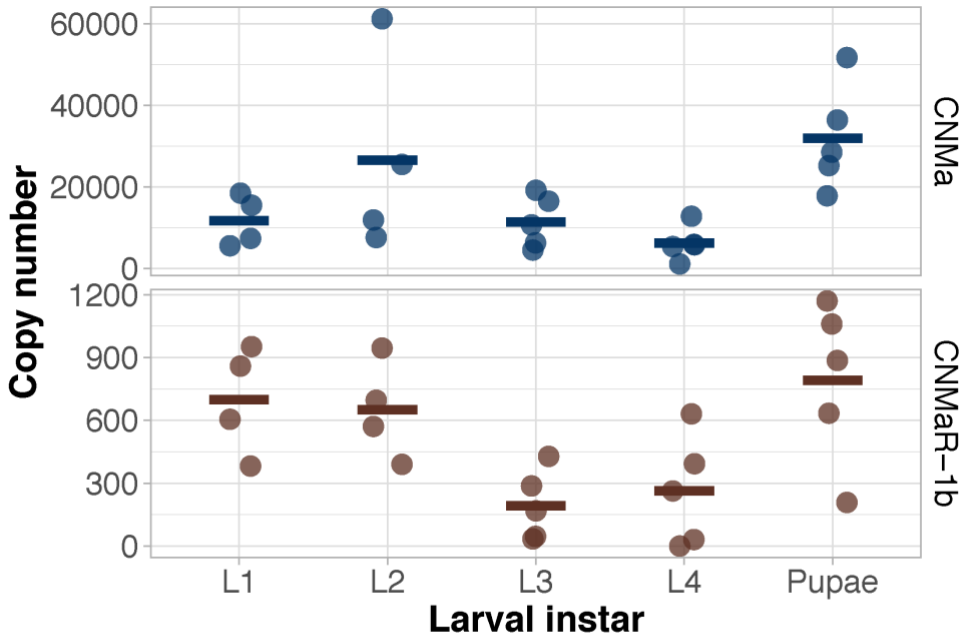

Figure S2: *AeCNMaR-1b* and *AeCNMa* expression in *Ae. aegypti* larvae and pupae. The receptor was expressed at low levels in early instars and pupae, while *AeCNMa* was expressed at levels lower than adults but in all stages tested.

Figure 2.S3

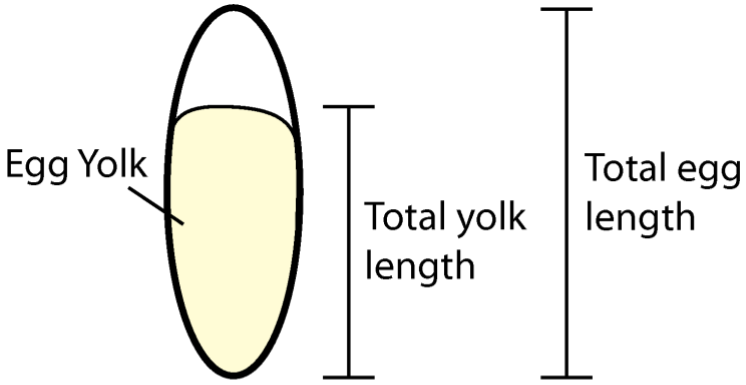

Figure S3: Yolk length is measured as the length, in μm, from the egg pole to the end of visible yolk deposition in the egg. As more yolk is deposited, the length of the region containing yolk increases.

CHAPTER 3

RNAI-MEDIATED KNOCKDOWN OF TWO ORPHAN G PROTEIN-COUPLED RECEPTORS REDUCES FECUNDITY IN THE YELLOW FEVER MOSQUITO *AEDES AEGYPTI* [2]

[2]Keyes-Scott NI, Swade KR, Allen LR, Vogel KJ. 2023. *Frontiers Insect Sci*. 3.

3.1 Abstract

G protein-coupled receptors (GPCRs) control numerous physiological processes in insects, including reproduction. While many GPCRs have known ligands, orphan GPCRs do not have identified ligands in which they bind. Advances in genomic sequencing and phylogenetics provide the ability to compare orphan receptor protein sequences to sequences of characterized GPCRs, and thus gain a better understanding of the potential functions of orphan GPCRs. Our study sought to investigate the functions of two orphan GPCRs, AAEL003647 and AAEL019988, in the yellow fever mosquito, *Aedes aegypti*. From our phylogenetic investigation, we found that AAEL003647 is orthologous to the SIFamide-2/SMYamide receptor. We also found that AAEL019988 is orthologous to the Trapped in endoderm (Tre1) receptor of *Drosophila melanogaster*. Next, we conducted a tissue-specific expression analysis and found that both receptors had highest expression in the ovaries, suggesting they may be important for reproduction. We then used RNA interference (RNAi) to knock down both genes and found a significant reduction in the number of eggs laid per individual female mosquito, suggesting both receptors are important for *Ae. aegypti* reproduction.

Keywords: Insect physiology, GPCR, reproduction, insect endocrinology

3.2 Introduction

Mosquitoes are a persistent threat to global health due to their ability to transmit pathogens among vertebrate hosts through blood feeding, which is required for many mosquito species to produce eggs. The events beginning with blood meal digestion and ultimately leading to egg production are coordinated by several reproductive hormones, including insulin-like peptide 3 (ILP3) and ovary ecdysteroidogenic hormone (OEH), which are released shortly after a blood meal is consumed (Brown et al. 2008; Dhara et al. 2013; Vogel et al. 2015). Release of

ILP3 from brain neurosecretory cells stimulates blood meal digestion, and ILP3 and OEH both stimulate secretion of 20-hydroxyecdysone (20E) from the ovaries (Brown et al. 2008; Dhara et al. 2013; Vogel et al. 2015; Roy et al. 2007). After 20E is released into the hemolymph, expression of yolk protein precursors (YPP) in the fat body is induced, initiating the production of yolk proteins, including vitellogenin, which are subsequently transported to the ovaries and packaged into oocytes resulting in egg formation (Hansen et al. 2014; Matsumoto et al. 1989).

Hormone signaling pathways have been exploited to control insect populations. Insect chemical growth regulators (IGRs), such as 20E antagonists, target insect hormonal pathways and have been utilized to control insect disease vectors (Siddal 1976; Ekoka et al. 2021). IGRs are attractive control measures due to their selective toxicity against insects and decreased rate of insecticide resistance developed against them relative to traditional pesticides (Hafez and Abbas 2021; Santos et al. 2020). IGR targets such as, JH and 20E and their receptors, are widely conserved in insects increasing the chances of negative effects on non-target species (Siddall 1976; Ekoka et al. 2021; El-Sheikh et al. 2016; Mulla 1995; Subramanian and Shankarganesh 2016). An attractive alternative to IGRs that act on JH or 20E are compounds that selectively target hormones or hormone receptors that are not widely conserved across all insect groups. G protein-coupled receptors (GPCRs) and their ligands may present taxa-specific targets, as insect genomes often encode unique GPCRs, including many that bind peptide hormones that regulate important aspects of insect physiology (Meyer et al. 2012; Hill et al. 2013; Audsley and Down 2015).

Hormone-binding GPCRs are essential in modulating insect physiology, including in metabolism (Kohyama-Koganeya et al. 2008; Alves-Bezzera et al. 2016), reproduction (Keyes-Scott et al. 2022), behavior (Petruccelli et al. 2020), immunity (Thuma et al. 2018), and

embryonic development (Benton et al. 2019), as they transduce systemic hormonal signals into target cells. In addition to modulating a diverse number of functions in insects, GPCRs are the largest class of receptor and bind a variety of ligands, including neurotransmitters (Kastner et al. 2014) and peptide hormones (Bainton et al. 2005; Wu et al. 2020). Peptide hormones govern many physiological functions in insects including feeding (Bloom et al. 2019; Aguilar et al. 2004; Martelli et al. 2017; Ayub et al. 2020), mating behavior (Terhzaz et al. 2007), development (Yamanaka et al. 2011; Sterkel et al. 2012; Wulff et al. 2017), metabolism (Brown et al. 2008; Alves-Bezerra et al. 2016; Zandawala et al. 2015; Nässel and Broeck 2016; Defferrari et al. 2016), immunity (Kin et al. 2014), diuresis (Te Brugge et al. 2011; Cannell et al. 2016; Capriotti et al. 2019), and reproduction (Brown et al. 2008; Keyes-Scott et al. 2022; Silva-Oliveira et al. 2021). While the ligands of many GPCRs have been identified, even well-studied organisms still encode GPCRs whose ligands are unknown.

Comparative genomics and phylogenetic analyses are useful tools in the identification of ligands of former orphan receptors (Vogel et al. 2015; Keyes-Scott et al. 2022). Phylogenetic placement of orphan receptors, such as in the case of the OEH receptor of *Aedes aegypti* mosquitoes, can provide insights into potential ligands. A Venus flytrap domain-containing receptor tyrosine kinase was found to be closely related to the mosquito insulin receptor, and also displayed the same species distribution pattern as neuroparsin peptide hormones including OEH. Subsequent biochemical and molecular studies determined that the gene in question was an OEH receptor (Vogel et al. 2015). Tissue-specific expression patterns are also useful in determining the functional roles and ligands of hormone receptors. We identified that the neuropeptide CNMa and its receptor, CNMaR, which were first identified in *Drosophila melanogaster*, were specifically expressed in *Ae. aegypti* ovaries and hypothesized that it was likely important for

reproduction (Vogel et al. 2015; Keyes-Scott et al. 2022; Vogel et al. 2013). In Culicidae, the CNMa receptor underwent gene duplication, resulting in two receptors, CNMaR-1a and CNMaR-1b, which both actively bind CNMa in vitro (Keyes-Scott et al. 2022). In *Ae. aegypti*, CNMa and CNMaR-1b are highly expressed in female ovaries and modulate the production of eggs (Keyes-Scott et al. 2022; Akbari et al. 2013).

We chose to examine two orphan GPCRs of *Aedes aegypti*, AAEL003647 and AAEL019988. These orphan GPCRs were chosen for further investigation based on their expression in female reproductive tissues following a blood meal (Akbari et al. 2013), suggesting a potential role in the modulation of reproductive physiology. We built phylogenetic trees to identify closely related receptors and provide insight into possible functions of the receptors. To understand the tissue tropism and temporal distribution of AAEL003647 and AAEL019988, we conducted a detailed expression analysis of both GPCRs in juvenile and adult mosquitoes. Using RNAi, we then investigated the functional consequences of silencing the GPCRs on fecundity. These results shed new light on the role of these orphan GPCRs on the reproductive physiology of *Ae. aegypti* mosquitoes.

3.3 Materials and Methods

Mosquitoes

UGAL strain *Aedes aegypti* were used for all experiments. Mosquito colonies were maintained at 27°C on a 16:8h L:D cycle. Larvae were fed Cichlid Gold fish pellets (Hikari, USA, Hayward, CA), and adult mosquitoes were fed an 8% sucrose solution until 2 days post-emergence. Adult females were fed defibrinated rabbit blood (Hemostat Laboratories, Dixon, CA, USA) by an artificial feeding apparatus warmed to 37°C.

Phylogenetic analysis

Putative AAEL003647 and AAEL019988 orthologs were identified using OrthoDB (Kuznetsov et al. 2023). Taxa were chosen to represent all possible insect orders with available genome sequences (tables S1 and S2). Protein sequences were aligned using hmmalign as implemented in HMMER (Eddy 2011) with the –trim option. Gaps in alignments were manually removed, and trimmed alignments were used to construct maximum likelihood phylogenies using PhyML (Guindon et al. 2010) using the options "-d aa -m LG -f e -o tl -b -2". FigTree version 1.4.4 was used for visualization of trees and trees were rooted on the midpoint. Accessions of included sequences are given in file S1.

Expression profiles

Eight to ten-day old, non-blood fed mated females were collected and dissected into head, gut, fat body, abdominal carcass ("pelt"), and clean ovaries without bursa or accessory glands in sterile, nuclease-free, *Aedes* saline. Additional ovary samples were collected from females at 2-hour intervals post-feeding (pbf) until 12 hours, then at 24, 48, and 72 hours pbf. Four or more tissue samples were collected for each tissue and time point. After collection, tissue samples were stored at -80°C prior to RNA extraction. Tissue samples were thawed on ice and homogenized with a rotor pestle. Total RNA was isolated from homogenized tissues using the RNeasy Mini kit (Qiagen, Venlo, The Netherlands) according to manufacturer instructions. DNA was removed from each RNA sample using the Turbo DNA-free kit (Ambion, Austin, TX, USA). One hundred nanograms of RNA was used as input to synthesize cDNA using the iScript cDNA synthesis kit (BioRad, Hercules, CA, USA). cDNA templates were used for quantitative

real-time PCR, with the Quantifast SYBR Green PCR kit (Qiagen) and gene specific primers (table S3). Standard curves for each gene were generated by cloning qPCR products into the pSCA vector with the Strataclone PCR cloning kit (Agilent, Santa Clara, CA, USA), isolating plasmid DNA using the GeneJET Plasmid Miniprep Kit (Thermo Scientific, Vilnius, Lithuania), and preparing plasmid standards to a known copy number. Expression levels of ribosomal protein S7 were used as a housekeeping gene to normalize transcript abundance.

RNAi knockdown of receptors and bioassays

A 400-500 bp region of each gene was chosen as a target for dsRNA synthesis for AAEL003647 and AAEL019988, subsequently referred to as *ds3647* and *ds19988*, respectively. Primers including the T7 promoter sequence were used to amplify each target using cDNA synthesized from RNA isolated from whole body, non-blood fed females (table S3). PCR products were cloned into the pSCA vector and plasmid DNA was extracted using methods listed above. Plasmid DNA from each target and an EGPF control were used as the templates for dsRNA synthesis. dsRNA was synthesized using the MEGAscript RNAi kit (Ambion, Vilnius, Lithuania), according to manufacturer instructions. Following dsRNA synthesis, dsRNA was precipitated in ethanol and resuspended in *Aedes* saline to a concentration of 2μg/μL.

Newly emerged (≤ 1d post eclosion) mated females were injected with 2 μg *ds3647*, *ds19988*, or *dsEGFP*. To validate receptor knockdown, whole body females were collected 7 days post-injection. qPCR was used to validate knockdown of each gene using the methods detailed above. Females were blood fed three days post-injection and separated into individual egg laying chambers consisting of a damp paper towel in a plastic cup with a lid and a dental wick with 8% sucrose solution, for yolk deposition and fecundity bioassays. For yolk deposition

bioassays, females were collected at 24, 48, and 72 hours PBF. Ovaries were dissected and yolk deposition per oocyte was measured along the anterior-posterior axis using an ocular micrometer. Five oocytes were measured and averaged per female, and 5 females were used per time point and treatment. Egg laying was measured by providing females with a wet paper towel at 72 h post blood feeding to stimulate egg deposition. Females were given 48 h to deposit eggs. After 48 h hours, the number of eggs laid per individual female was counted. Another cohort of knockdown females were allowed to lay eggs then dissected and the number of retained, mature oocytes were counted. Eggs that were laid were separated by parent and allowed to hatch, and the proportion of hatched versus unhatched eggs was recorded for each treatment.

3.4 Results

Phylogenetic comparison of AAEL003647 and AAEL019988

Our phylogenetic analysis included diverse insect species to identify the closest receptor relatives across both holometabolous and hemimetabolous insects. Our results for AAEL003647 indicate this receptor groups in a strongly supported clade of receptors that are distinct from, but sister to, the SIFamide receptors (figure 3.1). These receptors are found in the genomes of culicids as well as cockroaches (*Periplaneta americana* and *Blattella germanica*), termites (*Zootermopsis nevadensis*). This robustly supported sister clade to SIFamide receptors suggest an ancient split between SIFamide receptors and the orthologs of AAEL003647 which predates the split of hemi- and holometabolous insects. Orthologs of AAEL003647 appear to have been lost in many lineages. No orthologs were found in lepidopteran, coleopteran or hymenopteran genomes. In contrast, most sequenced hemipteran genomes contained orthologs, several of which have subsequently duplicated. In the order Diptera, AAEL003647 orthologs were found in most nematoceran genomes, but absent from many available brachyceran genomes, including

sequences from all members of the genus *Drosophila.* This loss was not complete in Brachycera, as *Rhagoletis zephyria* and *Hermetia illucens* both encode AAEL003647 orthologs in their genomes.

Within the Culicidae, each species examined has a single ortholog of AAEL003647 with the notable exception of *Anopheles maculatus*, which has five orthologous sequences in OrthoDB (Kuznetsov et al. 2023). Two sequences were identified as orthologs of the SIFamide receptor (AMAM023590 and AMAM011260), and two orthologs identified as orthologs of AAEL003647 (AMAM023042 and AMAM009506). All of these sequences are lacking the complete 7 transmembrane region of canonical GPCRs and it seems likely that these sequences do not reflect true orthologs but rather annotation artefacts, potentially fragments of a single ortholog to the SIFamide receptor and AAEL003647. An additional duplication in *Anopheles maculatus* groups with the SIFamide-like receptor of *Thrips palmi*. Further investigation of this

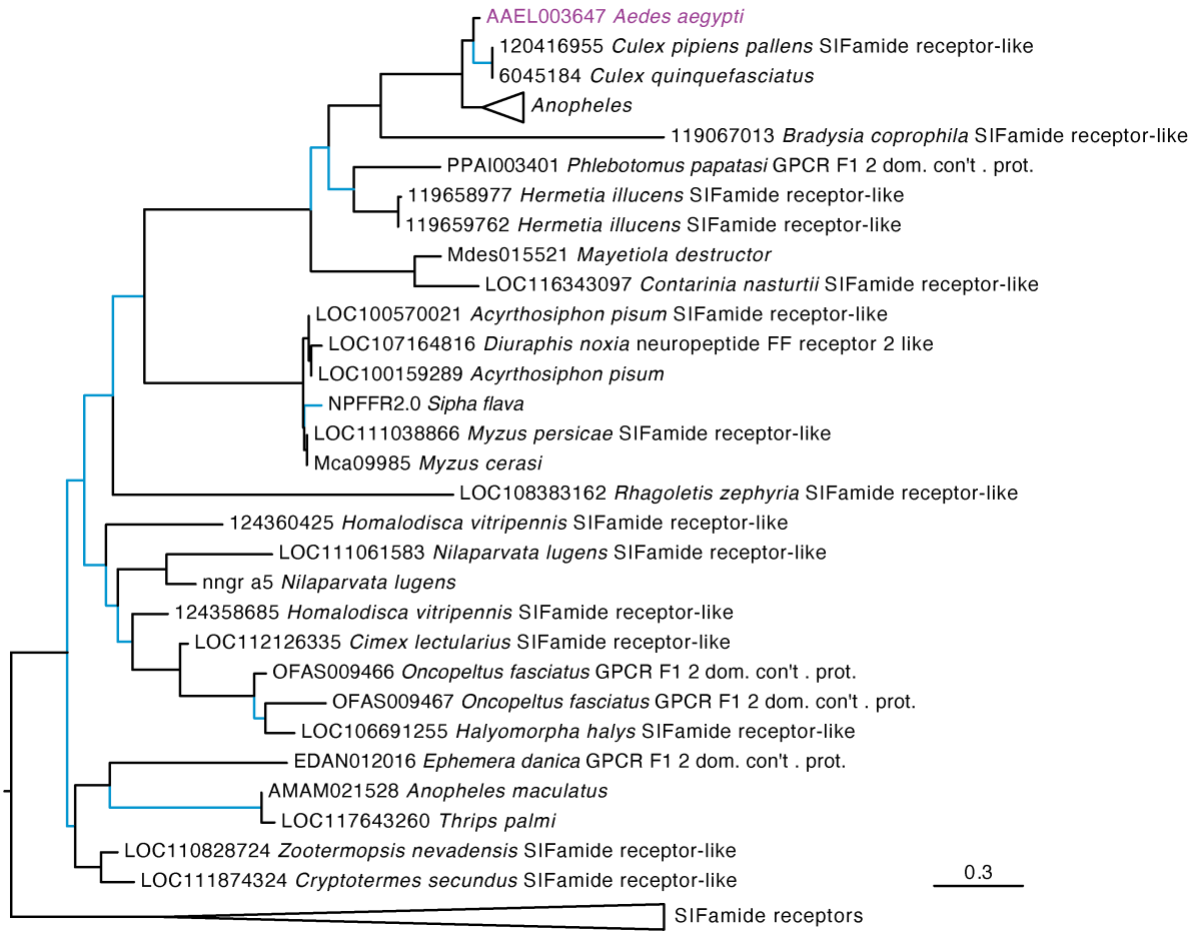

Figure 3.1: Maximum likelihood tree of AAEL003647 and its orthologs in other insects. Orthologs of AAEL003647 have been lost in many brachyceran taxa, including members of the genus *Drosophila*. AAEL003647 is most closely related to the SIFamide receptor. Sequences were downloaded from OrthoDB and aligned against a 7 transmembrane GPCR model (7tm-1.hmm) in hmmalign. Trees were built in PhyML. Support values are aLRT SH-like, and branches with support values < 0.95 are colored light blue. F1 2 domain containing protein is abbreviated as "F1 2 dom. con't. prot." Due to space constraints, orthologs of AAEL003647 in *Anopheles* species and SIFamide receptor sequences were collapsed. A full tree containing the *Anopheles* taxa is available in supplementary figure 3.S1.

Figure 3.2. Maximum likelihood tree of AAEL019988 and its orthologs in other insects. AAEL019988 is absent in most but not all hemimetabolous insects and is conserved in most holometabolous lineages. The tree was rooted at the midpoint which formed two major clades, the orthologs of Trapped in endoderm 1 (tre1) and the orthologs of moody and moody-like. Sequences were downloaded from OrthoDB and aligned against a 7 transmembrane GPCR model (7tm-1.hmm) in hmmalign. Trees were built in PhyML. F1 2 domain containing protein is abbreviated as "F1 2 dom. con't. prot." Support values are aLRT SH-like and branches with low support (< 0.95) are highlighted in blue. Due to space constraints, sequences from *Anopheles*, *Drosophila*, and *Apis* species, as well as Moody and Moody-like sequences, were collapsed. A full tree with the expanded AAEL019988 orthologs is shown in figure 3.S2.

ortholog suggests that it is unique to *An. maculatus*, and that its grouping with non-mosquito sequences is likely an artifact of the alignment. Improved sequencing of the *An. maculatus* genome will likely resolve this in the future.

Our analysis identified AAEL019988 as an ortholog of the *D. melanogaster* trapped in endoderm (tre1) GPCR with strong support (figure 3.2). Tre1 appears to be highly conserved among holometabolous insects but is absent from many hemimetabolous lineages. Only the orders Blattodea, Odonata, Thysanoptera, and Grylloblattidae encode orthologs. The sister group to this clade includes both the GPCRs Moody and Moody-like, which are known to be important to blood-brain barrier in *Drosophila melanogaster* (Hatan et al. 2011).

Tissue tropism of orphan receptors

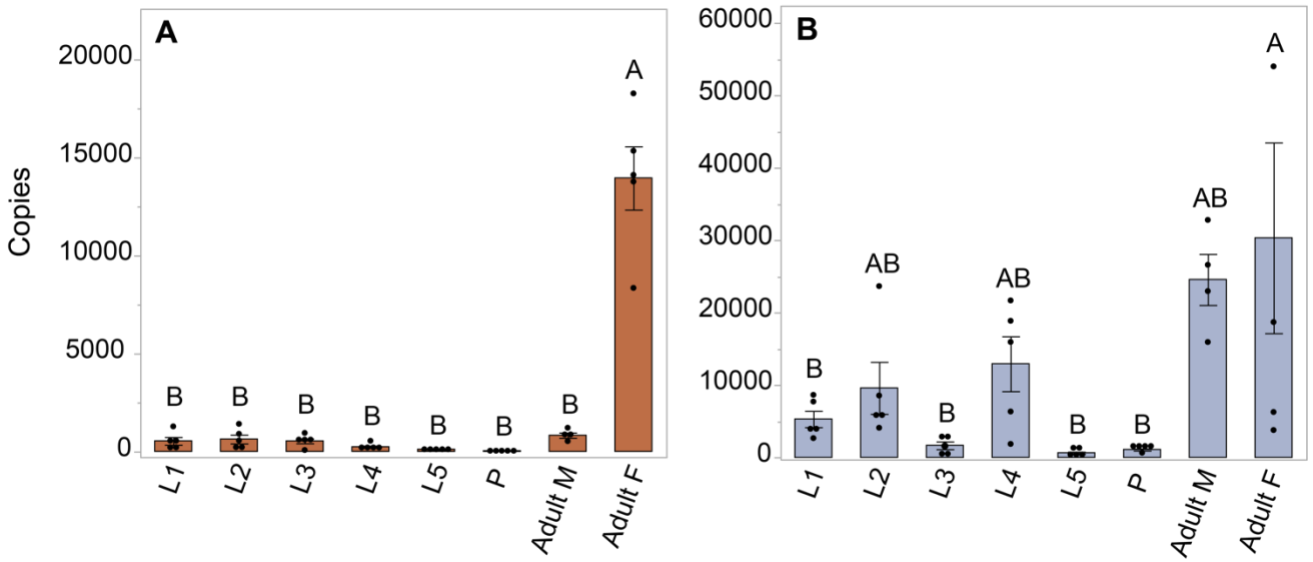

Figure 3.3. Expression profile of AAEL003647 and AAEL019988 in whole bodies of mosquitoes across life stages and sexes. The x-axis represents the number of copies of AAEL003647 and AAEL019988 per 100ng of RNA. **(A)** Expression of AAEL003647 is significantly higher in adult females (one-way ANOVA, $p < 0.0001$). **(B)** Expression of AAEL019988 was also significantly higher in adult females relative to 1st, 3rd, and 5th stage larvae and pupae (one-way ANOVA, $p < 0.05$). Treatments connected by the same letter are not significantly different ($p > 0.05$, one-way ANOVA).

We investigated expression patterns of *AAEL003647* and *AAEL019988* among life stages, sexes, and tissues. Expression of *AAEL003647* was highest in females relative to males and immature stages (one-way ANOVA, $p < 0.0001$) (figure 3.3A). Expression of *AAEL019988* was higher in adult females relative to 1st, 3rd, 5th instar larval, and pupal stage mosquitoes (one-way ANOVA, $p < 0.05$). There was no significant difference in expression between females and

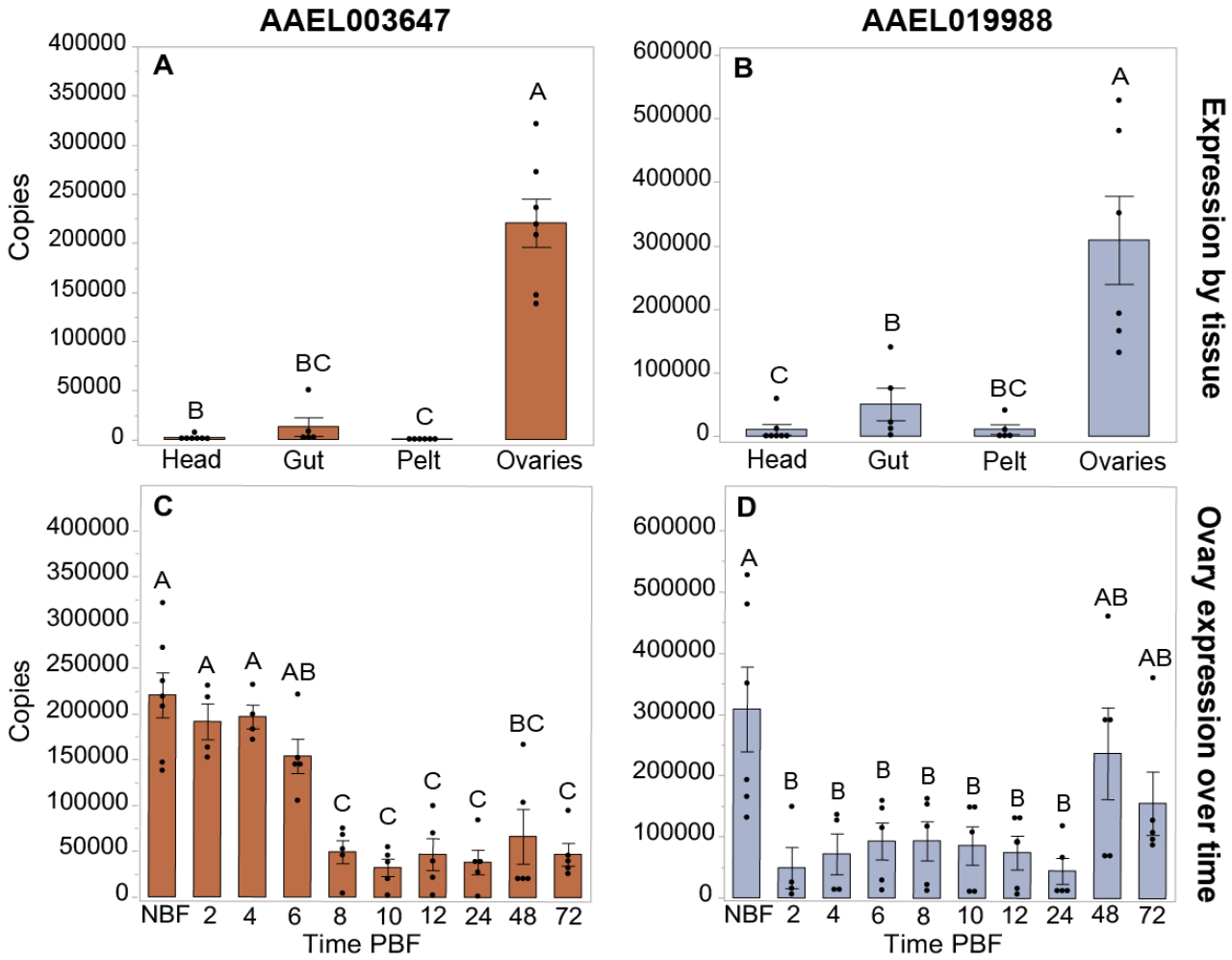

Figure 3.4. Expression profiles of AAEL003647 and AAEL019988 in NBF *Ae. aegypti* tissues **(A, B)** and in whole bodies following a blood meal **(C, D)**. Expression of AAEL003647 and AAEL019988 is highest in the ovaries for **(A)** AAEL003647 (one-way ANOVA, $p \leq 0.003$) and **(B)** AAEL019988 (one-way ANOVA, $p \leq 0.0092$). **(C)** Expression of AAEL003647 is significantly higher in the ovaries of NBF, 2h, 4h, and 6h pbf females (one-way ANOVA, $p < 0.05$). **(D)** Expression of AAEL019988 is significantly higher in the ovaries of NBF females (one-way

males (figure 3.3B). We next examined tissue tropism of the receptors in females. The highest expression of *AAEL003647* and *AAEL019988* was observed in the ovaries (figure 3.4A-B). We next measured receptor expression across a time series following a blood meal. Our results demonstrate that expression of *AAEL003647* was highest in non-blood fed, 2h, 4h, and 6h pbf

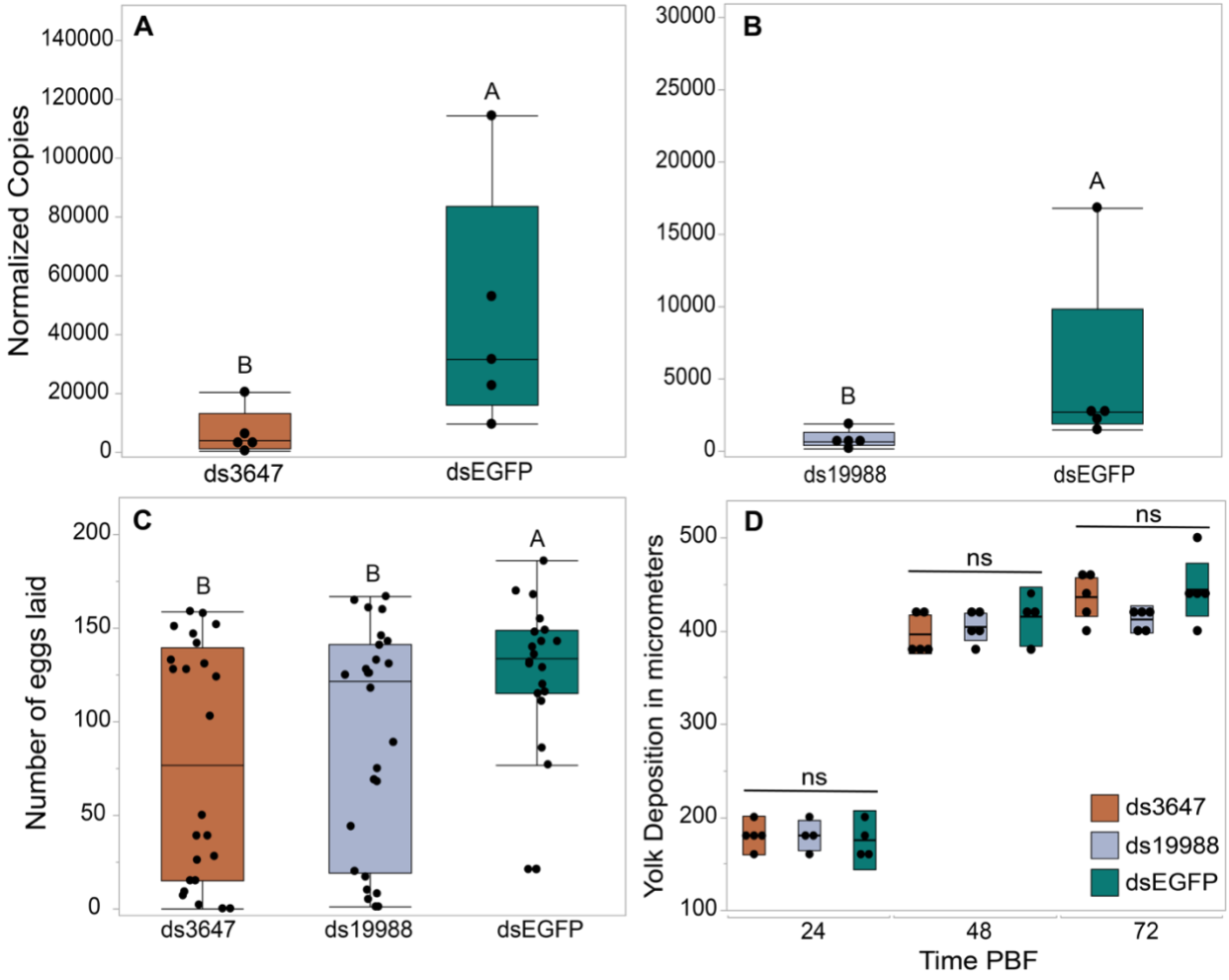

Figure 3.5. RNAi knockdowns **(A-B)**, oviposition bioassays **(C)**, and yolk deposition **(D)**. **(A-B)** Receptor knockdown validation. We achieved an 85% whole body transcript knockdown for AAEL003647 **(A)** (Wilcoxon rank-sum test, $p = 0.0163$) and AAEL019988 **(B)** (Wilcoxon rank-sum test, $p = 0.0163$). The x-axis represents the number of copies of AAEL003647 and AAEL019988 per 100ng of RNA. Transcripts were normalized by ribosomal S7 expression. **(C)** Knockdown of AAEL003647 and AAEL019988 resulted in a significant decrease in the number of eggs laid relative to dsEGFP controls (Wilcoxon rank-sum test, $p = 0.0184$, $p = 0.0393$, respectively). **(D)** Knockdown of AAEL003647 and AAEL019988 had no effect on yolk uptake (Wilcoxon rank-sum test, $p > 0.05$).

female ovaries (figure 3.4C). Expression of *AAEL019988* was highest in NBF ovaries (figure 3.4D).

Effects of knockdown of AAEL003647 and AAEL019988 on female reproduction

The peaks of expression prior to feeding and nearing the time of oviposition informed our hypothesis that AAEL003647 and AAEL019988 may be important in regulation of egg production and/or oviposition. To understand the effects of both orphan GPCRs on oviposition, we injected newly eclosed female mosquitoes with 2 µg of *ds3647*, *ds19988*, or *dsEGFP*. For each receptor, we were able to achieve an 85% whole body transcript knockdown (one-way ANOVA, $p < 0.0163$, $p < 0.0163$, respectively; figure 3.5A-B). Following dsRNA injection, females were allowed to mate and were fed 3 days post-injection. After feeding, females were separated into individual enclosures for oviposition assays. We found that *ds3647* and *ds19988*

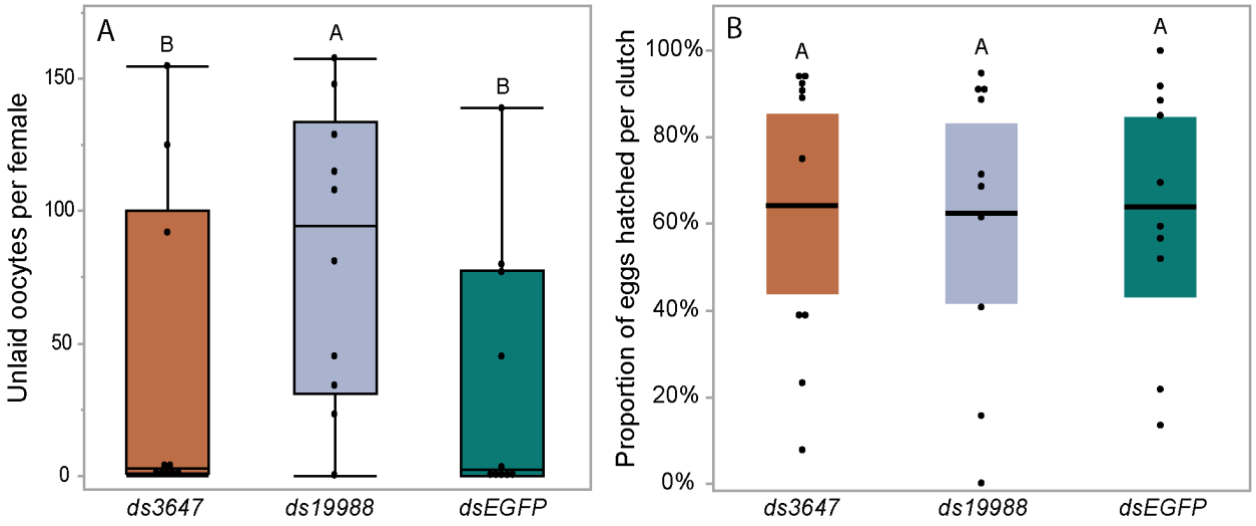

Figure 3.6: Effect of RNAi knockdown of AAEL003647 and AAEL019988 on egg retention **(A)** and egg hatching **(B)** of *Ae. aegypti*. Knockdown females were blood fed then allowed to lay eggs in individual cups. Females were then dissected and the number of unlaid, retained eggs were counted. Eggs were then allowed to hatch under standard conditions and successfully hatched larvae were counted. dsAAEL019988 females retained significantly more eggs than controls ($p = 0.0476$; Wilcoxon rank-sum test) while there was no significant difference between AAEL003647 knockdowns and controls.

injected females laid significantly fewer eggs than *dsEGFP* injected females (one-way ANOVA, $p = 0.0184$, $p = 0.0393$, respectively; figure 3.5C).

The observed reduction in egg laying by mosquitoes treated with *ds3647* or *ds19988* could be due to a disruption of egg maturation or egg laying. To disentangle this, we examined whether yolk deposition of *ds3647* and *ds19988* injected females was impaired, which would suggest that the receptors are important in post-vitellogenic egg development. We injected newly eclosed females with *dsEGFP, ds3647* or *ds19988*, fed females a blood meal at 3 days post injection, and dissected ovaries from blood fed females at 24, 48, and 72h pbf. Following dissection, we measured the packaged yolk in per individual oocyte with an ocular micrometer. We found no significant difference among oocyte yolk lengths in *ds3647*, *ds19988*, or *dsEGFP* injected females (one-way ANOVA, $p > 0.05$; figure 5D), suggesting that the receptors mediate physiological events after egg maturation. We then examined the effect of receptor knockdown on the egg retention and egg hatching. Knockdown of *AAEL003647* did not result in retained eggs in females, but *AAEL019988* knockdown mosquitoes retained more mature oocytes than dsEGFP controls (figure 3.6A, $p = 0.0476$; Wilcoxon rank-sum test). Of eggs that were laid, there was no difference in the proportion of eggs that hatched, suggesting that knockdown of the receptors does not interfere with fertilization (figure 3.6B).

3.5 Discussion

Our phylogenetic analysis identified that ancestor of SIFaR underwent gene duplication early in arthropod evolution. This paralog is retained in several arthropod lineages including members of the Culicidae, *Ae. aegypti* (AAEL003647) and *Anopheles gambiae* (AGAP003335). The SIFamide receptor binds the peptide hormone SIFamide, which is localized to

neurosecretory cells in the insect brain and central nervous system (Martelli et al. 2017; Sellami and Veenstra 2015; Siju et al. 2014). SIFamide is conserved among hemimetabolous and holometabolous insects and acts as a neurohormone to modulate appetitive behavior (Matrelli et al. 2017), feeding (Ayub et al. 2020), heart contractions (Ayub et al. 2020), and mating behavior (Terhzaz et al. 2007; Kunwar et al. 2008). The phylogenetic relationships of insect SIFaR receptors indicate an ancient divergence early in arthropod evolution, as evidenced by the presence of two receptor genes in diverse insect species including aphids, cockroaches, and mosquitoes. Veenstra recently identified a novel peptide hormone, SMYamide, in the genome of the American cockroach *Periplaneta americana* (Sellami and Veenstra 2015; Veenstra 2021). Phylogenetic analysis of the novel peptide revealed that it was sister to the *P. americana* SIFamide peptide, and though binding assays were not performed, the results suggest that SMYamide likely binds the protein encoded by the *SIFaR-2* gene of *P. americana*. Our expanded phylogenetic analysis indicates that the *P. americana* SIFaR-2 is an ortholog of AAEL003647, though we could not identify an ortholog of SMYamide in the *Ae. aegypti* genome. Future binding studies of AAEL003647 will focus on determining if the receptor binds SIFamide, a distant ortholog of SMYamide, or a novel peptide hormone.

The *Drosophila melanogaster* orphan GPCR, Trapped in Endoderm 1 (Tre1), was identified as an ortholog of AAEL019988 in our phylogenetic analysis. Tre1 is essential for the transepithelial migration of germ cells through the posterior midgut during embryogenesis (Ma et al. 2020; LeBlanc and Lehmann 2017; Kunwar et al. 2003; Kamps et al. 2010; Luu et al. 2016). Tre1 is also important for the initiation of courtship behavior *D. melanogaster* (Luu et al. 2016). The role of Tre1 in germ cell migration and in courtship may have led to the co-option of this

signaling system to regulate reproduction in *Ae. aegypti*. Interestingly, Tre1 is absent in most hemimetabolous insects.

Our expression profiles of *AAEL003647* and *AAEL019988* indicate that transcript abundance of both receptors is highest in adult females' ovaries, suggesting potential roles in egg production. To determine the potential roles of each orphan receptor in female reproductive physiology, we carried out a series of knockdown experiments which resulted in fecundity reduction in *ds3647*- and *ds19988*-injected females. Subsequently, we found that knockdown of both orphan receptors did not affect the amount of yolk packaged into oocytes, suggesting limited interactions with ILP3 and OEH, which are reproductive hormones that are known to modulate oogenesis (Brown et al. 2008; Dhara et al. 2013; Vogel et al. 2015). These results point to a role in oviposition rather than egg production.

The role of the SIFamide, a sister clade to AAEL003647, provides potential clues towards the mechanism of this receptor and its as-yet unknown ligand. SIFamide has been implicated in modulation of feeding and mating behavior in *Drosophila* (Martelli et al. 2017; Ayub et al. 2020; Kunwar et al. 2008). SIFamidergic neurons are activated during starving conditions and are inhibited by the myosin inhibitory peptide (MIP) which modulates satiation (Martelli et al. 2017). This SIFa/MIP neuropathway governs feeding behavior in *Drosophila*, but also directly affects mating behavior (Martelli et al. 2017; Ayub et al. 2020). SIFa acts on *fruitless* in *Drosophila*, which modulates courtship behavior; upon inhibition of SIFaR, male flies exhibited bisexual mating behaviors (Terhzaz et al. 2007; Kunwar et al. 2008). Although AAEL003647 and SIFaR belong to phylogenetically sister clades, it does not guarantee functional similarity. However, there is a possibility these receptors share similar functions, including modulation of oviposition by interaction with MIP.

AAEL019988 is an ortholog of Tre1, which in *Drosophila* regulates mating behavior. Luu *et al.* 2016 found that some *fruitless* expressing neurons also expressed *Tre1*, and that male and female flies exhibited expression of *Tre1* in a sexually dimorphic fashion (Luu et al. 2016). Female *Tre*1 expression was induced in males by generating transgenic males expressing the female Tre1 splice form, tra^{f}. This *Tre1* "feminization" in males resulted in latency in initiation of courtship behavior and complete absence of courtship initiation behavior in some males. However, there was no significant effect of *Tre1* feminization on the number of offspring per *Tre1* mutant male that mated with a female (Luu et al. 2016). We found that knockdown of AAEL019988 disrupts egg laying but not egg development, suggesting that it may have evolved an alternative function not involved in mating behaviors in *Ae. aegypti*. Future studies of AAEL003647 and AAEL019988 will examine the impacts of these orphan receptors on feeding and mating behavior, including through interactions with *fruitless* in *Ae. aegypti*.

3.6 Acknowledgments and Funding

The authors would like to express their gratitude to Jena Johnson, Logan Harrell, Lilith South, and Severen Brown for their maintenance of the mosquito colony used for this study. This research was grant funded by the National Institutes for Allergy and Infectious Diseases of the National Institutes of Health awarded to KJV (Award #K22AI127849).

Table 3.S1. List of accessions for full AAEL003647 phylogeny.

Table 3.S1: AAEL003647 ortholog accessions		
Accession	**Species**	**Description**
LOC108038247	*Drosophila rhopaloa*	LOC108038247
LOC108652677	*Drosophila navojoa*	neuropeptide.SIFamide.receptor
124791884	*Schistocerca piceifrons*	neuropeptide.SIFamide.receptor-like
LOC111683253	*Lucilia cuprina*	neuropeptide.SIFamide.receptor
NPFFR2	*Sipha flava*	NPFFR2
LOC116165108	*Photinus pyralis*	neuropeptide.SIFamide.receptor-like
LOC106660883	*Cimex lectularius*	A0A7E4SAB4
PPAI003401	*Phlebotomus papatasi*	GPCR F1_2 domain-containing protein
LOC107992660	*Apis cerana*	neuropeptide.SIFamide.receptor-like.isoform.X1
ASIS009403	*Anopheles sinensis*	undef
LOC108110268	*Drosophila eugracilis*	neuropeptide.SIFamide.receptor
LOC105687571	*Athalia rosae*	neuropeptide.SIFamide.receptor
123272567	*Cotesia glomerata*	neuropeptide.SIFamide.receptor-like
LOC111602638	*Drosophila hydei*	LOC111602638
LOC110832520	*Zootermopsis nevadensis*	neuropeptide.SIFamide.receptor-like
Pn.13150	*Polypedilum nubifer*	undef
LOC111867121	*Cryptotermes secundus*	neuropeptide.SIFamide.receptor
LOC100869437	*Apis florea*	neuropeptide.SIFamide.receptor
LOC116343097	*Contarinia nasturtii*	neuropeptide.SIFamide.receptor-like
6045184	*Culex quinquefasciatus*	6045184
120904938	*Anopheles arabiensis*	GPCR F1_2 domain-containing protein
Dgri\\GH18883	*Drosophila grimshawi*	Dgri\\GH18883
ACHR003668	*Anopheles christyi*	GPCR F1_2 domain-containing protein
Mdes002691	*Mayetiola destructor*	undef
AMIN000559	*Anopheles minimus*	GPCR F1_2 domain-containing protein
124613002	*Schistocerca americana*	neuropeptide.SIFamide.receptor-like
120895708	*Anopheles arabiensis*	neuropeptide.SIFamide.receptor-like

A0A1D2MZJ6	*Orchesella cincta*	
5572310	*Aedes aegypti*	5572310
AMIN002868	*Anopheles minimus*	GPCR F1_2 domain-containing protein
LOC108061875	*Drosophila takahashii*	LOC108061875
LOC108075454	*Drosophila kikkawai*	LOC108075454
LOC116337840	*Contarinia nasturtii*	neuropeptide.SIFamide.receptor-like
123292797	*Chrysoperla carnea*	neuropeptide.SIFamide.receptor-like
BomSIFR	*Bombyx mori*	J7RNN2
A0A1D2MDE5	*Orchesella cincta*	
LOC112686836	*Sipha flava*	neuropeptide.SIFamide.receptor-like
120416955	*Culex pipiens pallens*	neuropeptide.SIFamide.receptor-like
120950332	*Anopheles coluzzii*	neuropeptide.SIFamide.receptor-like
AMAM009506	*Anopheles maculatus*	GPCR F1_2 domain-containing protein
AFAF007709	*Anopheles farauti*	GPCR F1_2 domain-containing protein
118502584	*Anopheles stephensi*	neuropeptide.SIFamide.receptor-like.isoform.X3
LOC107164816	*Diuraphis noxia*	neuropeptide.FF.receptor.2-like
Mca09985	*Myzus cerasi*	undef
LOC111874324	*Cryptotermes secundus*	neuropeptide.SIFamide.receptor-like.isoform.X1
OFAS012396	*Oncopeltus fasciatus*	GPCR F1_2 domain-containing protein
SIFR	*Apis mellifera*	A9X454
LOC105223151	*Bactrocera dorsalis*	LOC105223151
GY_00000339-RA	*Galloisiana yuasai*	
LOC108615695	*Drosophila arizonae*	neuropeptide.SIFamide.receptor
118737274	*Rhagoletis pomonella*	neuropeptide.SIFamide.receptor
LOC112126335	*Cimex lectularius*	neuropeptide.SIFamide.receptor-like
LOC108155192	*Drosophila miranda*	neuropeptide.SIFamide.receptor.isoform.X1
LOC111061583	*Nilaparvata lugens*	neuropeptide.SIFamide.receptor-like
120950824	*Anopheles coluzzii*	neuropeptide.SIFamide.receptor-like

LOC109402751	*Aedes albopictus*	neuropeptide.SIFamide.receptor
AATE020562	*Anopheles atroparvus*	GPCR F1_2 domain-containing protein
118506506	*Anopheles stephensi*	neuropeptide.SIFamide.receptor-like.isoform.X1
LOC103524969	*Diaphorina citri*	LOC103524969
A0A1D2MLL8	*Orchesella cincta*	
LOC108601613	*Drosophila busckii*	neuropeptide.SIFamide.receptor
LOC117643260	*Thrips palmi*	LOC117643260
LOC110188270	*Drosophila serrata*	neuropeptide.SIFamide.receptor
LOC100159289	*Acyrthosiphon pisum*	A0A0I9QPX6
124358685	*Homalodisca vitripennis*	neuropeptide.SIFamide.receptor-like
LOC108556933	*Nicrophorus vespilloides*	neuropeptide.SIFamide.receptor-like
Dvir\\GJ14438	*Drosophila virilis*	GPCR F1_2 domain-containing protein
GPPI044149	*Glossina palpalis*	undef
ASIS014193	*Anopheles sinensis*	undef
AFUN008599	*Anopheles funestus*	undef
AMAM023042	*Anopheles maculatus*	GPCR F1_2 domain-containing protein
LOC106691255	*Halyomorpha halys*	neuropeptide.SIFamide.receptor-like.isoform.X1
NPFFR2	*Melanaphis sacchari*	NPFFR2
119652500	*Hermetia illucens*	neuropeptide.SIFamide.receptor-like
LOC110850949	*Folsomia candida*	neuropeptide.SIFamide.receptor-like
Dana\\GF17259	*Drosophila ananassae*	GPCR F1_2 domain-containing protein
LOC113207659	*Frankliniella occidentalis*	LOC113207659
LOC108691036	*Atta colombica*	neuropeptide.SIFamide.receptor-like
LOC109598616	*Aethina tumida*	neuropeptide.SIFamide.receptor
LLUN010603	*Limnephilus lunatus*	undef
Mdes015521	*Mayetiola destructor*	undef
121603638	*Anopheles merus*	GPCR F1_2 domain-containing protein
LLOJ008012	*Lutzomyia longipalpis*	A0A1B0CT13
LOC102671200	*Apis dorsata*	neuropeptide.SIFamide.receptor-like
nngr-a5	*Nilaparvata lugens*	nngr-a5

118460327	*Anopheles albimanus*	neuropeptide.SIFamide.receptor-like
LOC111356337	*Spodoptera litura*	neuropeptide.SIFamide.receptor-like
LOC117574210	*Drosophila albomicans*	LOC117574210
119638868	*Glossina fuscipes*	neuropeptide.SIFamide.receptor
LOC108013852	*Drosophila suzukii*	LOC108013852
EDAN012016	*Ephemera danica*	GPCR F1_2 domain-containing protein
CAUGE_22845	*Campodea augens*	
A0A1J1INC1	*Clunio marinus*	
LOC4800861	*Drosophila pseudoobscura*	neuropeptide.SIFamide.receptor
Dmoj\\GI10832	*Drosophila mojavensis*	Dmoj\\GI10832
AFUN007817	*Anopheles funestus*	GPCR F1_2 domain-containing protein
LOC5578735	*Aedes aegypti*	A0A411JK97
Mca26103	*Myzus cerasi*	undef
OFAS009466	*Oncopeltus fasciatus*	GPCR F1_2 domain-containing protein
GMOY008798	*Glossina morsitans*	undef
LOC100647319	*Bombus terrestris*	LOC100647319
AEPI001119	*Anopheles epiroticus*	GPCR F1_2 domain-containing protein
118468886	*Anopheles albimanus*	GPCR F1_2 domain-containing protein
LOC106681898	*Halyomorpha halys*	neuropeptide.SIFamide.receptor-like
ADIR002471	*Anopheles dirus*	GPCR F1_2 domain-containing protein
LOC105153454	*Acromyrmex echinatior*	neuropeptide.FF.receptor.2
LOC111032586	*Myzus persicae*	neuropeptide.SIFamide.receptor-like
ADAC004022	*Anopheles darlingi*	W5JIN1
LOC103522734	*Diaphorina citri*	LOC103522734
A0A1D2MAK0	*Orchesella cincta*	
EDAN005016	*Ephemera danica*	GPCR F1_2 domain-containing protein
GPRNNA7	*Anopheles gambiae str PEST*	AGAP003335-PA
SIFaR	*Drosophila melanogaster*	Neuropeptide.SIFamide.receptor
124360425	*Homalodisca vitripennis*	neuropeptide.SIFamide.receptor-like
OFAS009467	*Oncopeltus fasciatus*	GPCR F1_2 domain-containing protein

118502576	*Anopheles stephensi*	neuropeptide.SIFamide.receptor-like.isoform.X1
AMAM011260	*Anopheles maculatus*	GPCR F1_2 domain-containing protein
LOC110828724	*Zootermopsis nevadensis*	neuropeptide.SIFamide.receptor-like
119658977	*Hermetia illucens*	neuropeptide.SIFamide.receptor-like
LOC6650970	*Drosophila willistoni*	neuropeptide.SIFamide.receptor
LOC111080460	*Drosophila obscura*	neuropeptide.SIFamide.receptor
ADIR006514	*Anopheles dirus*	GPCR F1_2 domain-containing protein
RPRC000835	*Rhodnius prolixus*	GPCR F1_2 domain-containing protein
LOC108737918	*Agrilus planipennis*	LOC108737918
LOC117792575	*Drosophila innubila*	neuropeptide.SIFamide.receptor
ADAC003213	*Anopheles darlingi*	GPCR F1_2 domain-containing protein
LOC107168167	*Diuraphis noxia*	neuropeptide.FF.receptor.2-like
ACUA002341	*Anopheles culicifacies*	GPCR F1_2 domain-containing protein
106083508	*Stomoxys calcitrans*	GPCR F1_2 domain-containing protein
LOC105211385	*Zeugodacus cucurbitae*	P2Y.purinoceptor.4
LOC111056579	*Nilaparvata lugens*	neuropeptide.SIFamide.receptor
122715679	*Apis laboriosa*	neuropeptide.SIFamide.receptor-like
119085776	*Bradysia coprophila*	neuropeptide.SIFamide.receptor-like
AMAM023590	*Anopheles maculatus*	GPCR F1_2 domain-containing protein
LOC108121568	*Drosophila bipectinata*	LOC108121568
LOC100750178	*Bombus impatiens*	LOC100750178
LOC108383162	*Rhagoletis zephyria*	neuropeptide.SIFamide.receptor-like
GAUT007169	*Glossina austeni*	GPCR F1_2 domain-containing protein
PHUM189320	*Pediculus humanus*	undef
AMAM021528	*Anopheles maculatus*	A0A182T834
LOC117589782	*Drosophila guanche*	neuropeptide.SIFamide.receptor
LOC116164873	*Photinus pyralis*	GPCR F1_2 domain-containing protein
1155016:002b6f	*Mengenilla moldrzyki*	undef

118434209	*Folsomia candida*	A0A226EQT0
105619544	*Atta cephalotes*	GPCR F1_2 domain-containing protein
Pv.03453	*Polypedilum vanderplanki*	undef
118269799	*Spodoptera frugiperda*	neuropeptide.SIFamide.receptor-like
LOC111428400	*Onthophagus taurus*	neuropeptide.SIFamide.receptor-like
119659762	*Hermetia illucens*	neuropeptide.SIFamide.receptor-like
AEPI003302	*Anopheles epiroticus*	GPCR F1_2 domain-containing protein
GBRI036855	*Glossina brevipalpis*	GPCR F1_2 domain-containing protein
100167549	*Acyrthosiphon pisum*	GPCR F1_2 domain-containing protein
LOC100570021	*Acyrthosiphon pisum*	neuropeptide.SIFamide.receptor-like
LOC108354948	*Rhagoletis zephyria*	neuropeptide.SIFamide.receptor-like
AFAF014500	*Anopheles farauti*	GPCR F1_2 domain-containing protein
A0A1D2ME65	*Orchesella cincta*	
119560877	*Drosophila subpulchrella*	neuropeptide.SIFamide.receptor
CSPLE_10334	*Calopteryx splendens*	
LOC106645722	*Copidosoma floridanum*	neuropeptide.SIFamide.receptor-like
LOC108141215	*Drosophila elegans*	neuropeptide.SIFamide.receptor
LOC111512591	*Leptinotarsa decemlineata*	neuropeptide.SIFamide.receptor-like
A0A1D2NFD1	*Orchesella cincta*	
119601256	*Lucilia sericata*	neuropeptide.SIFamide.receptor
LOC111038866	*Myzus persicae*	neuropeptide.SIFamide.receptor-like
LOC108098657	*Drosophila ficusphila*	LOC108098657
121590202	*Anopheles merus*	neuropeptide.SIFamide.receptor-like
LOC115764080	*Drosophila novamexicana*	neuropeptide.SIFamide.receptor.isoform.X1
A0A1D2MLR2	*Orchesella cincta*	
120417916	*Culex pipiens pallens*	neuropeptide.SIFamide.receptor-like.isoform.X1
LOC113518978	*Galleria mellonella*	LOC113518978

119067013	*Bradysia coprophila*	neuropeptide.SIFamide.receptor-like
ACUA006288	*Anopheles culicifacies*	GPCR F1_2 domain-containing protein
120453180	*Drosophila santomea*	neuropeptide.SIFamide.receptor.isoform.X1
6051290	*Culex quinquefasciatus*	GPCR F1_2 domain-containing protein
LOC116769126	*Danaus plexippus plexippus*	neuropeptide.SIFamide.receptor
AATE019535	*Anopheles atroparvus*	GPCR F1_2 domain-containing protein
LOC117650282	*Thrips palmi*	LOC117650282
LOC110858557	*Folsomia candida*	neuropeptide.SIFamide.receptor.isoform.X1
A0A1D2N6V2	*Orchesella cincta*	
LOC110854061	*Folsomia candida*	A0A226DZL9
GPRCCK2	*Anopheles gambiae str PEST*	AGAP001379-PA
NPFFR2	*Melanaphis sacchari*	NPFFR2

Table 3.S2. List of accessions for full AAEL019988 phylogeny.

Table 3.S2: AAEL019988 ortholog accessions		
Accession	**Species**	**Description**
LOC113512885	*Galleria mellonella*	LOC113512885
LOC116770562	*Danaus plexippus plexippus*	G-protein coupled receptor moody-like isoform X1
AFUN001240	*Anopheles funestus*	GPCR F1_2 domain-containing protein
LOC100642395	*Bombus terrestris*	LOC100642395
LOC108124815	*Drosophila bipectinata*	LOC108124815
118267410	*Spodoptera frugiperda*	G-protein coupled receptor moody-like
LOC111058775	*Nilaparvata lugens*	G-protein coupled receptor moody
LOC111356401	*Spodoptera litura*	G-protein coupled receptor moody-like
LOC113369860	*Ctenocephalides felis*	protein trapped in endoderm-1-like
118267537	*Spodoptera frugiperda*	G-protein coupled receptor moody-like
119078897	*Bradysia coprophila*	protein trapped in endoderm-1-like
LOC100577758	*Apis mellifera*	G-protein coupled receptor moody
GBRI045038	*Glossina brevipalpis*	GPCR F1_2 domain-containing protein
LOC111075044	*Drosophila obscura*	G-protein coupled receptor moody
BGER022585	*Blattella germanica*	undef
106093090	*Stomoxys calcitrans*	GPCR F1_2 domain-containing protein
OFAS005065	*Oncopeltus fasciatus*	GPCR F1_2 domain-containing protein
LOC117563852	*Drosophila albomicans*	LOC117563852
LOC108016644	*Drosophila suzukii*	LOC108016644
LOC100866444	*Apis florea*	protein trapped in endoderm-1
119676607	*Teleopsis dalmanni*	G-protein coupled receptor moody isoform X1
LOC111604048	*Drosophila hydei*	LOC111604048
LOC106141093	*Amyelois transitella*	G-protein coupled receptor moody-like
GPROPDR	*Anopheles gambiae str PEST*	AGAP001498-PA
120455393	*Drosophila santomea*	protein trapped in endoderm-1 isoform X1

LOC117903044	*Drosophila subobscura*	protein trapped in endoderm-1
LOC115765416	*Drosophila novamexicana*	G-protein coupled receptor moody
LOC6600449	*Drosophila persimilis*	G-protein coupled receptor moody
LOC116413950	*Apis florea*	dopamine receptor 3-like
LOC111038866	*Myzus persicae*	neuropeptide SIFamide receptor-like
118267756	*Spodoptera frugiperda*	G-protein coupled receptor moody-like
119611629	*Lucilia sericata*	G-protein coupled receptor moody
Rpa00016.t1	*Rhopalosiphum padi*	undef
LOC105233352	*Bactrocera dorsalis*	LOC105233352
Dsim\\GD16244	*Drosophila simulans*	protein trapped in endoderm-1
LOC113521286	*Galleria mellonella*	LOC113521286
120896968	*Anopheles arabiensis*	G-protein coupled receptor moody
118272317	*Spodoptera frugiperda*	protein trapped in endoderm-1-like isoform X1
LOC409159	*Apis mellifera*	GPCR F1_2 domain-containing protein
LOC108016751	*Drosophila suzukii*	LOC108016751
GY00015349-RA	*Galloisiana yuasai*	
LOC111681491	*Lucilia cuprina*	G-protein coupled receptor moody isoform X1
LOC113206307	*Frankliniella occidentalis*	LOC113206307
LOC103505448	*Diaphorina citri*	LOC103505448
Dper\\GL18324	*Drosophila persimilis*	Dper\\GL18324
119601614	*Lucilia sericata*	protein trapped in endoderm-1 isoform X1
119078698	*Bradysia coprophila*	protein trapped in endoderm-1-like isoform X1
E6466C4BA369DEAAC0B542211B262904	*Clunio marinus*	A0A1J1HQP6
LOC113553289	*Rhopalosiphum maidis*	G-protein coupled receptor moody
LOC108063874	*Drosophila takahashii*	LOC108063874
GAUT032041	*Glossina austeni*	GPCR F1_2 domain-containing protein
119070870	*Bradysia coprophila*	G-protein coupled receptor moody isoform X1

LOC108104374	*Drosophila eugracilis*	G-protein coupled receptor moody
119666442	*Teleopsis dalmanni*	protein trapped in endoderm-1
LOC116166267	*Photinus pyralis*	GPCR F1_2 domain-containing protein
Mdes006942	*Mayetiola destructor*	undef
LOC117568881	*Drosophila albomicans*	LOC117568881
Mca26103	*Myzus cerasi*	undef
AGAP004930	*Anopheles gambiae*	A0A1S4GMK0
LOC108360438	*Rhagoletis zephyria*	protein trapped in endoderm-1
LOC4816028	*Drosophila pseudoobscura*	G-protein coupled receptor moody
LOC111356400	*Spodoptera litura*	G-protein coupled receptor moody
119658060	*Hermetia illucens*	protein trapped in endoderm-1
LOC100864393	*Apis florea*	G-protein coupled receptor moody isoform X1
Dsec\\GM18925	*Drosophila sechellia*	Dsec\\GM18925
GAUT014222	*Glossina austeni*	GPCR F1_2 domain-containing protein
124171018	*Ischnura elegans*	protein trapped in endoderm-1
ADIR009859	*Anopheles dirus*	GPCR F1_2 domain-containing protein
124551153	*Schistocerca americana*	G-protein coupled receptor moody-like
LOC108136303	*Drosophila elegans*	G-protein coupled receptor 84
LOC109596346	*Aethina tumida*	protein trapped in endoderm-1
LOC108097316	*Drosophila ficusphila*	LOC108097316
121589080	*Anopheles merus*	GPCR F1_2 domain-containing protein
119085496	*Bradysia coprophila*	protein trapped in endoderm-1-like
EDAN001528	*Ephemera danica*	GPCR F1_2 domain-containing protein
AFAF008557	*Anopheles farauti*	GPCR F1_2 domain-containing protein
6034428	*Culex quinquefasciatus*	6034428
Mdes006710	*Mayetiola destructor*	undef
LOC6612380	*Drosophila sechellia*	protein trapped in endoderm-1
LOC116770874	*Danaus plexippus plexippus*	G-protein coupled receptor moody-like
LOC108684917	*Atta colombica*	A0A195BMR5

ACHR005590	*Anopheles christyi*	GPCR F1_2 domain-containing protein
119069233	*Bradysia coprophila*	G-protein coupled receptor moody isoform X1
LOC111075024	*Drosophila obscura*	G-protein coupled receptor moody
LOC101737500	*Bombyx mori*	G-protein coupled receptor moody
LOC107996919	*Apis cerana*	protein trapped in endoderm-1
GY_00009018-RA	*00009018-RA*	
moody	*Melanaphis sacchari*	moody
119633803	*Glossina fuscipes*	G-protein coupled receptor moody
GPRMTN	*Anopheles gambiae str PEST*	AGAP001499-PB
LOC110832520	*Zootermopsis nevadensis*	neuropeptide SIFamide receptor-like
Dvir\\GJ17048	*Drosophila virilis*	GPCR F1_2 domain-containing protein
ADIR009858	*Anopheles dirus*	GPCR F1_2 domain-containing protein
120951550	*Anopheles coluzzii*	G-protein coupled receptor moody-like isoform X1
GMOY003467	*Glossina morsitans*	undef
LOC108056430	*Drosophila takahashii*	LOC108056430
LOC108618271	*Drosophila arizonae*	G-protein coupled receptor moody
LOC108024225	*Drosophila biarmipes*	protein trapped in endoderm-1
Rpa00010.t1	*Rhopalosiphum padi*	undef
ACUA012861	*Anopheles culicifacies*	GPCR F1_2 domain-containing protein
LOC115765265	*Drosophila novamexicana*	G-protein coupled receptor moody
LOC102681241	*Apis dorsata*	G-protein coupled receptor moody-like isoform X1
Mca09985	*Myzus cerasi*	undef
LOC108071748	*Drosophila kikkawai*	LOC108071748
5571506	*Aedes aegypti*	GPCR F1_2 domain-containing protein
GY	*00003523-RA*	Galloisiana yuasai
LOC102670969	*Apis dorsata*	muscarinic acetylcholine receptor M3-like
AFAF009723	*Anopheles farauti*	GPCR F1_2 domain-containing protein

AMIN002396	*Anopheles minimus*	GPCR F1_2 domain-containing protein
EDAN001526	*Ephemera danica*	GPCR F1_2 domain-containing protein
106083909	*Stomoxys calcitrans*	GPCR F1_2 domain-containing protein
AMAM004845	*Anopheles maculatus*	GPCR F1_2 domain-containing protein
LOC108049742	*Drosophila rhopaloa*	LOC108049742
LOC115564075	*Drosophila navojoa*	GPCR F1_2 domain-containing protein
LOC108567174	*Nicrophorus vespilloides*	G-protein coupled receptor moody-like isoform X1
LOC100648479	*Bombus terrestris*	LOC100648479
118755384	*Rhagoletis pomonella*	uncharacterized protein LOC118755384
ASIS001664	*Anopheles sinensis*	undef
LOC117903751	*Drosophila subobscura*	G-protein coupled receptor moody
AFUN007074	*Anopheles funestus*	GPCR F1_2 domain-containing protein
LOC100741539	*Bombus impatiens*	LOC100741539
123294409	*Chrysoperla carnea*	G-protein coupled receptor moody isoform X1
LOC111425617	*Onthophagus taurus*	protein trapped in endoderm-1-like
LOC105233335	*Bactrocera dorsalis*	LOC105233335
LOC116349961	*Contarinia nasturtii*	uncharacterized protein LOC116349961
LOC113389048	*Ctenocephalides felis*	G-protein coupled receptor moody-like
PPAI010520	*Phlebotomus papatasi*	A0A1B0DPT3
LOC105686273	*Athalia rosae*	G-protein coupled receptor moody isoform X2
119655773	*Hermetia illucens*	G-protein coupled receptor moody isoform X1
LOC117794287	*Drosophila innubila*	G-protein coupled receptor moody
ASIS010062	*Anopheles sinensis*	undef
LOC100649542	*Bombus terrestris*	LOC100649542
LOC108097159	*Drosophila ficusphila*	LOC108097159
BGER021446	*Blattella germanica*	undef
LLOJ000164	*Lutzomyia longipalpis*	GPCR F1_2 domain-containing protein

Dper\\GL15127	*Drosophila persimilis*	Dper\\GL15127
Mdes012035	*Mayetiola destructor*	undef
118734271	*Rhagoletis pomonella*	protein trapped in endoderm-1
122720408	*Apis laboriosa*	protein trapped in endoderm-1 isoform X1
118267591	*Spodoptera frugiperda*	G-protein coupled receptor moody-like
ADAC008043	*Anopheles darlingi*	GPCR F1_2 domain-containing protein
LOC108606688	*Drosophila busckii*	A0A0M4F907
LOC103505811	*Diaphorina citri*	LOC103505811
AMAM019542	*Anopheles maculatus*	GPCR F1_2 domain-containing protein
LOC113366797	*Ctenocephalides felis*	protein trapped in endoderm-1-like
124357072	*Homalodisca vitripennis*	G-protein coupled receptor moody
AEPI006197	*Anopheles epiroticus*	GPCR F1_2 domain-containing protein
LOC116413236	*Galleria mellonella*	LOC116413236
Dmoj\\GI15171	*Drosophila mojavensis*	GPCR F1_2 domain-containing protein
LOC105152358	*Acromyrmex echinatior*	F4X3L3
AGAP001498;GPROPDR	*Anopheles gambiae*	A0A1S4GC54
PPAI003818	*Phlebotomus papatasi*	GPCR F1_2 domain-containing protein
LOC6648527	*Drosophila willistoni*	G-protein coupled receptor moody
119655195	*Hermetia illucens*	G-protein coupled receptor moody
LOC115767594	*Drosophila novamexicana*	protein trapped in endoderm-1
LOC117591157	*Drosophila guanche*	A0A3B0KW52
LOC117569517	*Drosophila albomicans*	LOC117569517
119673162	*Teleopsis dalmanni*	G-protein coupled receptor moody
CSPLE	*1134*	Calopteryx splendens
122719695	*Apis laboriosa*	G-protein coupled receptor moody-like
AATE012834	*Anopheles atroparvus*	GPCR F1_2 domain-containing protein
120952214	*Anopheles coluzzii*	protein trapped in endoderm-1-like
LOC108080324	*Drosophila kikkawai*	LOC108080324
124551194	*Schistocerca americana*	G-protein coupled receptor moody-like

CSPLE	*6094*	Calopteryx splendens
LOC116770760	*Danaus plexippus plexippus*	A0A212FJK6
LFUL019070	*Ladona fulva*	undef
LLUN001788	*Limnephilus lunatus*	undef
105626419	*Atta cephalotes*	GPCR F1_2 domain-containing protein
LOC113204198	*Frankliniella occidentalis*	LOC113204198
LOC113389613	*Ctenocephalides felis*	G-protein coupled receptor 84
LOC111683130	*Lucilia cuprina*	protein trapped in endoderm-1 isoform X1
LOC108361516	*Rhagoletis zephyria*	cholecystokinin receptor-like isoform X1
LOC117793386	*Drosophila innubila*	protein trapped in endoderm-1
LOC108103713	*Drosophila eugracilis*	protein trapped in endoderm-1
GMOY005600	*Glossina morsitans*	undef
LOC110180449	*Drosophila serrata*	G-protein coupled receptor moody
LOC108619174	*Drosophila arizonae*	protein trapped in endoderm-1
moody	*Drosophila melanogaster*	moody
LOC111868440	*Cryptotermes secundus*	protein trapped in endoderm-1
120950599	*Anopheles coluzzii*	protein trapped in endoderm-1
LOC116349859	*Contarinia nasturtii*	G-protein coupled receptor moody isoform X1
GPPI025988	*Glossina palpalis*	undef
AEPI005391	*Anopheles epiroticus*	GPCR F1_2 domain-containing protein
LFUL011698	*Ladona fulva*	undef
LOC108164524	*Drosophila miranda*	G-protein coupled receptor moody
LOC113206313	*Frankliniella occidentalis*	LOC113206313
LOC108015377	*Drosophila suzukii*	LOC108015377
LOC100749439	*Bombus impatiens*	LOC100749439
118267592	*Spodoptera frugiperda*	A0A2H1X154
120894962	*Anopheles arabiensis*	GPCR F1_2 domain-containing protein
LOC111032586	*Myzus persicae*	neuropeptide SIFamide receptor-like

119556972	*Drosophila subpulchrella*	G-protein coupled receptor moody
109431381	*Aedes albopictus*	GPCR F1_2 domain-containing protein
LOC108685206	*Atta colombica*	G-protein coupled receptor moody isoform X1
119644908	*Glossina fuscipes*	G-protein coupled receptor moody
LOC117581121	*Drosophila guanche*	A0A3B0JRZ4
ADIR001668	*Anopheles dirus*	GPCR F1_2 domain-containing protein
Dmoj\\GI16297	*Drosophila mojavensis*	GPCR F1_2 domain-containing protein
124357071	*Homalodisca vitripennis*	G-protein coupled receptor moody isoform X1
LOC113513007	*Galleria mellonella*	LOC113513007
LOC108041898	*Drosophila rhopaloa*	LOC108041898
AMIN002397	*Anopheles minimus*	GPCR F1_2 domain-containing protein
LOC111418077	*Onthophagus taurus*	G-protein coupled receptor moody-like isoform X1
EDAN002678	*Ephemera danica*	GPCR F1_2 domain-containing protein
LOC116168571	*Photinus pyralis*	GPCR F1_2 domain-containing protein
LOC111604051	*Drosophila hydei*	LOC111604051
LOC111593654	*Drosophila hydei*	LOC111593654
122624164	*Drosophila teissieri*	G-protein coupled receptor moody
GMOY009566	*Glossina morsitans*	undef
LOC110828724	*Zootermopsis nevadensis*	neuropeptide SIFamide receptor-like
LOC108001168	*Apis cerana*	G-protein coupled receptor moody
Dana\\GF20907	*Drosophila ananassae*	GPCR F1_2 domain-containing protein
GBUE013208	*Gerris buenoi*	undef
LOC116344279	*Contarinia nasturtii*	protein trapped in endoderm-1 isoform X1
LOC109427701	*Aedes albopictus*	protein trapped in endoderm-1 isoform X1
122623085	*Drosophila teissieri*	protein trapped in endoderm-1
LOC100866323	*Apis florea*	protein trapped in endoderm-1-like
AFAF001669	*Anopheles farauti*	GPCR F1_2 domain-containing protein
LFUL010416	*Ladona fulva*	undef

LOC109598991	*Aethina tumida*	G-protein coupled receptor moody-like isoform X1
LOC108657262	*Drosophila navojoa*	GPCR F1_2 domain-containing protein
AATE001298	*Anopheles atroparvus*	GPCR F1_2 domain-containing protein
GPPI004155	*Glossina palpalis*	undef
LOC117794291	*Drosophila innubila*	G-protein coupled receptor moody
LOC111044985	*Nilaparvata lugens*	G-protein coupled receptor moody
118505213	*Anopheles stephensi*	G-protein coupled receptor moody isoform X1
AgaP	*AGAP004930*	Anopheles gambiae str PEST
LOC106671026	*Cimex lectularius*	A0A7E4SGQ3
CSPLE	*1139*	Calopteryx splendens
118267411	*Spodoptera frugiperda*	G-protein coupled receptor moody-like
LOC111867646	*Cryptotermes secundus*	G-protein coupled receptor moody-like
LOC111868344	*Cryptotermes secundus*	G-protein coupled receptor 84-like
LLUN002809	*Limnephilus lunatus*	undef
LOC108056426	*Drosophila takahashii*	LOC108056426
LOC117581119	*Drosophila guanche*	A0A3B0JZT1
LOC106690378	*Halyomorpha halys*	G-protein coupled receptor moody
LFUL019073	*Ladona fulva*	undef
LOC111681493	*Lucilia cuprina*	G-protein coupled receptor moody
LOC106688042	*Halyomorpha halys*	G-protein coupled receptor moody isoform X1
124154251	*Ischnura elegans*	G-protein coupled receptor moody
LOC4814990	*Drosophila pseudoobscura*	uncharacterized protein
121593680	*Anopheles merus*	GPCR F1_2 domain-containing protein
RPRC011268	*Rhodnius prolixus*	GPCR F1_2 domain-containing protein
118750830	*Rhagoletis pomonella*	G-protein coupled receptor moody
LOC108165240	*Drosophila miranda*	protein trapped in endoderm-1-like
101893638	*Musca domestica*	GPCR F1_2 domain-containing protein
AMAM008514	*Anopheles maculatus*	GPCR F1_2 domain-containing protein
Pn.11647	*Polypedilum nubifer*	undef

Pn.11270	*Polypedilum nubifer*	undef
PVEN013100	*Pachypsylla venusta*	undef
GBRI045041	*Glossina brevipalpis*	GPCR F1_2 domain-containing protein
LOC6648526	*Drosophila willistoni*	G-protein coupled receptor moody
LOC100165337	*Acyrthosiphon pisum*	G-protein coupled receptor moody isoform X1
LOC112592105	*Melanaphis sacchari*	G-protein coupled receptor moody
120419905	*Culex pipiens pallens*	protein trapped in endoderm-1
Pv.16028	*Polypedilum vanderplanki*	undef
LOC725008	*Apis mellifera*	GPCR F1_2 domain-containing protein
AGAP001499	*Anopheles gambiae*	A0A1S4GC96
LOC110180416	*Drosophila serrata*	LOW QUALITY PROTEIN: protein trapped in endoderm-1
LOC102681990	*Apis dorsata*	G-protein coupled receptor moody-like
BGER000660	*Blattella germanica*	undef
LOC108097092	*Drosophila ficusphila*	LOC108097092
Dwil\\GK19905	*Drosophila willistoni*	GPCR F1_2 domain-containing protein
120456293	*Drosophila santomea*	protein trapped in endoderm-1
Pv.12662	*Polypedilum vanderplanki*	undef
LOC105686247	*Athalia rosae*	G-protein coupled receptor moody isoform X1
RPRC004128	*Rhodnius prolixus*	GPCR F1_2 domain-containing protein
Dana\\GF21984	*Drosophila ananassae*	Dana\\GF21984
LOC116772735	*Danaus plexippus plexippus*	protein trapped in endoderm-1 isoform X1
Mdes018372	*Mayetiola destructor*	undef
LOC117650282	*Thrips palmi*	LOC117650282
LOC108606689	*Drosophila busckii*	A0A0M4ELY9
1155016:000d58	*Mengenilla moldrzyki*	undef
Dmoj\\GI15426	*Drosophila mojavensis*	Dmoj\\GI15426
LOC108152416	*Drosophila miranda*	protein trapped in endoderm-1
LOC108001224	*Apis cerana*	G-protein coupled receptor moody isoform X1

124717108	*Schistocerca piceifrons*	G-protein coupled receptor moody-like
105618427	*Atta cephalotes*	GPCR F1_2 domain-containing protein
GAUT014227	*Glossina austeni*	GPCR F1_2 domain-containing protein
LOC111509334	*Leptinotarsa decemlineata*	G-protein coupled receptor moody-like isoform X2
LOC113389611	*Ctenocephalides felis*	G-protein coupled receptor moody-like
LOC108080367	*Drosophila kikkawai*	LOC108080367
LOC4815666	*Drosophila pseudoobscura*	uncharacterized protein
LOC102674665	*Apis dorsata*	protein trapped in endoderm-1 isoform X1
LOC103505446	*Diaphorina citri*	LOC103505446
LOC105683977	*Athalia rosae*	protein trapped in endoderm-1 isoform X1
GBUE012266	*Gerris buenoi*	undef
AATE010230	*Anopheles atroparvus*	GPCR F1_2 domain-containing protein
LOC111072298	*Drosophila obscura*	protein trapped in endoderm-1
LOC110182568	*Drosophila serrata*	protein trapped in endoderm-1
LOC101744412	*Bombyx mori*	G-protein coupled receptor moody isoform X1
LOC105225884	*Bactrocera dorsalis*	LOC105225884
Dvir\\GJ16387	*Drosophila virilis*	Dvir\\GJ16387
37DFD20BDF9821FFD83C75501E61BE53	*Clunio marinus*	A0A1J1I7J0
GBRI011759	*Glossina brevipalpis*	GPCR F1_2 domain-containing protein
LOC113553237	*Rhopalosiphum maidis*	G-protein coupled receptor moody
118734128	*Rhagoletis pomonella*	cholecystokinin receptor-like
101888711	*Musca domestica*	GPCR F1_2 domain-containing protein
LOC108685827	*Atta colombica*	protein trapped in endoderm-1
LOC111501990	*Leptinotarsa decemlineata*	protein trapped in endoderm-1
124716881	*Schistocerca piceifrons*	G-protein coupled receptor moody-like
OFAS016762	*Oncopeltus fasciatus*	undef
124418669	*Lucilia cuprina*	protein trapped in endoderm-1

Dvir\\GJ16684	*Drosophila virilis*	Dvir\\GJ16684
LOC108136247	*Drosophila elegans*	protein trapped in endoderm-1
LOC108124085	*Drosophila bipectinata*	LOC108124085
AEPI006198	*Anopheles epiroticus*	GPCR F1_2 domain-containing protein
LOC108023279	*Drosophila biarmipes*	G-protein coupled receptor moody
Pv.01215	*Polypedilum vanderplanki*	undef
Dgri\\GH24563	*Drosophila grimshawi*	Dgri\\GH24563
LOC108606550	*Drosophila busckii*	A0A0M3QZR8
ASIS013534	*Anopheles sinensis*	undef
LOC115564076	*Drosophila navojoa*	G-protein coupled receptor moody
AFUN001241	*Anopheles funestus*	GPCR F1_2 domain-containing protein
Pn.11395	*Polypedilum nubifer*	undef
122624167	*Drosophila teissieri*	protein trapped in endoderm-1 isoform X1
100164199	*Acyrthosiphon pisum*	GPCR F1_2 domain-containing protein
122710367	*Apis laboriosa*	G-protein coupled receptor moody isoform X1
Dsim\\GD26931	*Drosophila simulans*	G-protein coupled receptor moody
LOC108164553	*Drosophila miranda*	G-protein coupled receptor moody
118461917	*Anopheles albimanus*	GPCR F1_2 domain-containing protein
GY	*00002861-RA*	Galloisiana yuasai
LOC111415354	*Onthophagus taurus*	protein trapped in endoderm-1-like isoform X1
121590950	*Anopheles merus*	G-protein coupled receptor moody isoform X1
LOC105150226	*Acromyrmex echinatior*	protein trapped in endoderm-1
LOC108136305	*Drosophila elegans*	G-protein coupled receptor moody
LOC117643260	*Thrips palmi*	LOC117643260
120455391	*Drosophila santomea*	G-protein coupled receptor moody
118505206	*Anopheles stephensi*	protein trapped in endoderm-1
LOC108023533	*Drosophila biarmipes*	G-protein coupled receptor moody isoform X1
101888758	*Musca domestica*	GPCR F1_2 domain-containing protein

LOC111359012	*Spodoptera litura*	protein trapped in endoderm-1-like isoform X1
LLUN010089	*Limnephilus lunatus*	undef
PHUM288250	*Pediculus humanus*	undef
ACUA009446	*Anopheles culicifacies*	GPCR F1_2 domain-containing protein
Tre1	*Drosophila melanogaster*	Tre1
120896444	*Anopheles arabiensis*	protein trapped in endoderm-1-like
118511880	*Anopheles stephensi*	protein trapped in endoderm-1-like
ACHR001850	*Anopheles christyi*	GPCR F1_2 domain-containing protein
105618428	*Atta cephalotes*	GPCR F1_2 domain-containing protein
ADAC002409	*Anopheles darlingi*	GPCR F1_2 domain-containing protein
124154249	*Ischnura elegans*	G-protein coupled receptor moody isoform X1
119644785	*Glossina fuscipes*	protein trapped in endoderm-1 isoform X1
LOC111356475	*Spodoptera litura*	G-protein coupled receptor moody-like isoform X1
LOC111356629	*Spodoptera litura*	G-protein coupled receptor moody-like
LLOJ003459	*Lutzomyia longipalpis*	GPCR F1_2 domain-containing protein
LLOJ008669	*Lutzomyia longipalpis*	A0A1B0CUN4
ACUA002480	*Anopheles culicifacies*	GPCR F1_2 domain-containing protein
LOC108369982	*Rhagoletis zephyria*	G-protein coupled receptor moody-like
ACHR007042	*Anopheles christyi*	GPCR F1_2 domain-containing protein
123300017	*Chrysoperla carnea*	G-protein coupled receptor moody-like
118267704	*Spodoptera frugiperda*	G-protein coupled receptor moody-like isoform X1
LOC108568736	*Nicrophorus vespilloides*	protein trapped in endoderm-1
Dgri\\GH24406	*Drosophila grimshawi*	Dgri\\GH24406
PPAI007746	*Phlebotomus papatasi*	GPCR F1_2 domain-containing protein
122710373	*Apis laboriosa*	dopamine receptor 3-like

LOC106671023	*Cimex lectularius*	G-protein coupled receptor moody isoform X1
LOC117903752	*Drosophila subobscura*	G-protein coupled receptor moody
LOC101737358	*Bombyx mori*	G-protein coupled receptor moody isoform X1
119556719	*Drosophila subpulchrella*	protein trapped in endoderm-1
GPPI025997	*Glossina palpalis*	undef
GBUE012265	*Gerris buenoi*	undef
LOC108124825	*Drosophila bipectinata*	LOC108124825
118456768	*Anopheles albimanus*	G-protein coupled receptor moody-like isoform X1
101888937	*Musca domestica*	GPCR F1_2 domain-containing protein
LOC105150171	*Acromyrmex echinatior*	G-protein coupled receptor moody isoform X1
Dgri\\GH12042	*Drosophila grimshawi*	Dgri\\GH12042
Dana\\GF22194	*Drosophila ananassae*	GPCR F1_2 domain-containing protein
LOC108367270	*Rhagoletis zephyria*	G-protein coupled receptor moody
LOC105211385	*Zeugodacus cucurbitae*	P2Y purinoceptor 4
LOC108041910	*Drosophila rhopaloa*	LOC108041910
F560DEB183A782A69D8917DC121EA2C6	*Clunio marinus*	A0A1J1ING5
LOC108618273	*Drosophila arizonae*	G-protein coupled receptor moody
LOC100747153	*Bombus impatiens*	LOC100747153
AMIN011421	*Anopheles minimus*	GPCR F1_2 domain-containing protein

Table 3.S3. Primers sequences used in this study.

Table 3.S3: Primer sequences				
Vectorbase accession	**Forward primer**	**Reverse primer**	**Primer type**	**qPCR Efficiency**
AAEL003647	TGTAATCATCACTTTCGCCA	CCAAAGATGATGGCTTGAAC	qPCR	0.87
	TAATACGACTCACTATAGGGAGAAGACCGTATCCTATCTTCAGG	TAATACGACTCACTATAGGGAGATACCATTTTGATGACCTTCAC	RNAi	
AAEL019988	CAATCCATTCATTTACGCCA	AGATTTGTTCACTTCGTCGA	qPCR	0.91
	TAATACGACTCACTATAGGGAGAGGTGAGGATTTGTGTAAAGTG	TAATACGACTCACTATAGGGAGAGAAGCATACGTAGATGGTCAG	RNAi	
AAEL009496	ACCGCCGTCTACGATGCCA	ATGGTGGTCTGCTGGTTCTT	qPCR	
Underlined sequences denote T7 sequence for dsRNA synthesis				

Figure 3.S1. Full AAEL003647 phylogeny.

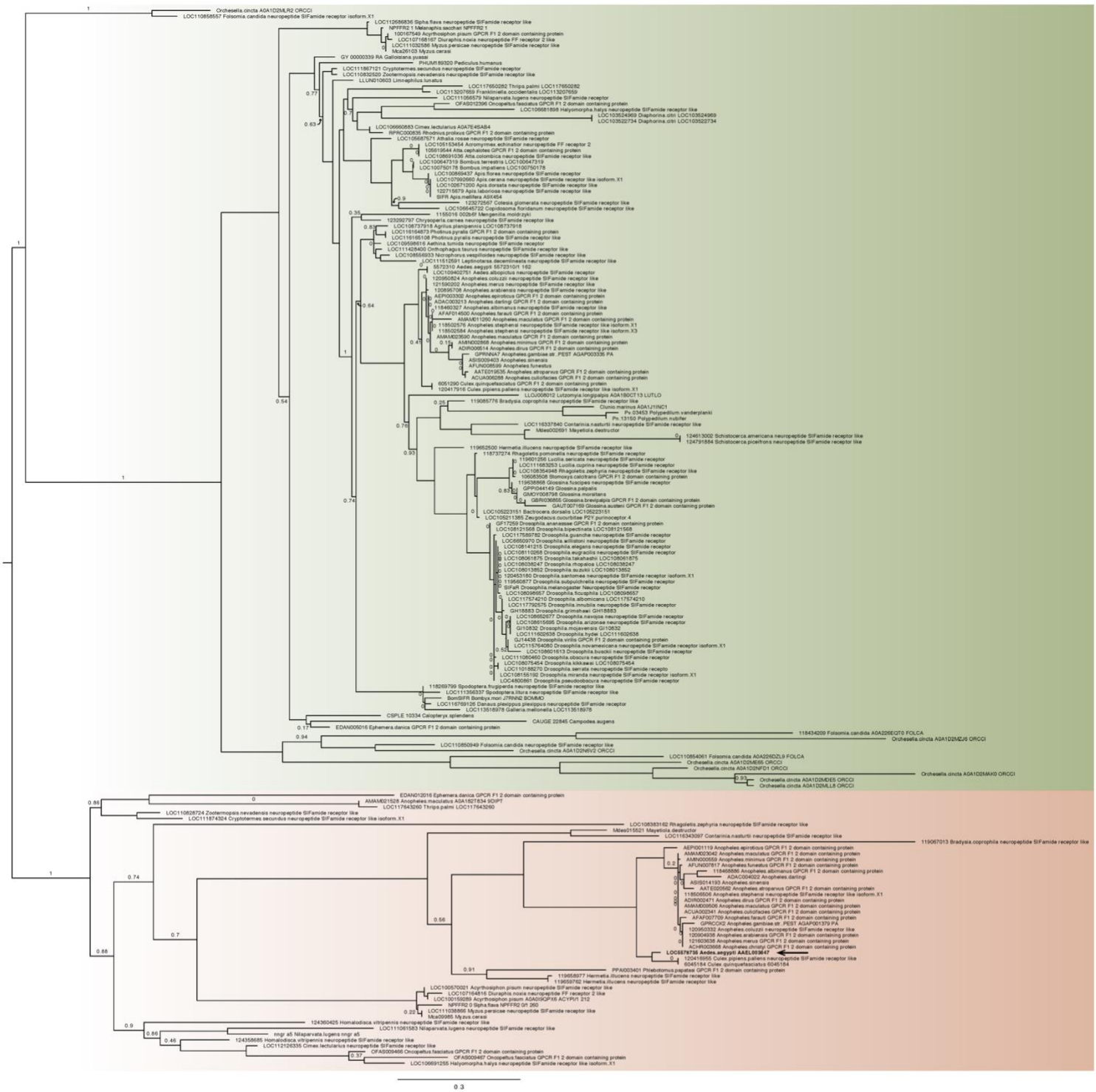

Figure S1: Expanded maximum likelihood tree of AAEL003647 and its orthologs in other insects. Orthologs of AAEL003647 have been lost in many brachyceran taxa, including members of the genus *Drosophila*. AAEL003647 is most closely related to the SIFamide receptor. Sequences were downloaded from OrthoDB and aligned against a 7 transmembrane GPCR model (7tm-1.hmm) in hmmalign. Trees were built in PhyML. Support values are aLRT SH-like, and branches with support values < 0.95 are labeled with their support values. F1 2 domain containing protein is abbreviated as "F1 2 dom. con't. prot."

Figure 3.S2. Full AAEL019988 phylogeny.

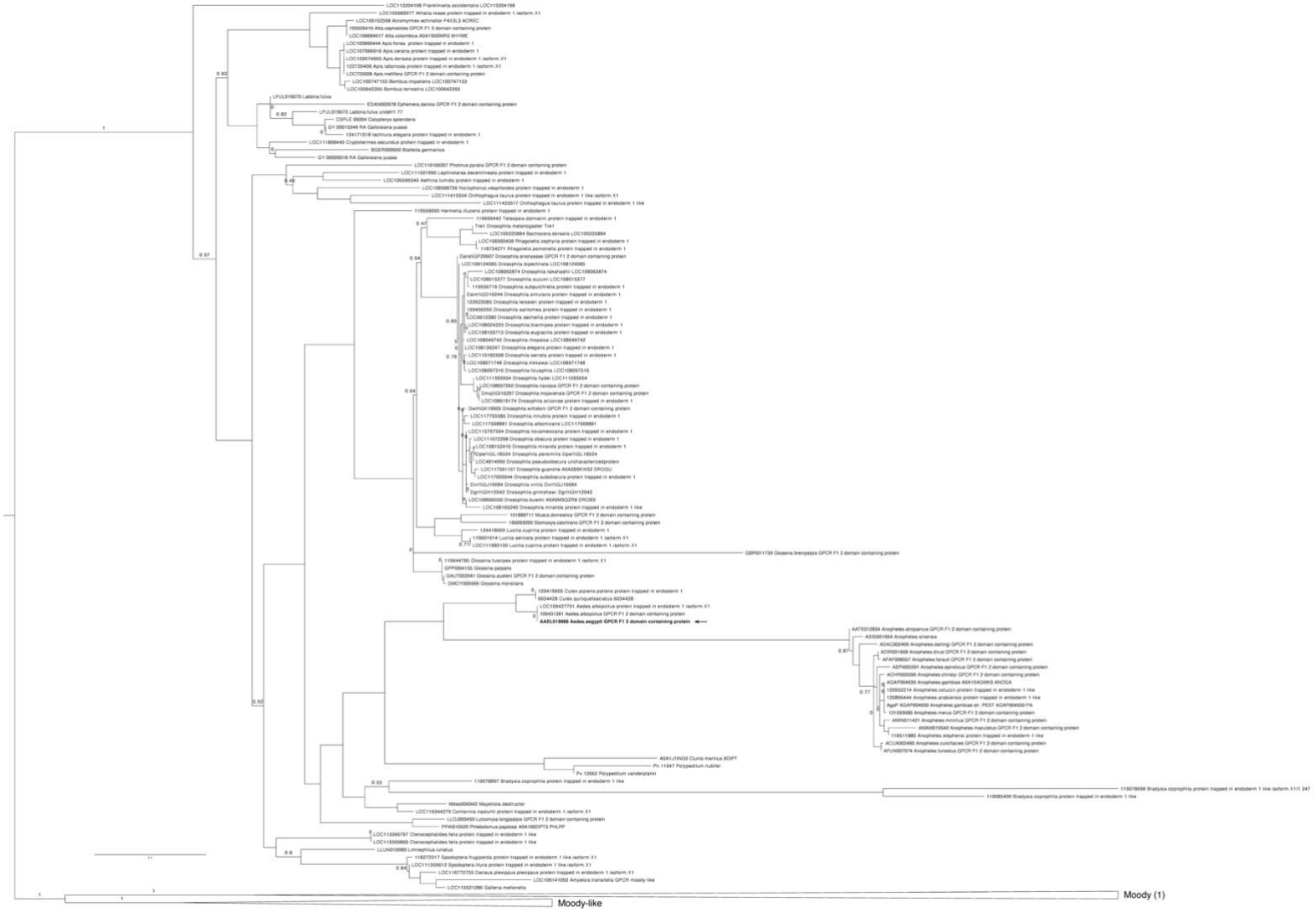

Figure S2: Expanded maximum likelihood tree of AAEL019988 and its orthologs in other insects. Genome sequences of most hemimetabolous insects do not encode an ortholog of AAEL019988. Sequences were downloaded from OrthoDB and aligned against a 7 transmembrane GPCR model (7tm-1.hmm) in hmmalign. Trees were built in PhyML. Support values are aLRT SH-like, and branches with support values < 0.95 are labeled with their support values.

CHAPTER 4

MICROBES INFLUENCE DE NOVO LIPOGENESIS AND BLOOD MEAL DIGESTION THROUGH MODULATION OF THE ACETYL-COA CARBOXYLASE AND FATTY ACID SYNTHASE GENES IN THE CHAGAS VECTOR *RHODNIUS PROLIXUS* [3]

[3]Keyes-Scott NI, Bimpeh K, Allen LR, Hines KM, Vogel KJ. To be submitted to MBio.

4.1 Abstract

The acetyl-CoA carboxylase (ACC) *de novo* lipogenesis pathway is conserved in mammals and insects, and it facilitates the conversion of dietary amino acids and glucose to lipids. This pathway is especially essential for obligately hematophagous insects, given there are nutritional components, such as lipids and vitamins, that are not highly abundant in a blood meal. Gut bacteria also play a role in nutrient supplementation, which subsequently promotes development and metabolism in insects. The symbiont, *Rhodococcus rhodnii*, in the kissing bug *Rhodnius prolixus* is able to function as a sole symbiont within the gut of *R. prolixus*, supporting development and reproduction. We sought to examine the role of the kissing bug microbiome in lipid metabolism in *R. prolixus* using axenic (germ-free), singly inoculated *R. rhodnii* (gnotobiotic), and conventional, unmanipulated fourth instar nymphs. We identified differences in fat body triglyceride levels among axenic, conventional, and gnotobiotic nymphs after a blood meal. Using quantitative PCR, we examined expression of *acc* and a fatty acid synthase ortholog, *fas289*, (RPRC011289) involved *in de novo* synthesis of fatty acids. Finally, we conducted lipidomic analysis of gut and fat body tissue to further interrogate the role of the microbiome in kissing bug lipid synthesis and metabolism. We found that the microbiome influences expression of *acc* and *fas289* and promotes the synthesis of several lipid classes in the fat body of *R. prolixus* nymphs.

4.2 Introduction

The kissing bug, *Rhodnius prolixus,* is an obligately hematophagous insect and vector of *Trypanosoma cruzi*, the causative agent of Chagas disease. Chagas disease is neglected tropical disease that affects an estimated six to eight million individuals per year (CDC 2023). In *R.*

prolixus, fatty acids and phospholipids are absorbed by midgut epithelial cells after consumption of a blood meal (Gondim et al. 2018). Lipases within the midgut hydrolyze diet-derived triacylglycerol (TAG) to free fatty acids which can be incorporated into phospholipids by the midgut epithelial cells to form the perimicrovillar membrane or alternatively can be transported through the hemolymph to the fat body or ovary by lipophorin carrier proteins (Atella et al. 1995; Bittencourt-Cunha et al. 2013; Grillo et al. 2003; Grillo et al. 2007; Entringer et al. 2013). In vertebrate blood, lipids are lower in abundance relative to proteins, thus hematophagous insects *de novo* synthesize fatty acids from amino acids and carbohydrates after lipid resources from a blood meal have been exhausted (Lynch et al. 2017; Sorapukdee and Narunatsopanon 2017; Gondim et al. 2018).

Acetyl-CoA carboxylase (ACC) is the rate limiting enzyme for *de novo* lipogenesis in hematophagous insects (Moraes et al. 2022; Gondim et al. 2018). Acetyl-CoA products from amino acid and glucose metabolism are converted to malonyl-CoA by ACC, and this process is biotin dependent (Wang et al. 2022; Lee et al. 2008). Malonyl-CoA subsequently serves as a substrate for the synthesis of long chain fatty acids by fatty acid synthases (FAS). In *R. prolixus*, *acc* is most highly expressed in the anterior and posterior midgut but is also expressed in the fat body and ovaries (Moraes et al. 2022). Inhibition of *acc* expression through RNA interference (RNAi) results in a reduction of all major lipid classes in the *R. prolixus* fat body (Moraes et al. 2022). *Acc* knockdown in *R. prolixus* also resulted in impairs blood meal digestion, reduces fecundity, and results in malformation of the eggshell (Moraes et al. 2022). Fatty acid metabolism is also connected to blood meal digestion in female *Aedes aegypti* mosquitoes (Alabaster et al. 2011).

In eukaryotes, ACCs are conserved, and one copy exists in insects and plants, while two isoforms exist in mammals (Abu-Elheiga et al. 2003, Wang et al. 2022, Wei et al. 2016). ACC activity is biotin dependent, and biotin is one among eight essential B vitamins that are unable to be synthesized by animals and must be acquired through dietary or microbial supplementation. In obligately hematophagous insects, symbionts are essential for provisioning B vitamins because it is widely accepted that B vitamins are not abundant in vertebrate blood (Bing et al. 2017; Hickin et al. 2022; Hosokawa et al. 2010). B vitamin supplementation is known to be a function of the bacterial symbionts in most hematophagous arthropods (Salcedo-Porras et al. 2020). For example, *Wigglesworthia*, in the tseste fly and *Wolbachia* in the bed bug are known to supplement B vitamins (Rio et al. 2016; Hosokawa et al. 2010; Hickin et al. 2022).

B vitamin provisioning is also thought to be the primary role of the extracellular gut-symbiont *Rhodococcus rhodnii* in its kissing bug host, *R. prolixus*. Removal of *R. rhodnii* via surface sterilization of eggs results in increased mortality, elongated nymphal developmental times, and complete developmental arrest at the fifth instar (Wigglesworth 1936; Gilliland et al. 2023). The genome sequence of *R. rhodnii* demonstrates that this bacteria can synthesize all eight essential B vitamins through *de novo* or salvage biosynthesis pathways (Gilliland et al. 2023). Microbes also aid lipid synthesis and mobilization in insects, where insects lacking symbiotic bacteria are unable to effectively synthesize and metabolize lipids (Zhou et al. 2021; Shin et al. 2011; Valzania et al. 2018a). Given the known function of B vitamin supplementation by symbionts and the role of symbionts in lipid synthesis and metabolism, we wanted to explore the contributions of the *R. prolixus* microbiome in lipogenesis.

We chose to first examine fat body triglyceride levels after feeding in *R. prolixus* fourth instar nymphs reared with a conventional or unmanipulated microbiome, singly inoculated with

R. rhodnii (gnotobiotic), or axenic (germ-free). We found that axenic bugs had significantly lower fat body triglyceride levels relative to conventional and gnotobiotic bugs, providing evidence that the microbiome promotes lipid synthesis. We further wanted to understand the mechanism in which the microbiome influenced lipid synthesis and examined expression of *acc* and an unannotated fas ortholog, *fas289* (RPRC011289), in the whole gut and fat body of axenic, conventional, and gnotobiotic fourth instar nymphs. We used RNA interference to determine the role of FAS289 in kissing bug lipogenesis. Finally, to identify potential deficiencies in free fatty acids, and to examine the role of the microbiome on the synthesis on other classes of lipids, we conducted a whole gut and fat body lipidomics analysis.

4.3 Methods and Materials

Insect rearing

Rhodnius prolixus were acquired from the lab of Dr. Ellen Dotson at the Center for Disease Control through BEI Resources. Insects were housed in a temperature-controlled incubator maintained at 28°C and 80% RH under a 12L:12D photoperiod cycle. Gnotobiotic and axenic insects were generated using methods described in Gilliland et al. 2023. *R. prolixus* eggs were surface sterilized with a series autoclaved deionized water, 70% ethanol, and iodine washes. Sterile eggs were placed in autoclaved mason jars which were secondarily contained in autoclaved plastic Nalgene containers. A small hole was created in lids of the autoclaved Nalgene containers for oxygen exchange, and the lids were covered with gas exchange membrane to maintain sterile conditions within the jar.

Gnotobiotic bugs were fed defibrinated rabbit blood (Hemostat Laboratories) inoculated with *Rhodococcus rhodnii* at a concentration of 10^6 CFU. Axenic bugs were fed sterile rabbit blood.

Gnotobiotic and axenic bugs were maintained in autoclaved mason jars and sterile secondary containment throughout development. Conventional bugs were fed defibrinated rabbit blood (Hemostat Laboratories) inoculated with *Rhodococcus rhodnii* at a concentration of 10^6 CFU but were not maintained in sterile conditions. All bugs were fed two to three weeks post-molt at each instar and were sorted by feeding status within one day following a blood meal. Fourth instar axenic, conventional, and gnotobiotic nymphs were used for all experiments. All non-blood fed insects used for experiments were starved and at least thirty days post fourth instar molt.

Expression analysis

Axenic, conventional, and gnotobiotic bugs were dissected, and whole gut (anterior midgut, posterior midgut, and hindgut) and fat body tissues were collected from non-blood fed bugs and at 4, 10, and 20 days post blood meal (pbm). The twenty-day pbm bugs followed the fourth to fifth instar molt. Tissues were placed in a 1.5 mL Eppendorf tube with 100 µL of *Aedes* saline (Hayes 1953) and were frozen at -80° C until RNA extraction. Tissues were placed in a 1.5 mL microcentrifuge tube with 100 µL of *Aedes* saline and were frozen at -80° C until RNA extraction. The Zymo Direct-zol RNA MagBead Kit with TRIzol kit, was used in a KingFisher Apex Dx system (ThermoFisher Scientific) for RNA extractions and DNase steps, per the manufacturer instructions.

One hundred nanograms of RNA was used as template to synthesize cDNA using the iScript cDNA synthesis kit (BioRad, Hercules, CA, USA). cDNA was used as template for quantitative real-time PCR, with the QuantiNova SYBR Green PCR kit (Qiagen) and gene specific primers (Table 4.S1). Standard curves for each gene were generated by cloning qPCR products into the pSCA vector with the Strataclone PCR cloning kit (Agilent, Santa Clara, CA, USA), isolating

plasmid DNA using the GeneJET Plasmid Miniprep Kit (Thermo Scientific, Vilnius, Lithuania), and preparing plasmid standards from 10^7 to 10^2 copies.

Preparation of dsRNAs and knockdown bioassays

Target regions of 300-500 bp were selected as targets for dsRNA synthesis for RNAi-mediated knockdown of the FAS ortholog (RPRC011289), subsequently referred to as *fas289*, and acetyl-CoA carboxylase (*acc*: RPRC013987), identified by Saraiva et al. 2021. Primers with the T7 promoter sequence were used to amplify each target using cDNA synthesized from RNA isolated from gnotobiotic fourth instar fed and unfed bug gut or fat body tissues (Table 4.S1). PCR products were cloned into the pSCA vector, and plasmid DNA was extracted as previously described. Plasmid DNA from each gene target and an EGPF control were used as the templates for dsRNA synthesis. dsRNA was synthesized using the Ambion™ MEGAscript RNAi kit (ThermoFisher Scientific, Vilnius, Lithuania), following manufacturer instructions. After dsRNA synthesis, dsRNA was precipitated in sodium acetate and ethanol, then resuspended in *Aedes* saline to a concentration of 1 μg/μL. Non-blood fed conventional fourth instar nymphs were injected with 1μL of dsRNA and were fed three days following microinjection. To examine the impacts of *fas289* and *acc* knockdown on triglyceride accumulation and blood meal digestion, the fat body and anterior midgut of knockdown bugs were collected at ten days pbm.

Triglyceride quantification

Non-blood fed axenic, conventional, and gnotobiotic bugs were blood fed and the fat body was dissected at 1, 4, 7, 10, and 20 days pbm. The fat body tissues were collected in 100 μL of 1x PBS with 0.5% Tween 20, and samples were frozen at −80°C for at least 24 hours prior to

triglyceride extraction. Samples were thawed on ice, then homogenized with an electric rotor pestle. Samples were incubated at 65°C for five minutes, then centrifuged for 3 minutes at 10,000 rpm. The supernatant was transferred to a new 1.5 mL Eppendorf tube, then centrifuged at 14,000 rpm for 3 minutes to remove all residual tissue. Lipid extracts were transferred to a new 0.6 mL tube. An additional 100 µl of 1x PBS with 0.5% Tween 20 was added to dilute samples, as necessary.

From each lipid extract, 10 µL was loaded on a 96-well polystyrene plate (Greiner Bio-One, USA) in triplicate. A standard line with pure triglyceride standard (MedTest Dx, Canton, MI, USA) ranging from 0.15 to 20mg was added to every plate of unknowns. Immediately following standard and sample loading, 100 µL of Infinity™ Triglycerides Liquid Stable Reagent by ThermoFisher was added to each well, and samples incubated in the dark at room temperature for 10 minutes. After incubation, the well plate was read on a colorimetric plate reader at 540nm.

Blood meal digestion quantification

To measure blood meal accumulation in non-blood fed insects, third instar conventional, gnotobiotic, and axenic bugs were fed and collected thirty days pbm following the fourth instar molt. To measure blood meal accumulation in fed insects, intact anterior midguts from axenic, conventional, and gnotobiotic fourth instar bugs were collected at 2 hours, 10 days, and 20 days pbm in 1.5 mL microcentrifuge tubes with 100 µl of 1x PBS. Samples were frozen at −80°C until protein quantification. For protein quantification, samples were thawed on ice then homogenized with an electric rotor pestle. To remove gut tissue, samples were centrifuged at 10,000 rpm for 1 minute. The supernatant was transferred to a new tube and were further diluted 1x PBS, as necessary. From each anterior midgut sample homogenate, 10 µl was loaded on a 96-well

polystyrene plate (Greiner Bio-One, USA) in triplicate. The Pierce BCA Protein quantification kit by ThermoFisher was used for protein quantification following manufacturer instructions. A BSA standard ranging from 0.01 to 2.5mg was added to every plate of unknowns. Plates were read on a colorimetric plate reader at 562nm.

LC-MS preparation and lipidomic analysis

The whole gut and fat body was collected from unfed and four day pbm axenic, conventional, and gnotobiotic fourth instar bugs. The anterior midgut of four day pbm bugs was severed to release blood contents and tissues were rinsed three times with sterile 1x PBS. Tissues were homogenized with an electric pestle and frozen at −80°C until later processing. To extract lipids, homogenized tissue samples in 0.5 mL of PBS were transferred glass tube and sonicated in an ice bath for 30 minutes. Next, the samples were extracted using the modified Bligh and Dyer extraction method (Carpenter et al. 2024). Briefly, 2mL of chilled 1:2(v/v) chloroform/methanol was added to the samples and vortexed for 5 min on ice. Following this, an additional volume of 0.5 mL each of water and chloroform was added to the mixture and vortexed for 1 min. The resulting mixture was centrifuged at 2000xg at 4°C for 10 min. The organic layer was then carefully transferred to a new glass tube, dried, and reconstituted in 1:1 (v/v) chloroform/methanol for storage at -80 °C until use.

Lipid extracts were analyzed using hydrophilic interaction liquid chromatography (HILIC) coupled with traveling wave ion mobility (TWIMS) mass spectrometry in both positive and negative ionization modes. Chromatographic separations were carried out with Waters Cortecs UPLC HILIC column (2.1 x 100 mm, 1.6 µm) over 7 minutes gradient method(cite). The effluent from the UPLC was connected to the electrospray ionization source of the TWIMS

instrument, and the experiments were conducted according to previously described ionization settings(cite). Peak Picking and alignment of LC-MS data were performed using Progenesis QI (v3.0, Nonlinear Dynamics, Waters). Multivariate statistical analysis with EZ Info (v3.0, Umetrics) was used to identify the features that significantly contributed to the experimental differences. Lipid species were identified using LipidPioneer (Ulmer et al. 2017) and the Human Metabolome Database (HMDB) (Wishart et al. 2007, 2009, 2013, 2018, 2022).

4.4 Results

Comparison of fat body triglyceride content among axenic, conventional, and gnotobiotic fourth instar nymphs

To investigate the role of the microbiome in metabolism, we first examined the fat body triglyceride levels in starved fourth instar axenic, conventional, and gnotobiotic fourth instar nymphs (figure 4.1). We found a significant difference in fat body triglyceride levels among axenic, conventional, and gnotobiotic bugs over multiple times pbm (Browne-Forsythe ANOVA, $F_{(2, 11)} = 31.22$, $p < 0.0001$). We found that fat body triglyceride levels were significantly higher in non-blood fed conventional nymphs compared to gnotobiotic nymphs (Welch's t, $p > 0.026$). One day pbm axenic bugs had significantly lower triglyceride stores than conventional (Welch's t, $p = 0.045$) and gnotobiotic bugs (Welch's t, $p = 0.004$).

Similarly at four days pbm, axenic bugs also had significantly lower fat body triglycerides relative to conventional (Welch's t, $p = 0.006$) and gnotobiotic bugs (Welch's t, $p = 0.038$). At ten days following a blood meal, conventional bugs had significantly higher triglyceride levels relative to axenic (Welch's t, $p < 0.0001$) and gnotobiotic bugs (Welch's t, $p = 0.002$). Twenty days following a blood meal, axenic bugs had significantly higher fat body triglyceride levels

compared to gnotobiotic bugs (Welch's t, $p = 0.041$). From these data, we concluded that axenic bugs underwent a delay in fat body triglyceride accumulation compared to conventional and gnotobiotic bugs until ten days pbm. At ten days pbm, conventional bugs exhibited the highest accumulation of triglycerides, suggesting that a higher bacterial abundance or diversity might be beneficial for triglyceride accumulation. Finally, the accumulation of triglyceride in the fat body of axenic bugs at twenty days pbm may be a symptom of delayed triglyceride mobilization.

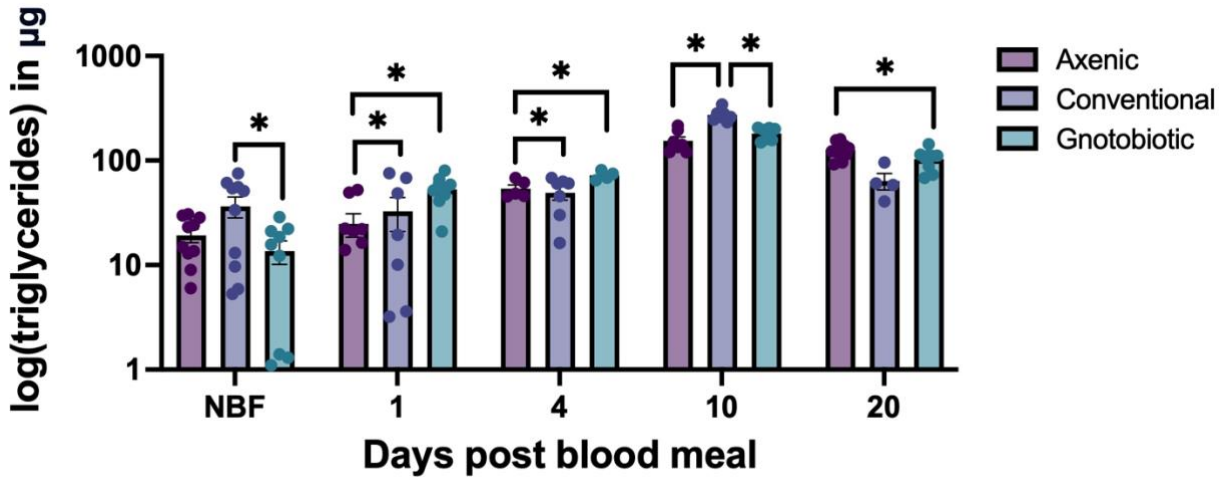

Figure 4.1. Triglycerides profiles of non-blood fed (NBF) fourth instar axenic, conventional, and gnotobiotic nymphs at multiple days post blood meal. Statistical significance was determined using the Browne-Forsythe ANOVA, followed by Welch's t, where *, **, ***, and **** represent $p < 0.05$, $p < 0.01$, $p < 0.001$, and $p < 0.0001$, respectively. Sample sizes were n ≧ 7 tissues per treatment and time point.

The microbiome differentially affects *acc* expression in the whole gut and fat body

Given that ACC is the rate limiting enzyme for *de novo* lipogenesis, we next wanted to investigate the role of the microbiome in modulation of *acc* expression in the whole gut and fat body across several times after feeding among axenic, conventional, and gnotobiotic fourth instar nymphs (figure 4.2). We discovered that there was an effect of the microbiome on *acc*

expression among axenic, conventional, and gnotobiotic bugs in the whole gut (two-way ANOVA, $F_{(2, 36)} = 6.15$, $p = 0.005$) and in the fat body (two-way ANOVA, $F_{(2, 33)} = 5.64$, $p = 0.008$).We found that four-day pbm gnotobiotic bugs had significantly higher expression of *acc* relative to axenic (Tukey's HSD, $p = 0.0001$) and conventional bugs (Tukey's HSD, $p < 0.0001$). There were no significant differences in whole gut expression of *acc* among non-blood fed axenic, gnotobiotic, or conventional bugs at ten or twenty days pbm (Tukey's HSD, $p > 0.05$). In the fat body of non-blood fed gnotobiotic bugs, we observed higher expression of *acc* compared to conventional bugs (Tukey's HSD, $p = 0.013$). Unexpectedly, at ten days pbm, the fat body of axenic bugs expressed *acc* at a significantly higher rate relative to conventional (Tukey's HSD, $p < 0.001$) and gnotobiotic bugs (Tukey's HSD, $p < 0.001$). There was no significant influence of the microbiome on fat body expression in axenic, conventional, or gnotobiotic nymphs at four or

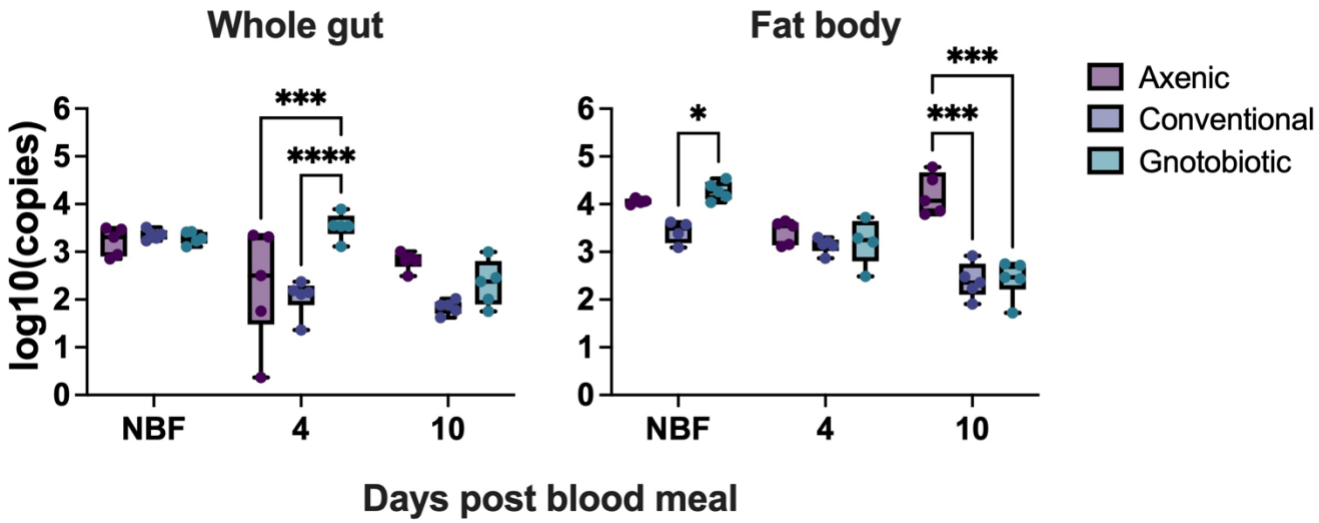

Figure 4.2. Expression profile of acetyl-CoA carboxylase (*acc*) in the whole gut and fat body in non-blood fed (NBF) and fed fourth instar axenic, conventional, and gnotobiotic bugs at multiple times post blood meal. Error bars represent one standard error above and below the mean. Statistical significance was determined using a two-way ANOVA followed by Tukey's HSD, where *, **, ***, and **** represent $p < 0.05$, $p < 0.01$, $p < 0.001$, and $p < 0.0001$, respectively. Sample sizes were n = 4-5 tissues per treatment, per time point.

twenty days pbm (Tukey's HSD, $p > 0.05$). From these data, we concluded that the gut microbiome does modulate *acc* expression in the whole gut and fat body, and that this may affect lipogenesis and expression of downstream genes involved in lipogenesis.

Impacts of the microbiome on blood meal digestion

We observed that axenic bugs had an accumulation of undigested blood in the anterior midgut after molting. We hypothesized that the microbiome may promote blood meal digestion, which in tandem promotes lipogenesis. To understand the impacts of the microbiome in blood meal digestion, we quantified the anterior midgut protein content of axenic, conventional, and gnotobiotic fourth instars bugs before and after a blood meal. We found a significant effect of

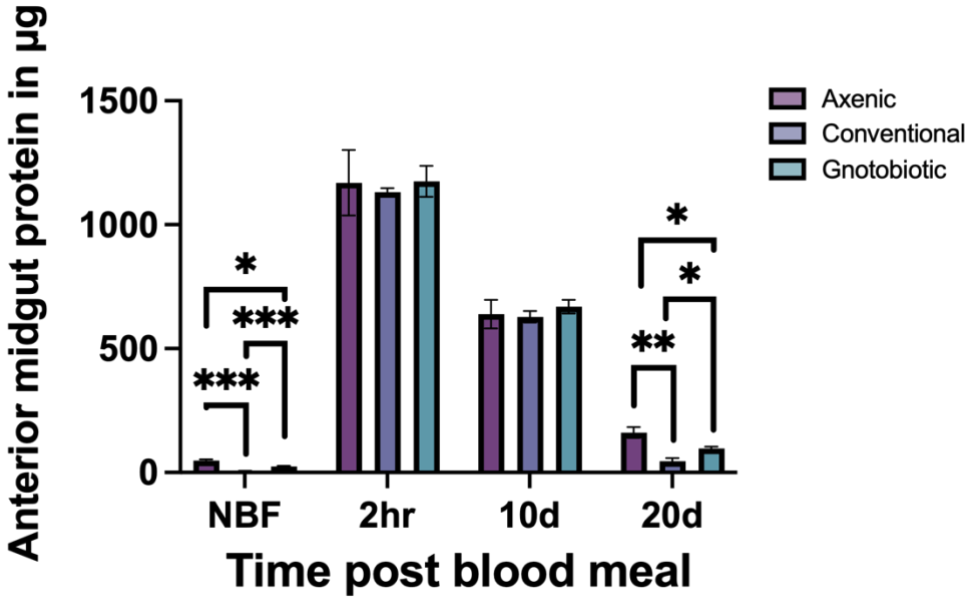

Figure 4.3. Anterior midgut protein content in non-blood fed (NBF), axenic, conventional, and gnotobiotic fourth instar bugs and at 2 hours, 10 days, and 20 days post blood meal. Error bars represent one standard error above and below the mean. Statistical significance was determined using the Browne-Forsythe ANOVA, followed by Welch's t, where *, **, ***, and **** represent $p < 0.05$, $p < 0.01$, $p < 0.001$, and $p < 0.0001$, respectively. Sample sizes were n = 3-10 tissues per treatment, per time point.

gnotobiotic state on anterior midgut protein content (Browne-Forsythe ANOVA, $F_{(2, 11)} = 31.22$, $p < 0.0001$). We found that axenic bugs exhibited a significant retention of blood in the anterior midgut relative to conventional (Welch's t, $p < 0.001$) and gnotobiotic bugs (Welch's t, $p < 0.001$), following a molt (figure 4.3). Only fully engorged individuals were selected at two hours pbm, and there was no significant difference in blood meal size among the treatments (Welch's t, $p > 0.05$). Further, was there no difference anterior midgut protein content at ten days pbm (Welch's t, $p > 0.05$). However, at twenty days following a blood meal and following the fourth to fifth instar molt, axenic bugs showed a significant retention of blood in the anterior midgut compared to conventional (Welch's t, $p < 0.001$) and gnotobiotic bugs (Welch's t, $p = 0.004$). From these data, we concluded that the microbiome promotes blood meal digestion or peristaltic activity that facilitates the movement of the blood meal from the anterior midgut through the digestive tract.

The microbiome differentially affects expression of *fas289* a fatty acid synthase ortholog

We next wanted to understand if the microbiome modulates expression of a fatty acid synthase ortholog, *fas289*, which is immediately downstream of ACC. To determine the role of the microbiome in *fas289* expression, we first conducted an expression analysis in non-blood fed, 4, and 10 day pbm axenic, conventional, and gnotobiotic fourth instar bugs comparing expression of *fas289* in the whole gut and fat body. We found a significant effect the gut microbiome on *fas289* expression in the fat body (two-way ANOVA, $F_{(2, 31)} = 3.33$, $p = 0.049$), but not in the whole gut (two-way ANOVA, $F_{(2, 32)} = 2.17$, $p > 0.05$) We found significantly higher expression of *fas289* in the fat body of axenic bugs at ten days pbm compared to conventional (Tukey's HSD, $p = 0.002$) and gnotobiotic bugs (Tukey's HSD, $p = 0.03$). From

these data, we concluded that the microbiome modulates expression of *fas289* in the fat body, which is immediately downstream of ACC, and that this may reflect differences in fat body lipogenesis among axenic, conventional, and gnotobiotic bugs.

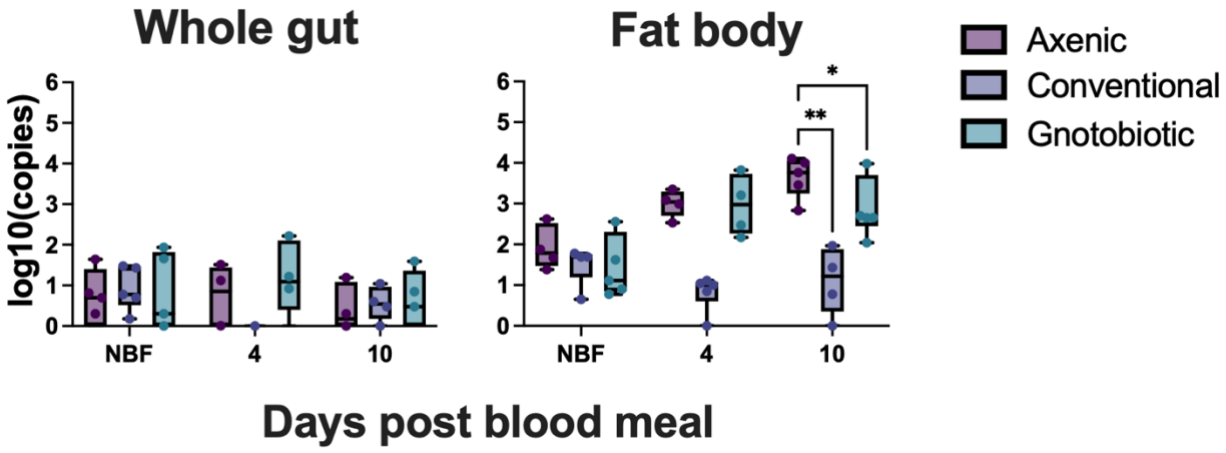

Figure 4.4. Expression profile of the fatty acid synthase ortholog (*fas289*) in the whole gut and fat body of non-blood fed (NBF) and fed axenic, conventional, and gnotobiotic fourth instar bugs at different times post blood meal. Error bars represent one standard error above and below the mean. Statistical significance was determined using a two-way ANOVA followed by Tukey's HSD, where * and ** represent $p < 0.05$, $p < 0.01$, respectively. Sample sizes were n = 4-5 tissues per treatment, per time point.

Knockdown of both *acc* and *fas289* decreases fat body triglyceride stores in conventional bugs

Fatty acid synthases are known to promote lipogenesis and triglyceride accumulation in insects, but the role of FAS289 in *R. prolixus* has not yet been described. We established that gut microbial communities impact lipogenesis and expression of *fas289.* Consequently, we wanted to assess the function of FAS289 in triglyceride accumulation. Our expectation was that knockdown of *fas289* would result in a decrease of triglyceride accumulation, as observed in axenic bugs. To test this, we carried out a series of RNAi knockdown experiments in which we

injected unfed fourth instar conventional bugs, fed them, and measured fat body triglyceride accumulation following a blood meal. It has been established by Saraiva et al. 2023 that knockdown of *acc* results in a significant reduction of fat body triglyceride stores in *R. prolixus*. We confirmed that *acc* knockdown results in decreased accumulation of fat body triglyceride, and we similarly found that knockdown of *fas289* results in a significant reduction of fat body triacylglycerol stores after ten days pbm (one-way ANOVA, $F_{(2, 11)} = 16.00$, $p < 0.0001$; Figure 4.5a). Saraiva et al. 2023 also established that knockdown of *acc* impairs digestion in *R. prolixus*. We found that while knockdown of *acc* does impair blood meal digestion (Welch's t, $p < 0.0001$;

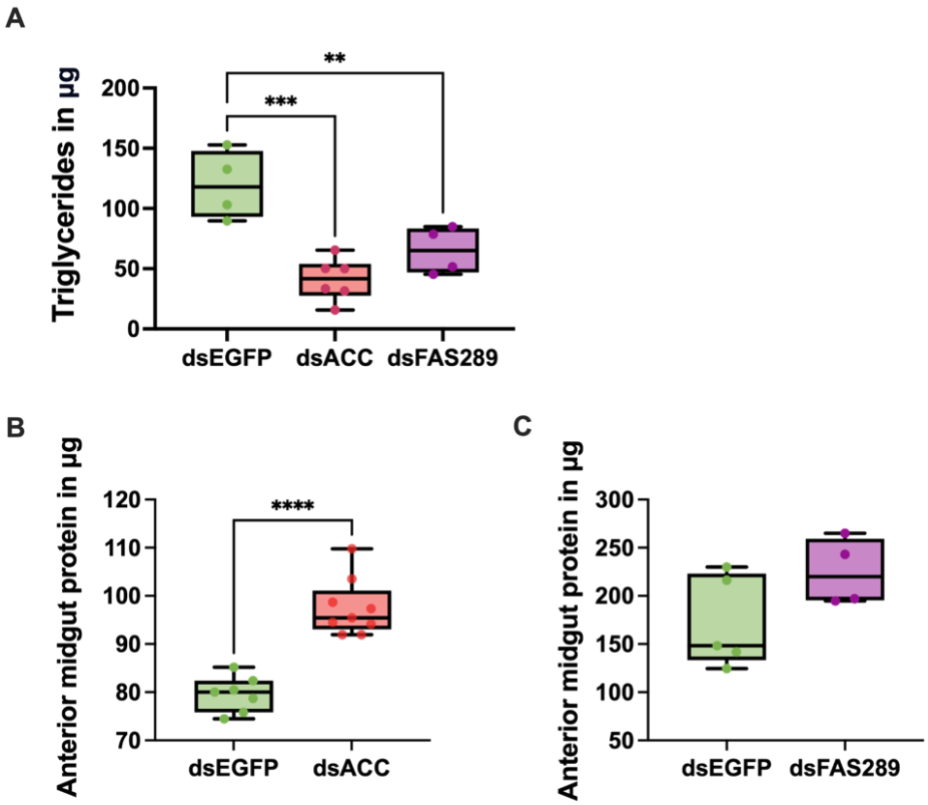

Figure 4.5. Effects of *acc* and *fas289* knockdown on (A) triacylglycerol levels and (B) and (C) blood meal digestion in ten days post blood meal (pbm) conventional bugs. Sample sizes were n ≧ 4 tissues per treatment. Error bars represent one standard error above and below the mean. Statistical significance was determined by one-way ANOVA (A) or Welch's t-test (B), where **, ***, and **** represent $p < 0.01$, $p < 0.001$, and $p < 0.0001$, respectively.

figure 4.5b), there was no significant effect of *fas289* knockdown on blood meal digestion (Welch's t, $p > 0.05$); figure 4.5c).

Contributions of the microbiome to whole gut and fat body lipogenesis

Because our triglyceride experiment revealed that axenic bugs had lower fat body triglyceride levels at one and four days post blood meal comparted to conventional and gnotobiotic bugs, we hypothesized that this might be due to having lower relative abundance of fatty acids available for triglyceride synthesis. Further, we hypothesized that the microbiome promotes the synthesis of additional lipid classes, including phospholipids and diacylglycerol. To test this, we conducted a whole gut and fat body lipidomics experiment using LC-MS in non-blood fed axenic, conventional, and gnotobiotic fourth instar bugs and at four days following a blood meal (figure 4.6 and figure 4.7). We identified significant differences in relative abundance of lipids in the whole gut of non-blood fed and four day pbm axenic, gnotobiotic, and conventional nymphs (two-way ANOVA, $F_{(2, 36)} = 14.71$, $p < 0.0001$). We found that in the whole gut of non-blood fed conventional bugs, there was significantly higher abundance of free FA 20:6 relative to gnotobiotic bugs (Tukey's HSD, $p = 0.031$; figure 4.6a). FA 20:6 is not a common fatty acid found in insects, however other 20 carbon chain fatty acids, such as arachidonic acid (FA 20:4) are implicated in insect immunity (Wrońska et al. 2023). There was no significant effect of the microbiome on whole gut free fatty acid levels of FA 17:6 or arachidonic acid (FA 20:4) in non-blood fed bugs (Tukey's HSD, $p > 0.05$). FA 17:6 is also not a common fatty acid found in insects, nor has a function been associated with this fatty acid in insects.

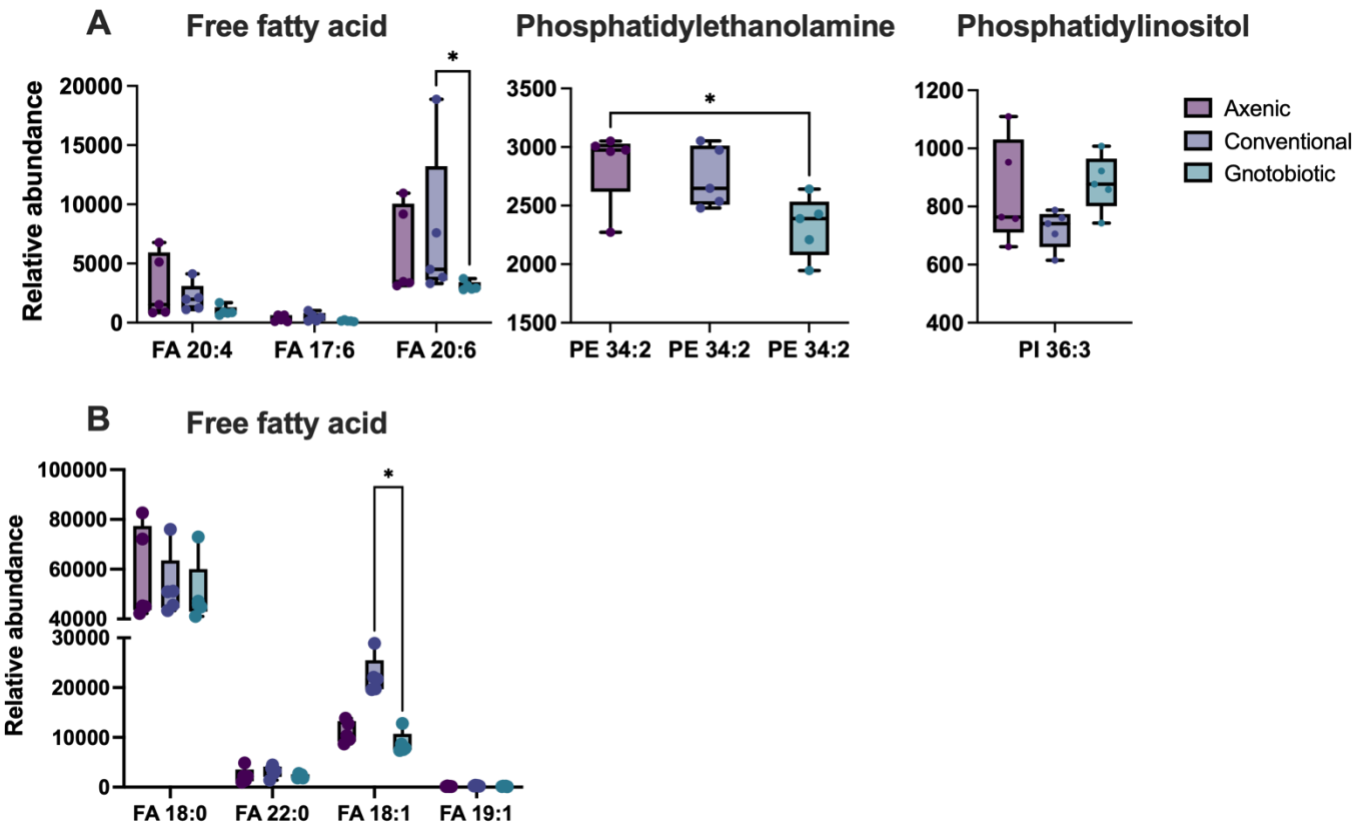

Figure 4.6. Whole gut lipidomics comparing axenic, conventional, and gnotobiotic fourth instar (A) non-blood fed nymphs and at (B) four days post blood meal, determined by LC-MS. Error bars represent one standard error above and below the mean. Sample sizes were n = 5 tissues per treatment and time point. Statistical significance was determined using one way and two-way ANOVA, followed by Tukey's HSD, where *, **, ***, and **** represent $p < 0.05$, $p < 0.01$, $p < 0.001$, and $p < 0.0001$, respectively. Fatty acids represented are (FA 17:6), stearic acid (FA 18:0), oleic acid (18:1), nonadecanoic acid (FA 19:1), arachidonic acid (FA 20:4), (FA 20:6), and behenic acid (FA 22:0).

There was significantly higher abundance of phosphatidylethanolamine (PE 32:4) in the whole gut among non-blood fed axenic, conventional and gnotobiotic bugs (one-way ANOVA, $F_{(2, 12)} = 4.83$, $p = 0.029$). Relative abundance of PE was higher in the fat body of axenic bugs compared to gnotobiotic bugs (Tukey's HSD, $p < 0.030$) but not to conventional bugs (Tukey's HSD, $p = 0.7978$). There was no significant impact of the microbiome on whole gut phosphatidylinositol abundance in non-blood fed bugs (two-way ANOVA, $p > 0.05$). In the

whole gut of four days pbm bugs, there was significantly higher abundance of lipids among axenic, conventional, and gnotobiotic bugs (two-way ANOVA, $F_{(3, 48)} = 156.4$, $p < 0.0001$). The relative abundance of oleic acid (FA 18:1) was higher in conventional bugs relative to gnotobiotic bugs (Tukey's HSD, $p = 0.020$), However, there was no difference between conventional and axenic bugs (Tukey's HSD, $p = 0.060$; figure 4.6b). There was no influence of the microbiome on whole gut stearic acid (FA 18:0), nonadecanoic acid (FA 19:0), or behenic acid (FA 22:0) abundance (Tukey's HSD, $p > 0.05$). Altogether, our non-blood fed nymphal whole gut lipidomics experiment revealed higher levels of phosphatidylethanolamine in axenic bugs. Phosphatidylethanolamine in eukaryotes is known to be involved in maintaining membrane fluidity, supporting the diffusion and function of molecules in cellular membranes (Dawaliby et al. 2016). We propose that the kissing bug gut microbiome may play a role in assimilation of cellular membrane components and function of molecules within the cellular membranes of gut cells.

In the fat body of non-blood fed bugs, we identified significant differences in relative abundance of several lipids (two-way ANOVA, $F_{(2, 60)} = 7.535$, $p = 0.001$). In the fat body of non-blood fed axenic bugs, there was significantly higher abundance of eicosapentaenoic acid (FA 20:5) relative to conventional (Tukey's HSD, $p < 0.001$) and gnotobiotic bugs (Tukey's HSD, $p = 0.007$; figure 4.7a). Eicosapentanoic acid is a derivative of arachidonic acid, which is deployed in the insect hemolymph in response to immune challenge (Wrońska et al. 2023). These results suggest that axenic bugs may have an accumulation of fatty acids involved in immune defense and these fatty acids are not being deployed into the hemolymph. There was no significant effect of the microbiome on abundance of palmitoleic acid (FA 16:1), (FA 17:6), arachidonic acid (FA 20:4), or (FA 20:6) in the fat body of non-blood fed bugs (Tukey's HSD,

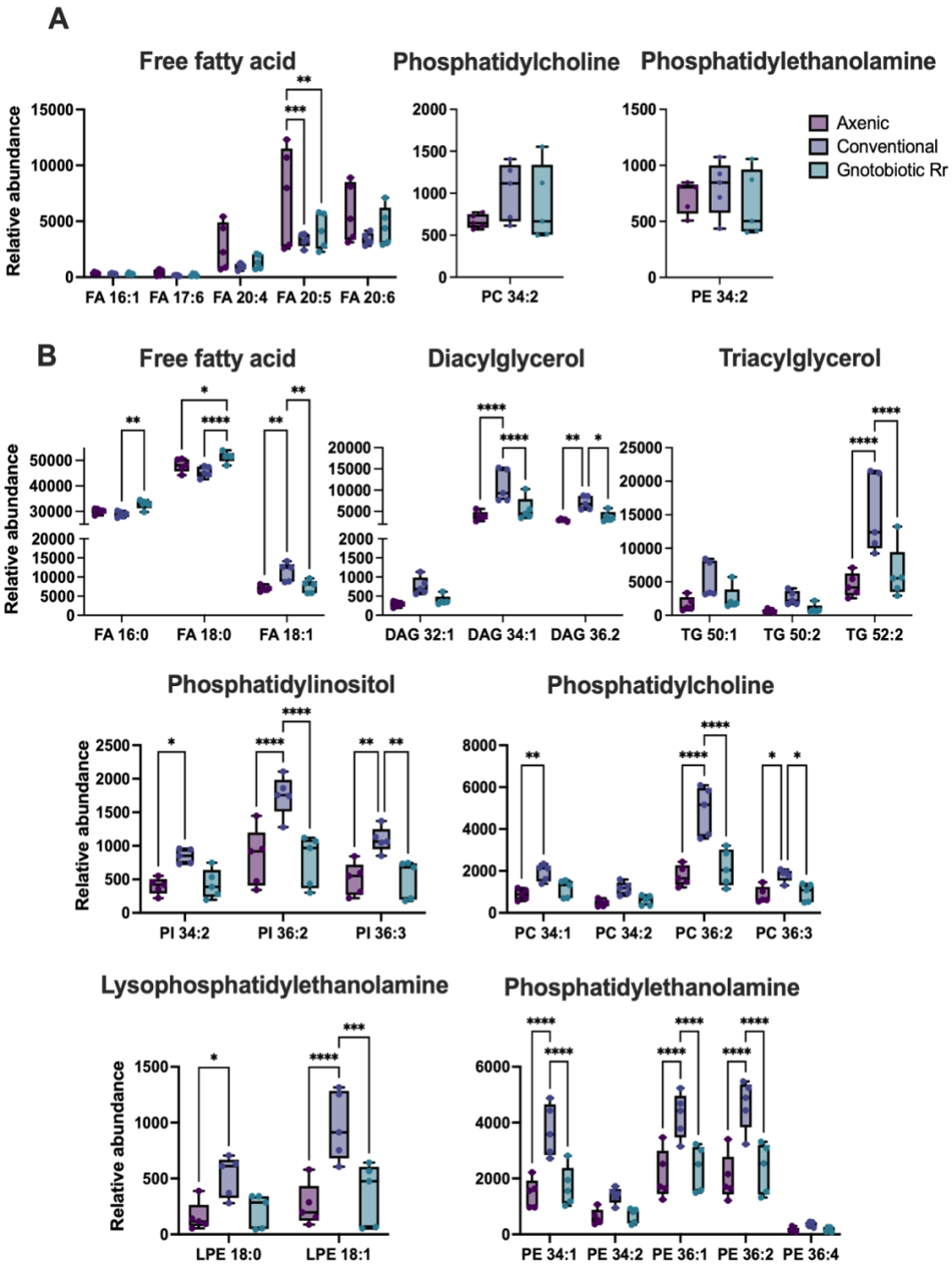

Figure 4.7. Fat body lipidomics comparing axenic, conventional, and gnotobiotic fourth instar (A) non-blood fed nymphs and at (B) four days post blood meal, determined by LC-MS. Error bars represent one standard error above and below the mean. Sample sizes were n = 5 per treatment and time point. Statistical significance was determined using a one way and two-way ANOVA followed by Tukey's HSD, where *, **, ***, and **** represent $p < 0.05$, $p < 0.01$, $p < 0.001$, and $p < 0.0001$, respectively. Fatty acids represented are palmitic acid (FA 16:0), palmitoleic acid (FA 16:1), (FA 17:6), stearic acid (FA 18:0), oleic acid (18:1), arachidonic acid (FA 20:4), eicosapentaenoic acid (20:5), and (FA 20:6).

$p > 0.05$). There was also no significant impact of the microbiome on fat body phosphatidylcholine or phosphatidylethanolamine relative abundance in non-blood-fed bugs (Tukey's HSD, $p > 0.05$).

At four days pbm, there were significantly higher abundance of several lipids in conventional or gnotobiotic bugs relative to axenic bugs (two-way ANOVA, $F_{(2, 36)} = 6.11$, $p = 0.005$). Relative abundance of palmitic acid (FA 16:0) was higher in the fat body of gnotobiotic bugs compared to conventional bugs (Tukey's HSD, $p = 0.007$; figure 4.7b) but not axenic bugs (Tukey's HSD, $p = 0.077$). There was also higher abundance of stearic acid (FA 18:0) in the fat body of gnotobiotic bugs compared to axenic (Tukey's HSD, $p = 0.023$) and conventional bugs (Tukey's HSD, $p < 0.0001$) at four days pbm. The fat body of conventional bugs also had significantly higher abundance of diacylglycerol (DAG 34:1) compared to axenic and gnotobiotic bugs (two-way ANOVA, $F_{(2, 36)} = 19.99$, $p < 0.0001$) Similarly, there was higher abundance of DAG 36:2 in conventional bugs compared to axenic (Tukey's HSD, $p = 0.002$) and gnotobiotic bugs (Tukey's HSD, $p < 0.016$).

There was significantly higher abundance of triacylglycerol (TAG 52:2) in conventional bugs compared to axenic and gnotobiotic bugs (two-way ANOVA $F_{(2, 36)} = 16.00$, $p < 0.0001$). One of the primary components of triacylglycerol in insects is palmitic acid (Zhou et al. 2021; Gondim et al. 2021; Municio et al.1975). As expected, we observed lower relative abundance of palmitic acid in the fat body of axenic bugs. Stearic acid is also incorporated into triglycerides in insects (Municio et al.1975), and we also observed lower relative abundance of stearic acid in the fat body of axenic bugs. Lower relative abundance of both palmitic and stearic acid may be potential cause for axenic bugs having lower fat body triglyceride levels. Lower fatty acid levels and triglyceride levels suggests that axenic bugs may have abnormal metabolism relative to

gnotobiotic and conventional bugs and may be a reason why these insects undergo delayed development, high mortality, and inability to reproduce (Gilliland et al. 2023).

4.5 Discussion

Gut bacteria contribute to multiple host physiological functions including provisioning nutrients (Rio et al. 2016; Shin et al. 2011; Douglas 2017), aiding in digestion (Gaio et al. 2011), immunity (Ramirez et al. 2012; Bai et al. 2019), promoting development (Gilliland et al. 2023; Coon et al. 2014; 2017), and supporting metabolism (Zhou et al. 2021; Shin et al. 2011). However, contributions of gut bacteria to lipid synthesis and metabolism in *R. prolixus* have not yet been considered. Because *R. rhodnii* can function as a sole symbiont in *R. prolixus*, we sought to understand the role of this symbiont in fatty acid synthesis, triglyceride accumulation, and blood meal digestion. Our triglyceride profiles showed that axenic bugs had lower fat body triglyceride levels than both conventional and gnotobiotic bugs at one and four days pbm. At ten days pbm conventional bugs had the highest fat body triglyceride levels compared to axenic and gnotobiotic bugs. However, at twenty days following the blood meal, axenic bugs had significantly higher triglyceride stores relative to gnotobiotic bugs.

From these data, we gathered that axenic bugs may be experiencing a delay in triglyceride synthesis and potentially a delay in fat body triglyceride mobilization. It is possible that the microbiome modulates AKH and Brummer lipase genes, which are involved in lipid metabolism and mobilization. Abnormal fat body triglyceride accumulation was observed in adult female *R. prolixus* following knockdown of Brummer lipase (Arêdes et al. 2024). AKH coordinates the mobilization of energy stores under starvation (Zandawala et al. 2015; Alves-Bezerra et al. 2016; Leyria et al. 2021). Upon knockdown of the adipokinetic hormone receptor in fifth instar *R.*

prolixus nymphs, there was a decrease fat body triglyceride mobilization at ten and sixteen days after a blood meal (Alves-Bezerra et al. 2016).

We next wanted to know if the microbiome differentially modulated *acc* expression, given that ACC is the rate limiting enzyme for *de novo* lipogenesis (Gondim et al. 2018). Our expression profiles indicated that gnotobiotic bugs had higher expression of *acc* in the whole gut at four days following a blood meal, among conventional and axenic bugs. These data demonstrate that gut microbiota modulate expression of *acc* and might subsequently affect downstream lipogenesis. In adult *R. prolixus*, Moraes et al. 2022 showed high expression of *acc* in the fat body at ten days pbm and this expression correlated with high fat body triglyceride stores. Thus, were surprised to find that axenic bugs had significantly higher expression of *acc* in the fat body compared to conventional and gnotobiotic bugs, especially given that fat body triglyceride stores were significantly lower in axenic bugs compared to conventional bugs. Similar to our *acc* expression findings among axenic, gnotobiotic, and conventional bugs, we found that expression of *fas289* was highest in axenic bugs at ten days pbm.

We thought axenic bugs might have overall lower accumulation of fat body triglycerides due to impaired digestion. We found no difference in anterior midgut protein content among axenic, conventional, and gnotobiotic bugs at ten days following a blood meal. However, we found a significant retention of blood in the anterior midgut following the both the third to fourth instar molt and fourth to fifth instar molt. Retention of blood in the anterior midgut was observed in *acc* knockdown adult *R. prolixus* (Moraes et al. 2022). A similar phenotype of blood meal retention in the anterior midgut was observed in mosquitoes, upon knockdown of *fasn1* demonstrating a link between blood meal digestion and fatty acid synthesis (Alabaster et al. 2011).

We found that knockdown of *acc* but not *fas289* resulted in significant blood accumulation in the anterior midgut of *R. prolixus* nymphs, while knockdown of both *acc* and *fas289* resulted in significant decrease in fat body triglycerides. The mechanism in which *acc* and *fas* knockdowns impair digestion is unknown. However, it has been hypothesized that digestion impairment may be a result of reduced midgut traffic or a result of disrupted regulatory feedback mechanisms due to abnormal accumulation of acetyl-CoA (Moraes et al. 2022; Alabaster et al. 2011). *Acc* knockdown in both mosquitoes and kissing bugs induced non-lipid related defects, such as malformation of the eggshell (Moraes et al. 2022; Alabaster et al. 2011). This supports the idea that disruption of ACC activity subsequently effects the fate of acetyl-CoA molecules, which are implicated in other cellular and biological processes, including but not limited to lipogenesis and lipid metabolism.

We hypothesize that the gut microbial community induces changes in *acc* and *fas289* expression by altering regulatory feedback mechanisms. By using a malonyl-CoA sensor actuator in *E. coli*, Liu et al. 2022 found that *acc* expression could be feedback modulated, where expression of *acc* was decreased when cellular concentrations of malonyl-CoA were high and increased when cellular malonyl-CoA concentrations were low. In *Brassica napus* cells, it was found that delivery of oleic acid (FA 18:1) bound to an acyl carrier protein reduced ACC enzymatic activity and subsequently the de novo synthesis of fatty acids (Andre et al. 2012). We propose that the increase in fat body expression of *acc* and *fas*289 in axenic bugs may be a feedback induced response, potentially to low cellular malonyl-CoA or free fatty acid abundance.

Our lipidomics analysis revealed that different gut microbial communities resulted in variation in the relative abundance of several fatty acids, phospholipids, diacylglycerol, and triacylglycerol among, axenic, conventional, and gnotobiotic bugs. We hypothesize that

conventional bugs might have higher relative abundance of lipids compared to axenic and gnotobiotic bugs due to the additive nutritional contributions from a more diverse and more highly abundant gut microbial community. We observed differences of oleic acid, palmitic acid, and stearic acid, all of which are all known fatty acid components of triacylglycerol (Zhou et al. 2021; Moore and Taft 1971). Phosphatidylethanolamine is known to make up half of the total phospholipids present in the cell membranes of eukaryotes (Gibellini and Smith 2010). Phosphatidylinositol and phosphatidylcholine are substrates for phospholipase A_2 degradation, and this reaction results in the synthesis of bioactive phospholipids in the insect (Gibellini and Smith 2010; Bittencourt-Cunha et al. 2013; Barletta et al. 2016). These bioactive phospholipids include lysophosphatidylcholine and lysophosphatidylethanolamine (Golodne et al. 2003; Yamamoto et al. 2022). Lysophosphatidylethanolamine extracted from the house fly, *Musca domestica*, is implicated in insect immunity due to its antimicrobial properties and inhibition of *Bacillus thuringiensis* and *Saccharomyces cerevisiae* growth (Van Rensburg et al. 1992; Meylaers et al. 2004). Future directions of this system may include further investigation of the role of the *R. prolixus* microbiome in synthesis of lipids involved in immune function.

Table 4.S1. *Rhodnius prolixus acc* and *fas289* primers used in this study.

Table 4.S1: Primer sequences			
Vectorbase accession	**Forward primer**	**Reverse primer**	**Primer type**
ACC: RPRC013987	TCAATAAACGTCTCCCTAACA	AGCACAAAAATCACCAAATAA	qPCR
	TAATACGACTCACTATAGGGAGAGATACTGCCTACCAGAACCTT	TAATACGACTCACTATAGGGAGACCATATCATCTTTGTGTCGAT	RNAi
FAS289: RPRC011289	CAATCCATTCATTTACGCCA	AGATTTGTTCACTTCGTCGA	qPCR
	TAATACGACTCACTATAGGGAGAGGTGAGGATTTGTGTAAAGTG	TAATACGACTCACTATAGGGAGAGAAGCATACGTAGATGGTCAG	RNAi
Underlined sequences denote T7 sequence for dsRNA synthesis			

CHAPTER 5

THE MICROBIOME PROMOTES DESICCATION TOLERANCE THROUGH MODULATION OF FATTY ACYL-COA REDUCTASE GENES IN THE KISSING BUG *RHODNIUS PROLIXUS* [4]

[4]Keyes-Scott NI, Wang Z, Bimpeh K, Lomax AD, Allen LR, Hines KM, Chung H, Vogel KJ. To be submitted to Insect Biochemistry and Molecular Biology.

5.1 Abstract

Bacterial symbionts are able to provide many benefits to insect hosts through nutrient supplementation and by promoting metabolism. The nutritional gains from the microbiome aid cell growth, promote development, metabolism, defense, and desiccation tolerance. Gut bacteria synthesize B vitamins or other essential precursor molecules that enable synthesis of lipids involved in metabolism and the synthesis of cuticular lipids. Cuticular lipids and waxes play a role in insect communication, defense, and desiccation prevention. The kissing bug *Rhodnius prolixus* midgut houses an extracellular, gram-positive symbiont, *Rhodococcus rhodnii*, which is known to have B vitamin biosynthesis capabilities. We propose that *R. rhodnii* and the *R. prolixus* microbiome may play an essential role in the synthesis of cuticular lipids and formation of the epicuticle. We identified differences in integument lipid levels among axenic (germ-free), singly inoculated gnotobiotic *R. rhodnii*, and conventional (unmanipulated) fourth instar nymphs using LC-MS. Our quantitative PCR analysis revealed differential expression of acetyl-CoA carboxylase (*acc*) in the abdominal integument and two fatty acyl-CoA reductase genes (*facrs*) in the fat body and abdominal integument. We further characterized the role of the microbiome in cuticular hydrocarbon synthesis, epicuticle formation, and desiccation tolerance. Finally, using RNA interference, we investigated the functions of three *facr* genes (*facr873*, *facr813*, and *facr223*) in desiccation tolerance, epicuticle formation, and development.

5.2 Introduction

Lipids are essential macromolecules required by all forms of life. In insects, lipids promote a diversity of functions including metabolism (Arrese and Soulages 2010), immune function (Wrońska et al. 2023), molting and development (Li et al. 2020; Cinnamon et al. 2016),

desiccation tolerance (Moriconi et al. 2019; Wang et al. 2022), reproduction (Li et al. 2020), and communication (Zeng et al. 2022; Würf et al. 2020). In the obligately hematophagous insect, *Rhodnius prolixus*, each developmental stage consumes a vertebrate blood meal which is primarily composed of protein and contains a limited amount of lipids and glucose (Lynch et al. 2017). The protein acquired through a blood meal is broken down into amino acids in the midgut, and the amino acids can be used for the *de novo* synthesis of lipids (Gondim et al. 2018). Blood feeding induces lipogenesis and expression of acetyl-CoA carboxylase (*acc*), which is the rate limiting enzyme for *de novo* lipogenesis in insects (Saraiva et al. 2020; Holze et at. 2021; Dean Goldring and Read 1993). ACC facilitates the conversion of acetyl-CoA to malonyl-CoA, which is an essential building block for long chain fatty acid synthesis by fatty acid synthases (FASNs) (Saraiva et al. 2020; Alabaster et al. 2011; Moraes et al. 2022).

Long chain fatty acids (LCFAs) which are produced in the oenocytes, or secretory cells associated with the insect fat body and epidermis, can undergo further modification through the ACC pathway to form cuticular lipids. Alternatively, LCFAs and hydrocarbons can be transported by fatty acid transport proteins to the oenocytes for cuticular lipid synthesis through the ACC pathway (Gondim et al. 2018; Holze et al. 2021). Modifications of LCFAs through the ACC pathway in oenocytes results in synthesis of pheromones, cuticular hydrocarbons, and cuticular waxes (Ferveur et al. 2018; Wang et al. 2022; Wigglesworth 1986; Holze et al. 2021; Moto et al. 2003; Teerawanichpan et al. 2010; Cinnamon et al. 2016). Downstream of ACC and FASNs, fatty acid elongase enzymes convert LCFAs into very long-chain fatty acids (VLCFAs) (Holze et al. 2021). Knockdown of the fatty acid elongase gene, *elof*, in *Drosophila* resulted in a significant reduction of C29 hydrocarbons and significant accumulation of C25 hydrocarbons in adult females (Chertemps et al. 2007). Following elongation, fatty acyl-CoA reductases (FACRs)

reduce VLCFAs into very long chain fatty alcohols, which promote development and waterproofing of the trachea (Holze et al. 2021; Li et al. 2020). Lastly, Cytochrome P450 enzymes in the 4G family (CYP4Gs) carry out the final step in hydrocarbon biosynthesis by conversion of long chain fatty alcohol products to hydrocarbons (Dulbecco et al. 2020; MacLean et al. 2018). Silencing of two *R. prolixus* CYP4Gs, CYP4G106 and CYP4G107, resulted in a significant decrease of straight-chain and methyl-branched cuticular hydrocarbons that promote survival and waterproofing of the cuticle (Dulbecco et al. 2020).

Bacterial symbionts are known to promote lipid synthesis within an insect host (Zhou et al. 2021; Shin et al. 2011). Axenic, or germ-free, and aposymbiotic insects which lack symbiotic bacteria exhibit nutrient deficiencies and an inability to metabolize lipids and carbohydrates (Valzania et al. 2018a; Valzania et al. 2018b). This inability to metabolize nutrients further impacts the ability of the insect to undergo normal development (Coon et al. 2017; Valzania et al. 2018; Gilliland et al. 2023; Engl et al. 2020). Bacterial symbionts also promote nutrient synthesis and can directly produce molecules such as vitamins, amino acids, or other substrates which are used by insect hosts for growth, development, and metabolism (Zhou et al. 2021; Shin et al. 2011; Engl et al. 2020). Removal of bacterial symbionts within the saw-toothed grain beetle, *Oryzaephilus surinamensis*, resulted in malformation of the integument, including improper melanization and decreased levels of cuticular hydrocarbons which caused increased desiccation sensitivity (Engl et al. 2018; Hirota et al. 2017; Kiefer et al. 2021). It was later found that one contribution of the bacterial symbiont *Candidatus Shikimatogenerans silvanidophilus* within *O. surinamensis* was supplementation of tyrosine, an essential amino acid required for cuticle sclerotization and melanization (Kiefer et al. 2021; Keifer et al. 2023; Kramer and

Hopkins 1987; Vigneron et al. 2014). Altogether, these studies demonstrate the impact of symbionts in nutrient provisioning which affects metabolism and formation of the insect cuticle.

The extracellular bacterial symbiont *Rhodococcus rhodnii* that resides within the midgut of the kissing bug, *Rhodnius prolixus*, is known to supplement essential B vitamins which are not thought to be highly abundant in vertebrate blood (Wigglesworth 1936; Gilliland et al. 2023; Lake and Friend 1968; Baines 1956). B vitamins are essential cofactors for fatty acid synthesis and lipid metabolism. Due to their pivotal role in providing B vitamins which are necessary for lipid synthesis and metabolism, we sought to investigate the role of *R. rhodnii* on synthesis of cuticular lipids in *R. prolixus*. We examined this potential interaction using fourth instar nymphs with an unmanipulated microbiome (conventional), those singly infected with *R. rhodnii* (gnotobiotic), or germ-free (axenic). We found that there was a significant accumulation of phospholipids within the abdominal integument of axenic insects, suggesting a role of the microbiome in synthesis and metabolism of cuticular lipids. We identified differences in the formation of the epicuticle, cuticular hydrocarbon profiles, and desiccation tolerance among axenic, conventional, and gnotobiotic bugs. We next examined expression of *acc* in addition to three fatty acyl-CoA reductase genes in the abdominal integument of axenic, conventional, and gnotobiotic fourth instar bugs (RPRC000223, RPRC000873, and RPRC011813). Finally, we used RNAi to identify the role of each fatty acyl-CoA reductase gene in epicuticle formation, desiccation tolerance, and development in *R. prolixus*.

5.3 Materials and Methods

Insect rearing

Rhodnius prolixus were acquired from the lab of Dr. Ellen Dotson at the Center for Disease Control through BEI Resources. Insects were housed in a temperature-controlled incubator maintained at 28°C and 80% RH under a 12L:12D photoperiod cycle. Gnotobiotic and axenic insects were generated using methods described in Gilliland et al. 2023. *R. prolixus* eggs were surface sterilized with a series autoclaved deionized water, 70% ethanol, and iodine washes. Sterile eggs were placed in autoclaved mason jars which were secondarily contained in autoclaved plastic Nalgene containers. A small hole was created in lids of the autoclaved Nalgene container for oxygen exchange, and the lids were covered with gas exchange membrane to maintain sterile conditions within the jar.

Gnotobiotic bugs were fed defibrinated rabbit blood (Hemostat Laboratories) inoculated with *Rhodococcus rhodnii* at a concentration of 10^6 CFU. Axenic bugs were fed sterile rabbit blood. Gnotobiotic and axenic bugs were maintained in autoclaved mason jars and sterile secondary containment throughout development. Conventional bugs were fed defibrinated rabbit blood (Hemostat Laboratories) inoculated with *Rhodococcus rhodnii* at a concentration of 10^6 CFU but were not maintained in sterile conditions. All bugs were fed two to three weeks post-molt at each instar and were sorted by feeding status within one day following a blood meal, and fourth and fifth instar axenic, conventional, and gnotobiotic nymphs were used for all experiments. All non-blood fed insects used were starved and at least thirty days post fourth instar molt.

Expression analysis

Starved fourth instar conventional, gnotobiotic, and axenic bugs were collected, and the dorsal and ventral layers of the abdominal integument were dissected from non-blood fed bugs and 4, 10, and 20 days post blood meal (pbm) bugs. The twenty-day pbm timepoint followed the fourth to fifth instar molt. Tissues were placed in a 1.5 mL Eppendorf tube with 100 µL of *Aedes* saline (Hayes 1953) and were frozen at -80° C until RNA extraction. Tissues were placed in a 1.5 mL microcentrifuge tube with 100 µL of *Aedes* saline and were frozen at -80° C until RNA extraction. The Zymo Direct-zol RNA MagBead Kit with TRIzol kit, was used in a KingFisher Apex Dx system (ThermoFisher Scientific) for RNA extractions and DNase steps, per the manufacturer instructions.

One hundred nanograms of RNA was used as template to synthesize cDNA using the iScript cDNA synthesis kit (BioRad, Hercules, CA, USA). cDNA was used as template for quantitative real-time PCR, with the QuantiNova SYBR Green PCR kit (Qiagen) and gene specific primers (Table 5.S1). Standard curves for each gene were generated by cloning qPCR products into the pSCA vector with the Strataclone PCR cloning kit (Agilent, Santa Clara, CA, USA), isolating plasmid DNA using the GeneJET Plasmid Miniprep Kit (Thermo Scientific, Vilnius, Lithuania), and preparing plasmid standards from 10^7 to 10^2 copies.

Desiccation bioassays

To examine the effects of the microbiome on desiccation resistance, water loss was measured using conventional, gnotobiotic, and axenic fourth instar bugs at two weeks post-molt. Bugs were collected, weighed on an Ohaus microbalance (Ohaus Corporation, NJ, USA), and placed in an individual well of a sterile 12-well cell culture plate (Advangene Consumables, Inc., IL,

USA). Well plates were placed in an incubator at 28° C and low humidity (35% RH ± 5%). Individual bugs weights were tracked for several days until seven days post-exposure, and survival was examined at fourteen days post-exposure.

RNAi knockdowns and bioassays

Target regions of 300-500 bp were selected as targets for RNAi-mediated knockdown of RPRC000873, RPRC011813, and RPRC000223, subsequently referred to as *facr873*, *facr813*, and *facr223*, respectively. Primers with the T7 promoter sequence were used to amplify each target using cDNA synthesized from RNA isolated from gnotobiotic fourth instar fed and unfed bug gut or fat body tissues (Table 5.S1). PCR products were cloned into the pSCA vector, and plasmid DNA was extracted following the aforementioned methods. Plasmid DNA from each gene target and an EGPF control were used as the templates for dsRNA synthesis. dsRNA was synthesized using the MEGAscript RNAi kit (Ambion, Vilnius, Lithuania), following manufacturer instructions. After dsRNA synthesis, dsRNA was precipitated in sodium acetate and ethanol, then resuspended in *Aedes* saline (Hayes 1953) to a concentration of 1 μg/μL for microinjections.

Non-blood fed conventional or gnotobiotic fourth instar nymphs were injected with 1μL of dsRNA and were fed three days following microinjection to examine the effects of *facr873*, *facr813*, and *facr223* on development and epicuticle formation. Molting was observed fourteen days pbm. To examine the impacts of *facr873*, *facr813*, and *facr223* knockdown on desiccation tolerance, gnotobiotic fourth instar bugs were collected and injected with *facr873*, *facr813*, *facr223*, or *EGFP* dsRNA. After three days, injected bugs weighed on an Ohaus microbalance (Ohaus Corporation, NJ, USA), and placed in an individual well of a sterile 12-well cell culture

plate (Advangene Consumables, Inc., IL, USA). Well plates were placed in an incubator at 28° C and low humidity (35% RH ± 5%). Individual bugs weights were tracked at four days and seven days post-exposure.

LC-MS

Fifth instar abdominal integuments were collected from conventional, gnotobiotic, and axenic bugs. Tissues were flash frozen with liquid nitrogen in Lysing Matrix Z tubes with 2.0 mm diameter yttria-stabilized zirconium oxide beads (MP Biomedicals, CA, USA) and shaken on a bead beater for 30 seconds. Samples were frozen at −80°C until later processing. Subsequently, the lipids from the integument samples were extracted using the modified Bligh and Dyer extraction method (Carpenter et al. 2024). Briefly, 2mL of chilled 1:2(v/v) chloroform/methanol was added to the samples and vortexed for 5 min on ice. Following this, an additional volume of 0.5 mL each of water and chloroform was added to the mixture and vortexed for 1 min. The resulting mixture was centrifuged at 2000xg at 4°C for 10 min. The organic layer was then carefully transferred to a new glass tube, dried, and reconstituted in 1:1 (v/v) chloroform/methanol for storage at -80 °C until use.

Lipid extracts were analyzed using hydrophilic interaction liquid chromatography (HILIC) coupled with traveling wave ion mobility (TWIMS) mass spectrometry in both positive and negative ionization modes. Chromatographic separations were carried out with Waters Cortecs UPLC HILIC column (2.1 x 100 mm, 1.6 µm) over 7 minutes gradient method(cite). The effluent from the UPLC was connected to the electrospray ionization source of the TWIMS instrument, and the experiments were conducted according to previously described ionization settings(cite). Peak Picking and alignment of LC-MS data were performed using Progenesis QI

(v3.0, Nonlinear Dynamics, Waters). Multivariate statistical analysis with EZ Info (v3.0, Umetrics) was used to identify the features that significantly contributed to the experimental differences. Lipid species were identified using LipidPioneer (Ulmer et al. 2017) and the Human Metabolome Database (HMDB) (Wishart et al. 2007, 2009, 2013, 2018, 2022).

Sectioning and microscopy

Fifth instar gnotobiotic and axenic thoracic carcasses, which were removed of the head and legs and were collected in 4% paraformaldehyde in 1x PBS. Samples were embedded and 1 μm sections were cut longitudinally from the space between the prothoracic and mesothoracic leg cavities using a microtome. Samples were stained with Trypan blue for fifteen minutes after cutting and were photographed under a light microscope at 500x magnification (Olympus). To determine the role of FACRs on epicuticle formation, thoracic carcasses from fifth instar conventional bugs injected with *dsFACR873*, *dsFACR813*, *dsFACR223*, and *dsEGFP* were collected. The thoracic carcasses were removed of the head and legs and were collected in 4% paraformaldehyde in 1x PBS. Samples were embedded and 1 μm sections were cut longitudinally from the space between the prothoracic and mesothoracic leg cavities using a microtome. Samples were stained with Trypan blue for fifteen minutes and were photographed under a light microscope at 500x magnification (Olympus).

5.4 Results

Axenic bugs have an accumulation of phospholipid in the abdominal integument

To first investigate the role of the microbiome in synthesis of cuticular hydrocarbons, we examined abdominal integument lipid levels of non-blood fed axenic and gnotobiotic fifth instar

bugs using LC-MS. We found no difference in phosphatidylglycerol (PG) 34:1 (Student's t, p = 0.064), but significantly higher levels of PG 34:2 in the abdominal integument of axenic bugs (Student's t, p = 0.004) compared to gnotobiotic bugs (figure 5.1). We also found significantly higher levels of phosphatidylinositol (PI) 36:3 (Student's t, p = 0.013), PI 34:2 (Student's t, p = 0.015), and PI 36:4 Student's t, p = 0.025) in the abdominal integument of axenic bugs compared to gnotobiotic bugs (figure 5.1). Phosphatidylglycerol and phosphatidylinositol are both components of cellular membranes, and phosphatidylinositol is implicated in cellular growth signaling in the oenocytes (Wrońska et al. 2023; Cinammon et al. 2016). Our integument lipidomics results suggest that axenic bugs may be exhibiting abnormal cellular signaling and

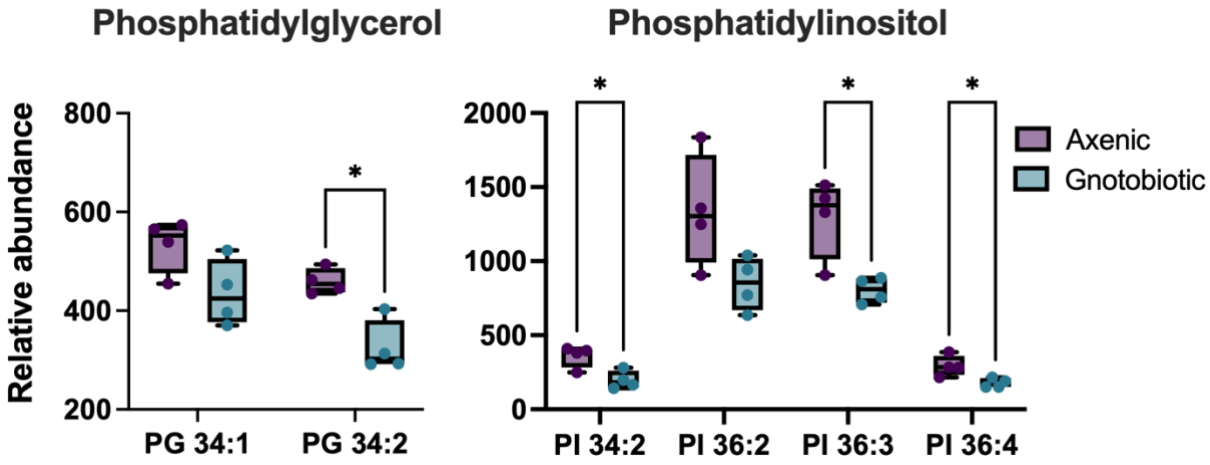

Figure 5.1. Abdominal integument phospholipid levels of non-blood fed axenic and gnotobiotic fifth instar nymphs determined by LC-MS. Error bars represent one standard error above and below the mean. Statistical significance was determined using a Student's t, where * represents $p < 0.05$. Sample sizes were n = 4 tissues per treatment.

growth in this tissue.

The microbiome affects expression of *acc* and downstream fatty acyl-CoA reductase genes

We next wanted to investigate if the microbiome influenced expression of genes that modulate lipid synthesis in fat body and epidermis of the abdominal integument. We first

conducted an expression analysis to measure expression of *acc* in the abdominal integument and found there was a significant impact of the microbiome on *acc* expression across multiple times pbm (two-way ANOVA, $F_{(2, 35)}$, $p < 0.0001$; figure 5.2). We found that non-blood fed axenic bugs had significantly lower expression of *acc* relative to conventional (Tukey's HSD, $p = 0.001$) and gnotobiotic bugs (Tukey's HSD, $p = 0.02$). There was no influence of the microbiome on *acc* expression in the abdominal integument post-feeding, as expression decreased after a blood meal and remained low at ten and twenty days pbm, which was after the fourth to fifth instar molt (Tukey's HSD, $p > 0.05$).

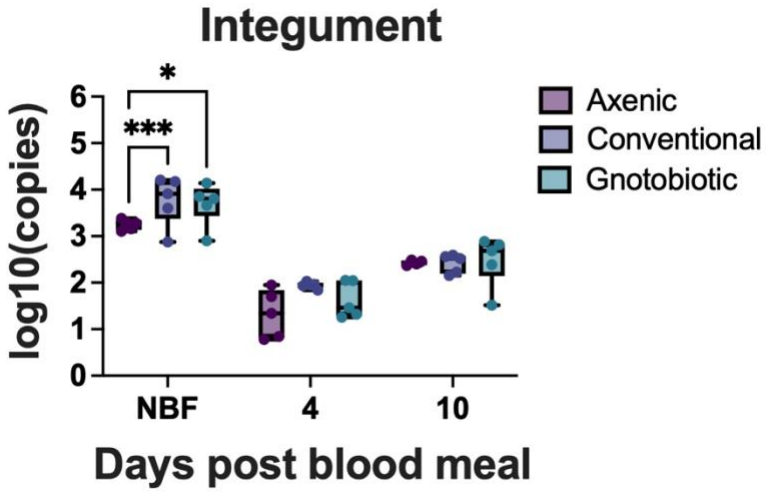

Figure 5.2. Expression profile of acetyl-CoA carboxylase (*acc*) in the abdominal integument of non-blood fed (NBF) and fed fourth instar axenic, conventional, and gnotobiotic bugs at different times post blood meal. Error bars represent one standard error above and below the mean. Statistical significance was determined using a two-way ANOVA followed by Tukey's HSD, where ** and *** represent $p < 0.01$ and $p < 0.001$, respectively. Sample sizes were n = 4-5 tissues per treatment, per time point.

Next, we examined tissue tropism of three uncharacterized fatty acyl-CoA reductase (*facr*) genes in axenic, conventional, and gnotobiotic fourth instar bugs. The *Rhodnius* genome encodes fifteen fatty acyl-CoA reductase genes (Majerowicz et al. 2017), but our preliminary transcriptomic data comparing differential expression of genes in axenic versus gnotobiotic first

instar nymphs showed that there was differential expression of *facr873*, *facr223*, and *facr813* in the whole gut. From our current fourth instar expression analysis in the fat body, we identified differential expression of *facr873* (two-way ANOVA, $F_{(2, 31)}$, $p = 0.042$) and *facr223* (two-way ANOVA, $F_{(2, 32)}$, $p = 0.045$; figure 5.3) among axenic, conventional, and gnotobiotic bugs. In the fat body, there was higher expression of *facr873* in axenic bugs compared to conventional bugs (Tukey's HSD, $p < 0.01$), however, there were no differences in fat body expression among

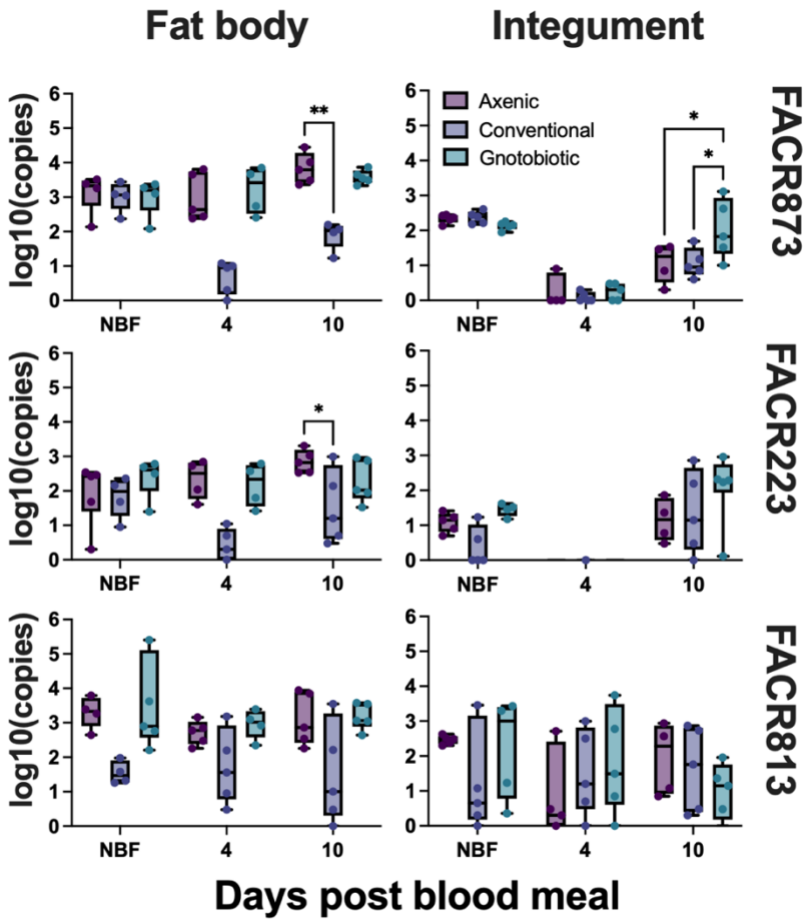

Figure 5.3. Expression profiles of *facr873*, *facr223*, and *facr813* in the fat body and abdominal integument of non-blood fed (NBF) axenic, conventional, and gnotobiotic fourth instar bugs and at four- and ten-days post blood meal. Error bars represent one standard error above and below the mean. Statistical significance was determined using a two-way ANOVA followed by Tukey's HSD, where * and ** represent $p < 0.05$ and $p < 0.01$, respectively. Sample sizes were n = 4-5 tissues per treatment, per time point.

non-blood fed or four-day pbm axenic, conventional, or gnotobiotic bugs (Tukey's HSD, $p > 0.05$). In the abdominal integument, there was also a significant difference in expression of *facr873* among axenic, conventional, and gnotobiotic bugs (two-way ANOVA, $F_{(2, 34)}$, $p = 0.027$). In the abdominal integument, we found higher expression of *facr873* in gnotobiotic bugs compared to axenic and conventional bugs (Tukey's HSD, $p < 0.01$ and $p < 0.01$, respectively). We observed no differences in *facr223* expression among axenic, conventional, and gnotobiotic bugs in the abdominal integument of non-blood fed, four day pbm, or ten day pbm bugs (two-way ANOVA, $p > 0.05$). Finally, we did not identify any differences in expression of *facr813* in non-blood fed, four-day pbm, or ten-day pbm bugs in the whole gut, fat body, or abdominal integument (two-way ANOVA, $p > 0.05$). Altogether, our expression data show that the microbiome modulates expression of *facr873* and *facr223*, which might in tandem influence the synthesis of cuticular lipids, including cuticular hydrocarbons.

Gut bacteria differentially affect cuticular hydrocarbon profiles and promote desiccation tolerance

We established that the microbiome modulates the expression of *facr* genes, which encode enzymes that are involved in cuticular hydrocarbon synthesis. Cuticular hydrocarbons (CHCs) aid desiccation tolerance in insects, and it is known that the microbiome also promotes desiccation tolerance and induces changes in insect CHC profiles (Guo et al. 1991; Engl et al. 2018). Thus, we next wanted to examine the role of the microbiome in synthesis of cuticular hydrocarbons using GC-MS. The three primary types of CHCs are the straight-chain CHCs, including n-alkanes and n-alkenes, and methyl-branched (mb) CHCs. We found a significant effect of the gut microbiome on epicuticular CHC abundance (two-way ANOVA, $F_{(2, 6)} = 29.48$,

$p < 0.0001$). We found that there was no significant difference in the straight-chain CHC, n-C31, among axenic, conventional, and gnotobiotic bugs (Tukey's HSD, $p > 0.05$), however, conventional bugs had significantly more straight-chain CHC, n-C33, relative to axenic (Tukey's HSD, $p < 0.001$) and gnotobiotic bugs (Tukey's HSD, $p = 0.004$; figure 5.4a). Longer chain CHCs are associated with increased desiccation tolerance (Wang et al. 2022), which suggests that conventional bugs may be more tolerant to desiccation due to higher abundance of n-C33 compared to axenic and gnotobiotic bugs.

Given the role of CHCs in desiccation prevention, we next wanted to know if differential CHC profiles among each gut microbiome treatment translated into differential desiccation sensitivity. Thus, we exposed non-blood fed axenic, conventional, and gnotobiotic fourth instar

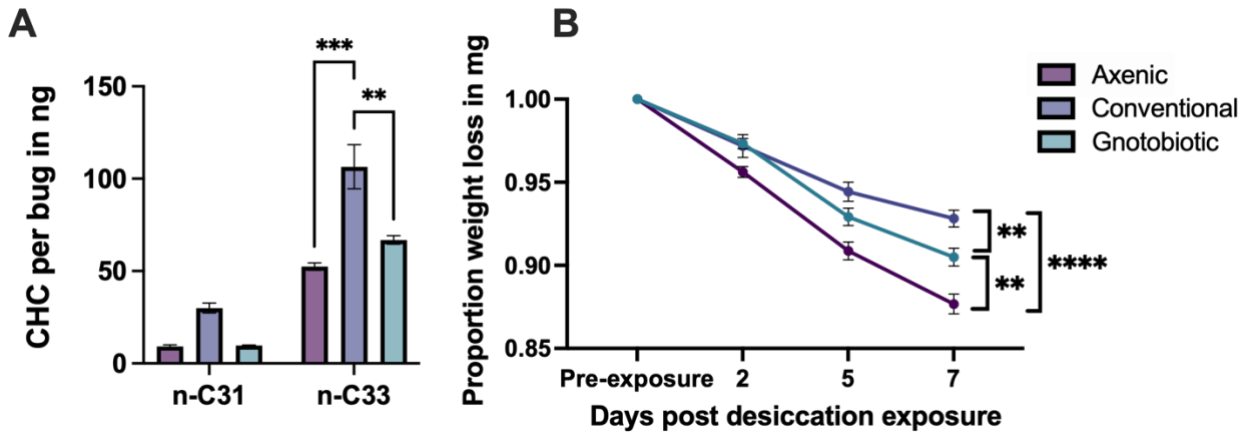

Figure 5.4. Impacts of the microbiome on cuticular hydrocarbon synthesis and desiccation tolerance. (A) Abundance of cuticular hydrocarbons on the surface of the integument of non-blood fed axenic, conventional, and gnotobiotic fourth instar nymphs, determined by GC-MS. Sample sizes were n = 2 per treatment. Statistical significance was determined using two-way ANOVA followed by Tukey's HSD, where ** and *** represent $p < 0.01$ and $p < 0.001$, respectively. (B) Proportion of water loss in unfed axenic, conventional, and gnotobiotic fourth instar bugs across multiple days following low humidity exposure (35% RH ± 5%). Error bars represent one standard error above and below the mean. Sample sizes were n = 24-44 individuals per treatment. Statistical significance was determined using two-way ANOVA followed by Tukey's HSD, where ** and **** represent $p < 0.01$ and $p < 0.0001$, respectively.

nymphs to low humidity (35% RH ± 5%), and measured water loss by relative net weight loss at different times post desiccation exposure. We found that the microbiome promotes desiccation tolerance in nymphs (two-way ANOVA, $F_{(2, 340)} = 25.53$, $p < 0.0001$). After five days of low humidity exposure, axenic bugs lost significantly more weight relative to conventional and gnotobiotic bugs (Tukey's HSD, $p < 0.0001$ and $p < 0.028$, respectively; figure 5.4b). After one week following desiccation exposure, gnotobiotic bugs lost significantly more weight than conventional bugs (Tukey's HSD, $p = 0.004$). These data suggest that a complete microbiome is most advantageous in terms of desiccation tolerance.

Gut bacteria promote formation of the epicuticle

Given the observed differences in hydrocarbon profiles and desiccation sensitivity among axenic, conventional, and gnotobiotic bugs, we next wanted to know if the gut microbiome promoted formation of the epicuticle. We embedded and sectioned the thoracic region between the prothorax and mesothorax and found a more conspicuous epicuticle of gnotobiotic bugs

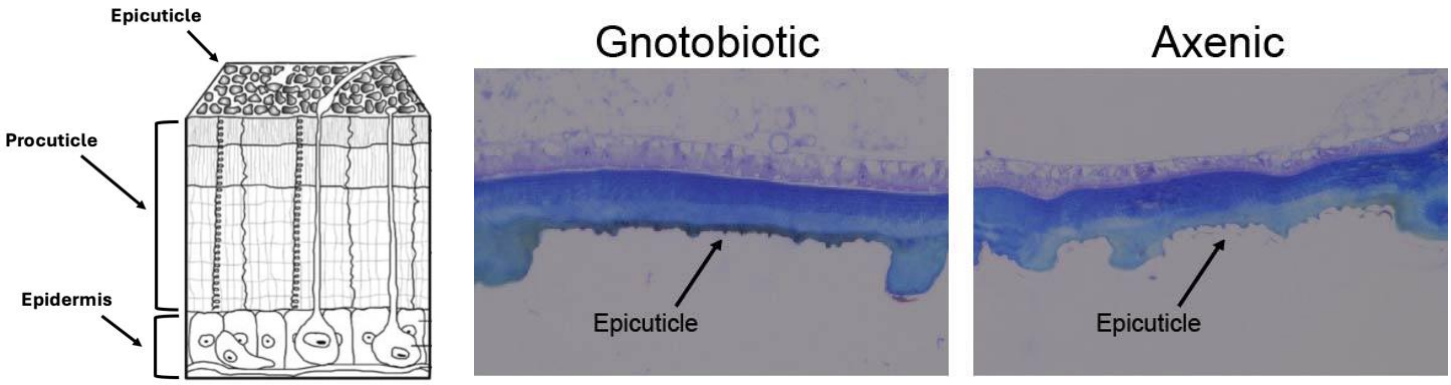

Figure 5.5. Epicuticle formation in gnotobiotic versus axenic bugs. Reference image of the layers of the insect integument (left) amended from Nation 2008. The epicuticle of gnotobiotic (middle) and axenic (right) fifth instar nymphs at ≤ one week post fifth instar molt. Images were taken at 500x magnification.

relative to axenic counterparts (figure 5.5). The epicuticle of the gnotobiotic bugs appears more darkened and punctate relative to the axenic epicuticle, which appears to be minimally darkened and less studded.

Knockdown of *facr223* and *facr873* induces desiccation sensitivity

To characterize the functions of FACR873, FACR223, and FACR813 in desiccation tolerance, we conducted knockdown experiments and examined desiccation sensitivity post knockdown (figure 5.6). We found that after four days of desiccation exposure, *dsFACR223* and *dsFACR873* injected bugs exhibited a significantly higher rate of weight loss relative to *dsEGFP* controls (two-way ANOVA, $F_{(3, 104)}$, $p < 0.0001$) respectively. There was no effect of *facr813*

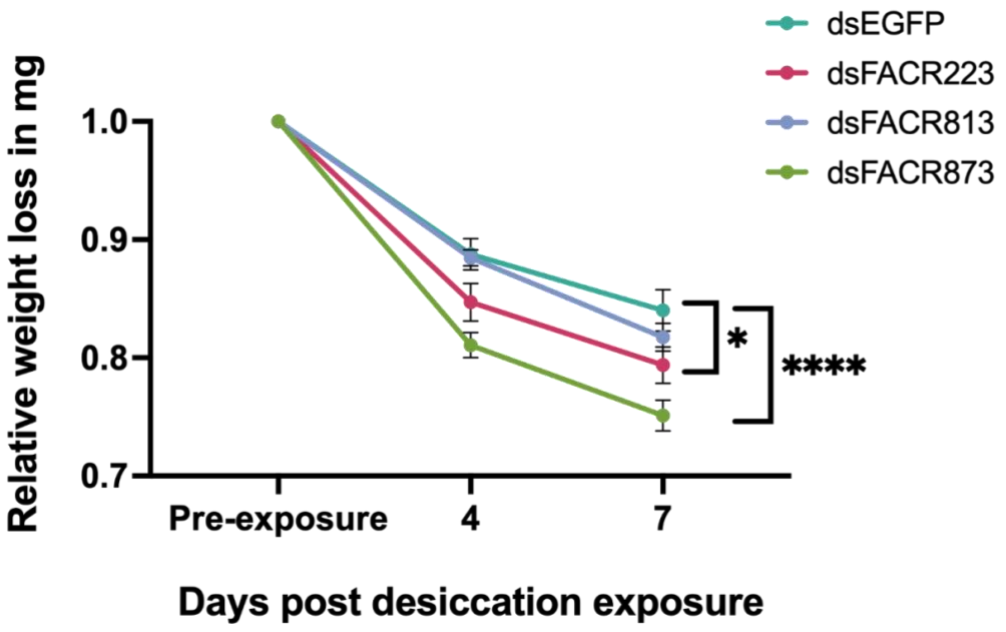

Figure 5.6. Impacts of *facr* knockdown on desiccation tolerance. Proportion of water loss in unfed gnotobiotic knockdown bugs injected with *dsFACR223*, *dsFACR813*, *dsFACR873*, or *dsEGFP* control at multiple days following desiccation exposure. Error bars represent one standard error above and below the mean. Sample sizes were n ≧ 10 individuals per treatment. Statistical significance was determined using one-way ANOVA followed by Tukey's HSD, where * and **** represent $p < 0.05$ and $p < 0.0001$, respectively

knockdown on desiccation tolerance (Tukey's HSD, $p > 0.05$). This trend persisted up until seven days post desiccation exposure, where *dsFACR223* and *dsFACR873* injected bugs lost significantly more weight than *dsEGFP* controls (Tukey's HSD, $p = 0.021$ and $p < 0.0001$, respectively). These data show that FACR223 and FACR873 are involved in desiccation tolerance and may play a role in synthesis of cuticlar lipids and formation of the epicuticle.

Knockdown of *facr813* and *facr873* induces malformation of the epicuticle

Using RNAi, we wanted to identify the role of FACR873, FACR813, and FACR223 in formation of the epicuticle. We injected fourth instar conventional bugs with *dsFACR873*, *dsFACR813*, *dsFACR223*, or *dsEGFP*, fed injected bugs at three days post injection, and allowed each treatment to develop to the fifth instar. We then embedded and sectioned the thoracic region

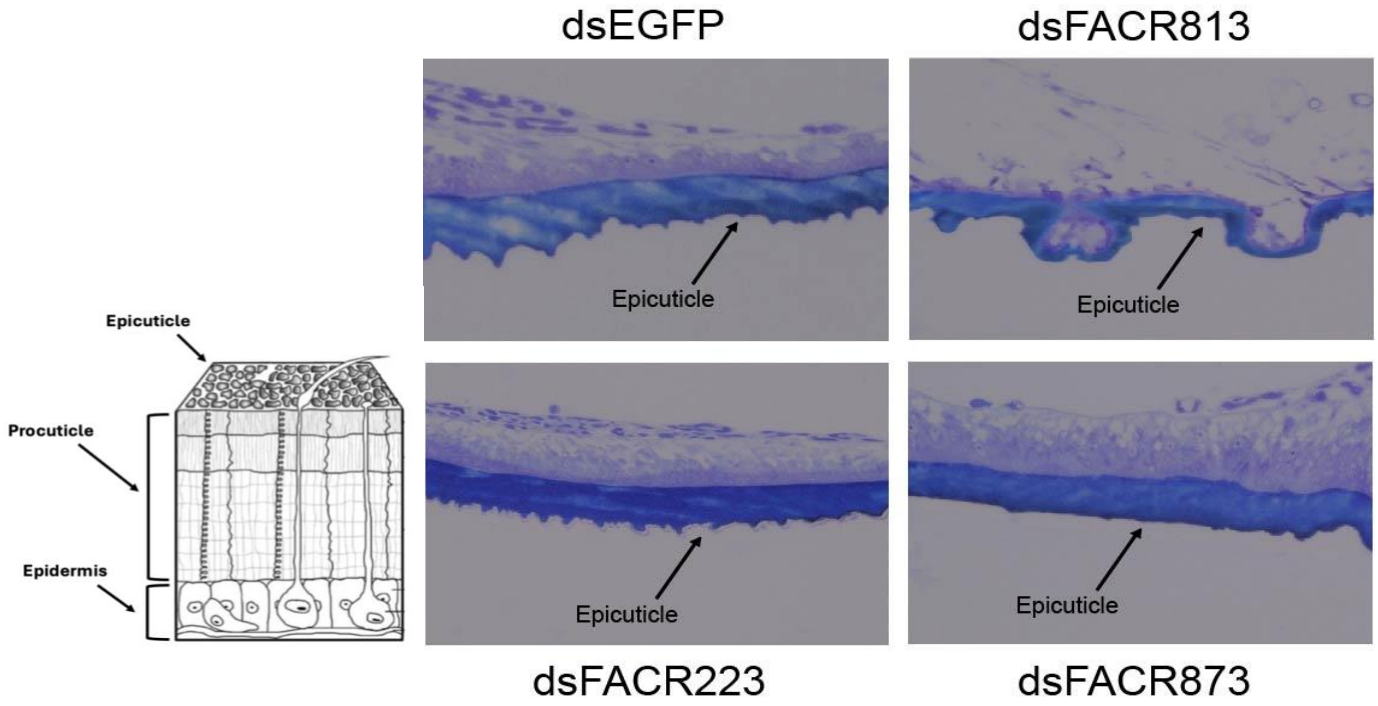

Figure 5.7. Effects of *facr* knockdown on epicuticle formation. Reference image of the layers of the insect integument (bottom left) amended from Nation 2008. Formation of the epicuticle in *dsEGFP* (top left), *dsFACR813* (top right), *dsFACR223* (bottom middle), and *dsFACR873* (bottom right) fifth instar nymphs at ≤ one week post fifth instar molt.

between the prothorax and mesothorax and found that knockdown of *facr813* and *facr873* induced changes in the formation of the epicuticle (figure 5.7). The epicuticle of *dsFACR813* and *dsFACR873* injected bugs resulted in a smooth looking epicuticle layer, with minimal spiked areas seen in the *dsEGFP* control. There were no marked differences in epicuticle formation between the *dsEGFP* and the *dsFACR223* epicuticle.

Knockdown of *facr873* and *facr813* disables ecdysis

Finally, we characterized the role of FACRs in development using RNAi. We injected fourth instar conventional nymphs with *dsFACR873*, *dsFACR813*, *dsFACR223*, or *dsEGFP*, fed them at three days post injection, then allowed them to develop to fifth instars. Individuals in the *dsFACR873* and *dsFACR813* treatments underwent 100% mortality within one week as a result

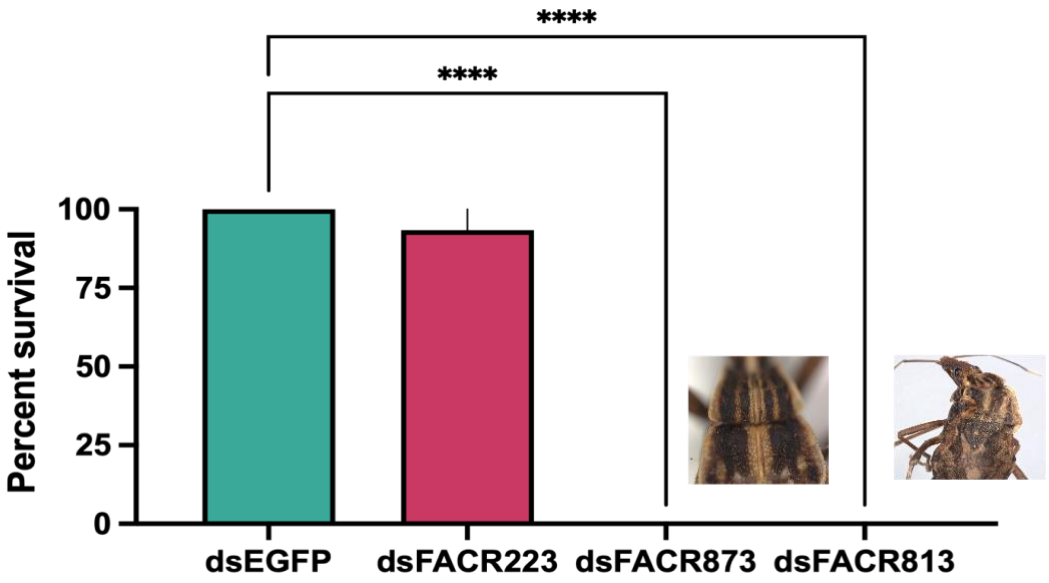

Figure 5.8. Percent survival of fourth instar conventional bugs injected with *dsEGFP*, *dsFACR223*, *dsFACR873*, or *dsFACR813* post molt or post molt attempt. Error bars represent one standard error above and below the mean. Sample sizes were n ≧ 15 individuals per treatment. Statistical significance was determined using one-way ANOVA followed by Tukey's HSD, where **** represents $p < 0.0001$.

of ecdysis failure, and none of these individuals successfully molted to fifth instars (one-way ANOVA, $F_{(3, 78)} = 542.0$, $p < 0.0001$; figure 5.8). These results demonstrate that FACR813 and FACR873 are essential for *R. prolixus* development.

5.5 Discussion

The first line of insect defense is the integument, which is coated with cuticular lipids and waxes that are synthesized by oenocytes and the epidermis and are secreted by pore canals (Locke 1959; Wigglesworth 1986; Botella-Cruz et al. 2021; Moriconi et al. 2019; Holze et al. 2021). Cuticular lipids, including cuticular hydrocarbons, wax esters, fatty alcohols, and fatty acids, are known to aid in desiccation prevention and also have antimicrobial properties (Holze et al. 2021; Krupp et al. 2020; Botella-Cruz et al. 2021; Ferveur et al. 2018; Wang et al. 2022; Batalha et al. 2020). Our integument lipidomic analysis revealed significantly higher phospholipid levels in the integument of axenic bugs compared to gnotobiotic bugs. Phosphatidylinositide, the phosphorylated form of phosphatidylinositol and membrane product of the phosphatidylinositide 3-kinase (PI3K) pathway, is implicated in modulating oenocyte cell growth in *Drosophila* (Cinnamon et al. 2016; Gutierrez et al. 2007). Interactions between PI3K and the fatty acyl-CoA reductase (FarO) and putative lipid dehydrogenase/reductase (Spidey/Kar) pathway allow for suppression of oenocyte growth and promotion of lipid droplet storage under nutrient restriction and promotion of oenocyte growth in the presence of nutrients (Cinnamon et al. 2016). We speculate that accumulation of phosphatidylinositol in axenic bugs be a result of abnormal nutrient signaling and consequence of dysbiosis.

In *Drosophila*, ACC and the fatty acyl-CoA reductase gene, *Waterproof*, are involved in tracheal waterproofing and promote tracheal airway clearance. Knockdown of both genes

resulted in an arrest in ecdysis due to airway blockage in the trachea (Jaspers et al. 2014; Parvy et al. 2012). We conducted an expression analysis that revealed significantly lower expression of *acc* in the abdominal integument of axenic bugs compared to conventional and gnotobiotic bugs, providing evidence that gut bacteria may be important for the modulating the synthesis of cuticular lipids through this pathway. We found differential expression of *facr873* in the abdominal integument and differential expression of *facr223* in the fat body among axenic, conventional, and gnotobiotic fourth instar nymphs, further providing support that the microbiome may contribute to cuticular lipid synthesis by the oenocytes. We observed similar phenotypes to those found in Li et al. 2022 and Parvy et al. 2012, where *dsFACR873* and *dsFACR813* injected bugs exhibited 100% mortality due to disabled ecdysis. We suggest that both FACR873 and FACR813 may be involved in the synthesis of lipids used for the formation of trachea or tracheal waterproofing (Jaspers et al. 2014; Parvy et al. 2012).

Using GC-MS, we found higher n-C33 methyl-branched cuticular hydrocarbon levels in conventional bugs relative to axenic and gnotobiotic control bugs. In *Drosophila*, increasing chain length of methyl-branched hydrocarbons is correlated with increased desiccation tolerance (Wang et al. 2022). Similarly, we found that conventional bugs were more desiccation tolerant among axenic and gnotobiotic bugs. We also demonstrated that gut bacteria contribute to the formation of the epicuticle, as gnotobiotic bugs appeared to have a more conspicuous epicuticle compared to axenic bugs. Guo et al. 1991 demonstrated that gut bacteria of the termite, *Zootermopsis nevadensis*, produced propionate in the termite gut. The propionate provisioned by the gut microbiota was subsequently used for the synthesis of methyl-branched cuticular hydrocarbon biosynthesis. B vitamins are also known to be cofactors for the synthesis of methyl-branched cuticular hydrocarbons (Guo et al. 1991). We propose that the *R. prolixus* gut

microbiota may provision precursor molecules or B vitamins that fuel the synthesis of cuticular hydrocarbons by the oenocytes and epidermis, thus aiding the formation of the epicuticle and promoting desiccation tolerance. Future directions of this work will investigate the potential direct contributions of the microbiome, including synthesis of substrates or precursor molecules that are used for the cuticular lipid biosynthesis.

Table 5.S1. *Rhodnius prolixus* ACC and FACR primers used in this study.

Table 5.S1: Primer sequences			
Vectorbase accession	**Forward primer**	**Reverse primer**	**Primer type**
ACC: RPRC013987	TCAATAAACGTCTCCCTAACA	AGCACAAAAATCACCAAATAA	qPCR
	TAATACGACTCACTATAGGGAGAGATACTGCCTACCAGAACCTT	TAATACGACTCACTATAGGGAGACCATATCATCTTTGTGTCGAT	RNAi
FACR873: RPRC000873	TCAGAAAATTGTACCAATCCA	GTTGATGGTGACAGACAGTTT	qPCR
	TAATACGACTCACTATAGGGAGAGGCAAAGTCTTAGTGGAG	TAATACGACTCACTATAGGGAGAGGTGTACTAGGCGTTTAGTT	RNAi
FACR223: RPRC000223	GATAACATTTACGGTCCAACA	AGTTTTGTTTTGTGGATAGCA	qPCR
	TAATACGACTCACTATAGGGAGAAAGGAACTTGAAGAAATGACC	TAATACGACTCACTATAGGGAGAGAATAACCGGATTTGATTGAAGT	RNAi
FACR813: RPRC011813	TTTGTCTCCGAAGTTAGTCAA	TTGCGATACTAGAGACTCTGC	qPCR
	TAATACGACTCACTATAGGGAGATTATGATGGAAATAGGTCGTG	TAATACGACTCACTATAGGGAGACATTGAAACTTCCATTCATGT	RNAi
Underlined sequences denote T7 sequence for dsRNA synthesis			

REFERENCES

Abu-Elheiga L, Oh W, Kordari P, Wakil SJ. Acetyl-CoA carboxylase 2 mutant mice are protected against obesity and diabetes induced by high-fat/high-carbohydrate diets. *Proc Natl Acad Sci* (2003) 100(18):10207-12. doi: 10.1073/pnas.1733877100

Akbari OS, Antoshechkin I, Amrhein H, Williams B, Diloreto R, Sandler J, Hay BA. The developmental transcriptome of the mosquito *Aedes aegypti*, an invasive species and major arbovirus vector. *G3: Genes|Genomes|Genetics* (2013) 3(9):1493-509. doi: 10.1534/g3.113.006742

Aguilar R, Maestro JL, Vilaplana L, Chiva C, Andreu D, Bellés X. Identification of leucomyosuppressin in the German cockroach, *Blattella germanica*, as an inhibitor of food intake. *Regulatory Peptides* (2004) 119(1-2):105-112. doi:10.1016/j.regpep.2004.01.005

Alabaster A, Isoe J, Zhou G, Lee A, Murphy A, Day WA, Miesfeld RL. Deficiencies in acetyl-CoA carboxylase and fatty acid synthase 1 differentially affect eggshell formation and blood meal digestion in *Aedes aegypti*. *Insect Biochem Mol Biol* (2011) 41(12):946-55. doi: 10.1016/j.ibmb.2011.09.004

Alves-Bezerra M, De Paula IF, Medina JM, Silva-Oliveira G, Medeiros JS, Gäde G, Gondim KC. Adipokinetic hormone receptor gene identification and its role in triacylglycerol metabolism in the blood-sucking insect *Rhodnius prolixus*. *Insect Biochem Mol Biol* (2016) 69:51-60. doi: 10.1016/j.ibmb.2015.06.013

Andersen JF, Gudderra NP, Francischetti IM, Ribeiro JM. The role of salivary lipocalins in blood feeding by *Rhodnius prolixus*. *Arch Insect Biochem Physiol* (2005) 58(2):97-105. doi: 10.1002/arch.20032

Andre C, Haslam RP, Shanklin J. Feedback regulation of plastidic acetyl-CoA carboxylase by 18:1-acyl carrier protein in *Brassica napus*. *Proc Natl Acad Sci* (2012) 109(25):10107-12. doi: 10.1073/pnas.1204604109

Arcà B, Ribeiro JM. Saliva of hematophagous insects: a multifaceted toolkit. *Curr Opin Insect Sci* (2018) 29:102-109. doi: 10.1016/j.cois.2018.07.012

Arêdes DS, Rios T, Carvalho-Kelly LF, Braz V, Araripe LO, Bruno RV, Meyer-Fernandes JR, Ramos I, Gondim KC. Deficiency of Brummer lipase disturbs lipid mobilization and locomotion and impairs reproduction due to defects in the eggshell ultrastructure in the insect vector *Rhodnius prolixus*. *Biochim Biophys Acta Mol Cell Biol Lipids* (2024) 1869(2):159442. doi: 10.1016/j.bbalip.2023.159442

Arias-Giraldo LM, Muñoz M, Hernández C, Herrera G, Velásquez-Ortiz N, Cantillo-Barraza O, Urbano P, Ramírez JD. Species-dependent variation of the gut bacterial communities across *Trypanosoma cruzi* insect vectors. *PLoS One* (2020) 15(11):e0240916. doi: 10.1371/journal.pone.0240916

Arrese EL, Soulages JL. Insect fat body: energy, metabolism, and regulation. *Annu Rev Entomol* (2010) 55:207-25. doi: 10.1146/annurev-ento-112408-085356

Atella GC, Gondim C, Masuda H. Loading of lipophorin particles with phospholipids at the midgut of *Rhodnius prolixus*. *Arch Insect Biochem Physiol* (1995) 30(2-3):337-50. doi: 10.1002/arch.940300404

Audsley N, Down RE. G protein-coupled receptors as targets for next generation pesticides. *Insect Biochem Mol Biol* (2015) 67:27-37. doi: 10.1016/j.ibmb.2015.07.014

Ayub M, Hermiz M, Lange AB, Orchard I. SIFamide Influences Feeding in the Chagas Disease Vector, *Rhodnius prolixus*. *Front Neurosci* (2020) 14:134. doi: 10.3389/fnins.2020.00134

de Azambuja P, Furtado AF, Garcia ES. Effects of juvenile hormone analogue on ecdysis prevention induced by precocene in *Rhodnius prolixus* (Hemiptera:Reduviidae). *Mem Inst Oswaldo Cruz* (1984) 79(4):419-23. doi: 10.1590/s0074-02761984000400004

Baines S. The role of the symbiotic bacteria in the nutrition of *Rhodnius prolixus* (Hemiptera). *J Exp Biol* (1956) 33: 533–41.

Bainton RJ, Tsai LTY, Schwabe T, DeSalvo M, Gaul U, Heberlein U. moody encodes two GPCRs that regulate cocaine behaviors and blood-brain barrier permeability in *Drosophila*. *Cell* (2005) 123(1):145-156. doi:10.1016/j.cell.2005.07.029

Baldini F, Gabrieli P, South A, Valim C, Mancini F, Catteruccia F. The interaction between a sexually transferred steroid hormone and a female protein regulates oogenesis in the malaria mosquito *Anopheles gambiae*. *PLoS Biol* (2013) 11(10):e1001695. doi: 10.1371/journal.pbio.1001695

Bai L, Wang L, Vega-Rodríguez J, Wang G, Wang S. A gut symbiotic bacterium *Serratia marcescens* renders mosquito resistance to *Plasmodium* infection through activation of mosquito immune responses. *Front Microbiol* (2019) 10:1580. doi: 10.3389/fmicb.2019.01580

Barletta AB, Alves LR, Silva MC, Sim S, Dimopoulos G, Liechocki S, Maya-Monteiro CM, Sorgine MH. Emerging role of lipid droplets in *Aedes aegypti* immune response against bacteria and Dengue virus. *Sci Rep* (2016) 6:19928. doi: 10.1038/srep19928

Batalha MMC, Goulart HF, Santana AEG, Barbosa LAO, Nascimento TG, da Silva MKH, Dornelas CB, Grillo LAM. Chemical composition and antimicrobial activity of cuticular and internal lipids of the *insect Rhynchophorus palmarum*. *Arch Insect Biochem Physiol* (2020) 105(1):e21723. doi: 10.1002/arch.21723

Benton MA, Frey N, Nunes da Fonseca R, von Levetzow C, Stappert D, Hakeemi MS, Conrads KH, Pechmann M, Panfilio KA, Lynch JA, Roth S. Fog signaling has diverse roles in epithelial morphogenesis in insects. *Elife* (2019) 8:e47346. doi: 10.7554/eLife.47346

Bing X, Attardo GM, Vigneron A, Aksoy E, Scolari F, Malacrida A, Weiss BL, Aksoy S. Unravelling the relationship between the tsetse fly and its obligate symbiont *Wigglesworthia*: transcriptomic and metabolomic landscapes reveal highly integrated physiological networks. *Proc Biol Sci* (2017) 284(1857):20170360. doi: 10.1098/rspb.2017.0360

Bittencourt-Cunha PR, Silva-Cardoso L, Oliveira GA, Silva JR, Silveira AB, Kluck GE, Souza-Lima M, Gondim KC, Dansa-Petretsky M, Silva CP, Masuda H, Silva Neto MA, Atella GC. Perimicrovillar membrane assembly: the fate of phospholipids synthesized by the midgut of *Rhodnius prolixus*. *Mem Inst Oswaldo Cruz* (2013) 108(4):494-500. doi: 10.1590/S0074-0276108042013016

Blaustein L, Kotler BP. Oviposition habitat selection by the mosquito, *Culiseta longiareolata*: effects of conspecifics, food, and green toad tadpoles. *Ecol Entomol* (1993) 18(2):104–8. doi: 10.1111/j.1365-2311.1993.tb01190.x

Bloom M, Lange AB, Orchard I. Identification, functional characterization, and pharmacological analysis of two sulfakinin receptors in the medically-important insect *Rhodnius prolixus*. *Sci Rep* (2019) 9(1):13437. doi: 10.1038/s41598-019-49790-x

Botella-Cruz M, Velasco J, Millán A, Hetz S, Pallarés S. Cuticle hydrocarbons show plastic variation under desiccation in saline aquatic beetles. *Insects* (2021) 12(4):285. doi: 10.3390/insects12040285

Brackney DE, LaReau JC, Smith RC. Frequency matters: How successive feeding episodes by blood-feeding insect vectors influences disease transmission. *PLoS Pathog* (2021) 17(6):e1009590. doi: 10.1371/journal.ppat.1009590

Brecher G, Wigglesworth VB. The transmission of *Actinomyces rhodnii* (Erikson) in *Rhodnius prolixus* Stål (Hemiptera) and its influence on the growth of the host. *Parasitology* (1944) 35(4): 220–24. doi: https://doi.org/10.1017/S0031182000021648

Brown MR, Clark KD, Gulia M, Zhao Z, Garczynski SF, Crim JW, Suderman RJ, Strand MR. An insulin-like peptide regulates egg maturation and metabolism in the mosquito *Aedes aegypti*. *Proc Natl Acad Sci* (2008) 105(15):5716-21. doi: 10.1073/pnas.0800478105

Brown JJ, Rodríguez-Ruano SM, Poosakkannu A, Batani G, Schmidt JO, Roachell W, Zima J Jr, Hypša V, Nováková E. Ontogeny, species identity, and environment dominate microbiome dynamics in wild populations of kissing bugs (Triatominae). *Microbiome* (2020) 8(1):146. doi: 10.1186/s40168-020-00921-x

Cannell E, Dornan AJ, Halberg KA, Terhzaz S, Dow JAT, Davies SA. The corticotropin-releasing factor-like diuretic hormone 44 (DH 44) and kinin neuropeptides modulate desiccation and starvation tolerance in *Drosophila melanogaster*. *Peptides (NY)* (2016) 80:96-107. doi:10.1016/j.peptides.2016.02.004

Capella-Gutiérrez S, Silla-Martínez JM, Gabaldón T. trimAl: a tool for automated alignment trimming in large-scale phylogenetic analyses. *Bioinformatics* (2009) 25(15):1972-3. doi: 10.1093/bioinformatics/btp348

Capriotti N, Ianowski JP, Gioino P, Ons S. The neuropeptide CCHamide2 regulates diuresis in the Chagas disease vector *Rhodnius prolixus*. *J Exp Biol* (2019) 222(Pt 10):jeb203000. doi: 10.1242/jeb.203000

Cardé RT. Multi-cue integration: how female mosquitoes locate a human host. *Curr Biol* (2015) 25(18):R793-5. doi: 10.1016/j.cub.2015.07.057

Carpenter JM, Hynds HM, Bimpeh K, Hines KM. HILIC-IM-MS for simultaneous lipid and metabolite profiling of bacteria. *ACS Meas Sci Au* (2023) 4(1):104-116. doi: 10.1021/acsmeasuresciau.3c00051

Cator LJ, Arthur BJ, Ponlawat A, Harrington LC. Behavioral observations and sound recordings of free-flight mating swarms of *Ae. aegypti* (Diptera: Culicidae) in Thailand. *J Med Entomol* (2011) 48(4):941-6. doi: 10.1603/me11019

Cator LJ, Wyer CAS, Harrington LC. Mosquito sexual selection and reproductive control programs. *Trends Parasitol* (2021) 37(4):330-339. doi: 10.1016/j.pt.2020.11.009

Canavoso LE, Jouni ZE, Karnas KJ, Pennington JE, Wells MA. Fat metabolism in insects. *Annu Rev Nutr* (2001) 21:23-46. doi: 10.1146/annurev.nutr.21.1.23

CDC. Mosquitoes. 2020. https://www.cdc.gov/mosquitoes/about/diseases.html. 9 April 2024

CDC. Parasites - American Trypanosomiasis (also known as Chagas Disease). 2023. https://www.cdc.gov/parasites/chagas/index.html. 9 April 2024

Champagne DE. Antihemostatic strategies of blood-feeding arthropods. *Curr Drug Targets Cardiovasc Haematol Disord* (2004) 4(4):375-96. doi: 10.2174/1568006043335862

Chertemps T, Duportets L, Labeur C, Ueda R, Takahashi K, Saigo K, Wicker-Thomas C. A female-biased expressed elongase involved in long-chain hydrocarbon biosynthesis and courtship behavior in *Drosophila melanogaster*. *Proc Natl Acad Sci* (2007) 104(11):4273-8. doi: 10.1073/pnas.0608142104

Christie AE, Hull JJ. What can transcriptomics reveal about the phylogenetic/structural conservation, tissue localization, and possible functions of CNMamide peptides in

decapod crustaceans*? Gen Comp Endocrinol* (2019) 282:113217. doi: 10.1016/j.ygcen.2019.113217

Cinnamon E, Makki R, Sawala A, Wickenberg LP, Blomquist GJ, Tittiger C, Paroush Z, Gould AP. *Drosophila* Spidey/Kar regulates oenocyte growth via PI3-Kinase signaling. *PLoS Genet* (2016) 12(8):e1006154. doi: 10.1371/journal.pgen.1006154

Clements AN. *The Biology of Mosquitoes*. Development, Nutrition and Reproduction. (1992) Volume 1. London: Chapman and Hall.

Clifton ME, Noriega FG. Nutrient limitation results in juvenile hormone-mediated resorption of previtellogenic ovarian follicles in mosquitoes. *J Insect Physiol* (2011) 57(9):1274-81. doi: 10.1016/j.jinsphys.2011.06.002

Clifton ME, Noriega FG. The fate of follicles after a blood meal is dependent on previtellogenic nutrition and juvenile hormone in *Aedes aegypti*. *J Insect Physiol* (2012) 58(7):1007-19. doi: 10.1016/j.jinsphys.2012.05.005

Cohen AC. Feeding adaptations of some predaceous Hemiptera." *Ann Entomol* (1990) 83(6):1215–23. doi: https://doi.org/10.1093/aesa/83.6.1215

Coon KL, Valzania L, McKinney DA, Vogel KJ, Brown MR, Strand MR. Bacteria-mediated hypoxia functions as a signal for mosquito development. *Proc Natl Acad Sci* (2017) 114(27):E5362-E5369. doi: 10.1073/pnas.1702983114

Coon KL, Vogel KJ, Brown MR, Strand MR. Mosquitoes rely on their gut microbiota for development. *Mol Ecol* (2014) 23(11):2727-39. doi: 10.1111/mec.12771

Coutinho-Abreu IV, Riffell JA, Akbari OS. Human attractive cues and mosquito host-seeking behavior. *Trends Parasitol* (2022) 38(3):246-264. doi: 10.1016/j.pt.2021.09.012

Dahalan FA, Churcher TS, Windbichler N, Lawniczak MKN. The male mosquito contribution towards malaria transmission: Mating influences the Anopheles female midgut transcriptome and increases female susceptibility to human malaria parasites. *PLoS Pathog* (2019) 15(11):e1008063. doi: 10.1371/journal.ppat.1008063

Dawaliby R, Trubbia C, Delporte C, Noyon C, Ruysschaert JM, Van Antwerpen P, Govaerts C. Phosphatidylethanolamine is a key regulator of membrane fluidity in eukaryotic cells. *J Biol Chem* (2016) 291(7):3658-67. doi: 10.1074/jbc.M115.706523

Defferrari MS, Orchard I, Lange AB. An insulin-like growth factor in *Rhodnius prolixus* is involved in post-feeding nutrient balance and growth. *Front Neurosci* (2016) 10:566. doi: 10.3389/fnins.2016.00566

Degner EC, Harrington LC. Polyandry depends on postmating time interval in the Dengue vector *Aedes aegypti*. *Am J Trop Med Hyg* (2016) 94(4):780-785. doi: 10.4269/ajtmh.15-0893

Dennell R. The occurrence and significance of phenolic hardening in the newly formed cuticle of Crustacea Decapoda. *Proc R Soc Med* (1947) 134(877):485-503. doi: 10.1098/rspb.1947.0027

Dhara A, Eum JH, Robertson A, Gulia-Nuss M, Vogel KJ, Clark KD, Graf R, Brown MR, Strand MR. Ovary ecdysteroidogenic hormone functions independently of the insulin receptor in the yellow fever mosquito, *Aedes aegypti*. *Insect Biochem Mol Biol* (2013) 43(12):1100-8. doi: 10.1016/j.ibmb.2013.09.004

Douglas AE. The B vitamin nutrition of insects: the contributions of diet, microbiome and horizontally acquired genes. *Curr Opin Insect Sci* (2017) 23:65-69. doi: 10.1016/j.cois.2017.07.012

Dulbecco AB, Moriconi DE, Lynn S, McCarthy A, Juárez MP, Girotti JR, Calderón-Fernández GM. Deciphering the role of Rhodnius prolixus CYP4G genes in straight and methyl-branched hydrocarbon formation and in desiccation tolerance. *Insect Mol Biol* (2020) 29(5):431-443. doi: 10.1111/imb.12653

Duvall LB. Mosquito host-seeking regulation: Targets for behavioral control. *Trends Parasitol* (2019) 35(9):704-714. doi: 10.1016/j.pt.2019.06.010

Duvall LB, Ramos-Espiritu L, Barsoum KE, Glickman JF, Vosshall LB. Small-molecule agonists of *Ae. aegypti* Neuropeptide Y receptor block mosquito biting. *Cell* (2019) 176(4):687-701.e5. doi: 10.1016/j.cell.2018.12.004

Eberhard FE, Klimpel S, Guarneri AA, Tobias NJ. Exposure to *Trypanosoma* parasites induces changes in the microbiome of the Chagas disease vector *Rhodnius prolixus*. *Microbiome* (2022) 10(1):45. doi: 10.1186/s40168-022-01240-z

Eddy SR. Accelerated profile HMM searches. *PLoS Comput Biol* (2011) 7(10):e1002195. doi: 10.1371/journal.pcbi.1002195

Ekoka E, Maharaj S, Nardini L, Dahan-Moss Y, Koekemoer LL. 20-Hydroxyecdysone (20E) signaling as a promising target for the chemical control of malaria vectors. *Parasit Vectors* (2021) 14(1):86. doi:10.1186/s13071-020-04558-5

El-Sheikh el-SA, Kamita SG, Hammock BD. Effects of juvenile hormone (JH) analog insecticides on larval development and JH esterase activity in two spodopterans. *Pestic Biochem Physiol* (2016) 128:30-6. doi: 10.1016/j.pestbp.2015.10.008

Engl T, Eberl N, Gorse C, Krüger T, Schmidt THP, Plarre R, Adler C, Kaltenpoth M. Ancient symbiosis confers desiccation resistance to stored grain pest beetles. *Mol Ecol* (2018) 27(8):2095-2108. doi: 10.1111/mec.14418

Engl T, Schmidt THP, Kanyile SN, Klebsch D. Metabolic cost of a nutritional symbiont manifests in delayed reproduction in a grain pest beetle. *Insects* (2020) 11(10):717. doi: 10.3390/insects11100717

Entringer PF, Grillo LA, Pontes EG, Machado EA, Gondim KC. Interaction of lipophorin with *Rhodnius prolixus* oocytes: biochemical properties and the importance of blood feeding. *Mem Inst Oswaldo Cruz* (2013) 108(7):836-44. doi: 10.1590/0074-0276130129

Ferveur JF, Cortot J, Rihani K, Cobb M, Everaerts C. Desiccation resistance: effect of cuticular hydrocarbons and water content in *Drosophila melanogaster* adults. *PeerJ* (2018) 6:e4318. doi: 10.7717/peerj.4318

Francis SE, Sullivan DJ Jr, Goldberg DE. Hemoglobin metabolism in the malaria parasite *Plasmodium falciparum*. *Annu Rev Microbiol* (1997) 51:97-123. doi: 10.1146/annurev.micro.51.1.97

Freitas L, Nery MF. Expansions and contractions in gene families of independently-evolved blood-feeding insects. *BMC Evol Biol* (2020) 20(1):87. doi: 10.1186/s12862-020-01650-3

Fuchs S, Rende E, Crisanti A, Nolan T. Disruption of aminergic signalling reveals novel compounds with distinct inhibitory effects on mosquito reproduction, locomotor function and survival. *Sci Rep* (2014) 4:5526. doi: 10.1038/srep05526

Garcia ES, Feder D, Gomes JE, de Azambuja P. Effects of precocene and azadirachtin in *Rhodnius prolixus*: some data on development and reproduction. *Mem Inst Oswaldo Cruz* (1987a) 82(3):67-73. doi: 10.1590/s0074-02761987000700014

Garcia ES, Furtado AF, de Azambuja P. Effect of allatectomy on ecdysteroid-dependent development of *Rhodnius prolixus* larvae." *J Insect Physiol* (1987b) 33(10). doi: https://doi.org/10.1016/0022-1910(87)90058-8

Gaio Ade O, Gusmão DS, Santos AV, Berbert-Molina MA, Pimenta PF, Lemos FJ. Contribution of midgut bacteria to blood digestion and egg production in *Aedes aegypti* (Diptera: Culicidae) (L.). *Parasit Vectors* (2011) 4:105. doi: 10.1186/1756-3305-4-105

Gibellini F, Smith TK. The Kennedy pathway--De novo synthesis of phosphatidylethanolamine and phosphatidylcholine. *IUBMB Life* (2010) 62(6):414-28. doi: 10.1002/iub.337

Gilliland CA, Patel V, McCormick AC, Mackett BM, Vogel KJ. Using axenic and gnotobiotic insects to examine the role of different microbes on the development and reproduction of the kissing bug *Rhodnius prolixus* (Hemiptera: Reduviidae). *Mol Ecol* (2023) 32(4):920-935. doi: 10.1111/mec.16800

Goldring JP, Read JS. Insect acetyl-CoA carboxylase: enzyme activity during adult development and after feeding in the tsetse fly, *Glossina morsitans. Comp Biochem Physiol Biochem Mol Biol* (1994) 108(1):27-33. doi: 10.1016/0305-0491(94)90160-0

Golodne DM, Monteiro RQ, Graca-Souza AV, Silva-Neto MA, Atella GC. Lysophosphatidylcholine acts as an anti-hemostatic molecule in the saliva of the blood-sucking bug *Rhodnius prolixus*. *J Biol Chem* (2003) 278(30):27766-71. doi: 10.1074/jbc.M212421200

Gondim KC, Atella GC, Pontes EG, Majerowicz D. Lipid metabolism in insect disease vectors. *Insect Biochem Mol Biol* (2018) 101:108-123. doi: 10.1016/j.ibmb.2018.08.005

Gorbatov VM. Collection and utilization of blood and blood proteins for edible purposes in the USSR." *Adv Meat Res* (1988) 5:167–95.

Grillo LA, Pontes EG, Gondim KC. Lipophorin interaction with the midgut of *Rhodnius prolixus*: characterization and changes in binding capacity. *Insect Biochem Mol Biol* (2003) 33(4):429-38. doi: 10.1016/s0965-1748(03)00007-9

Grillo LA, Majerowicz D, Gondim KC. Lipid metabolism in *Rhodnius prolixus* (Hemiptera: Reduviidae): role of a midgut triacylglycerol-lipase. *Insect Biochem Mol Biol* (2007) 37(6):579-88. doi: 10.1016/j.ibmb.2007.03.002

Gu L, Liu H, Gu X, Boots C, Moley KH, Wang Q. Metabolic control of oocyte development: linking maternal nutrition and reproductive outcomes. *Cell Mol Life Sci* (2015) 72(2):251-71. doi: 10.1007/s00018-014-1739-4

Guindon S, Dufayard JF, Lefort V, Anisimova M, Hordijk W, Gascuel O. New algorithms and methods to estimate maximum-likelihood phylogenies: assessing the performance of PhyML 3.0. *Systems Biol*ogy (2010) 59(3):307-321. doi:10.1093/sysbio/syq010

Gulia-Nuss M, Robertson AE, Brown MR, Strand MR. Insulin-like peptides and the target of rapamycin pathway coordinately regulate blood digestion and egg maturation in the mosquito *Aedes aegypti. PLoS One* (2011) 6(5):e20401. doi: 10.1371/journal.pone.0020401

Guo L, Quilici DR, Chase J, Blomquist GJ. Gut tract microorganisms supply the precursors for methyl-branched hydrocarbon biosynthesis in the termite, *Zootermopsis nevadensis*. *Insect Biochem* (1991) 21(3):327-333. doi: https://doi.org/10.1016/0020-1790(91)90023-8

Gutierrez E, Wiggins D, Fielding B, Gould AP. Specialized hepatocyte-like cells regulate *Drosophila* lipid metabolism. *Nature* (2007) 445(7125):275-80. doi: 10.1038/nature05382

Gwadz RW, Spielman A. Corpus allatum control of ovarian development in *Aedes aegypti*. *J Insect Physiol* (1973) 19:1441–1448.

Hafez AM, Abbas N. Insecticide resistance to insect growth regulators, avermectins, spinosyns and diamides in *Culex quinquefasciatus* in Saudi Arabia. *Parasit Vectors* (2021) 14(1):558. doi:10.1186/s13071-021-05068-8

Hansen IA, Attardo GM, Rodriguez SD, Drake LL. Four-way regulation of mosquito yolk protein precursor genes by juvenile hormone-, ecdysone-, nutrient-, and insulin-like peptide signaling pathways. *Front Physiol* (2014) 5. doi:10.3389/fphys.2014.00103

Hartberg WK. Observations on the mating behaviour of *Aedes aegypti* in nature. *Bull World Health Organ* (1971) 45(6): 847–50.

Hatan M, Shinder V, Israeli D, Schnorrer, Volk T. The *Drosophila* blood brain barrier is maintained by GPCR-dependent dynamic actin structures. *J Cell Biol* (2011) 192(2):307-19. doi: 10.1083/jcb.201007095

Hayes RO. Determination of a physiological saline solution for *Aedes aegypti* (L.), *J Econ Entomol* (1953) 46(4):624-627. doi: https://doi.org/10.1093/jee/46.4.624

Helinski ME, Deewatthanawong P, Sirot LK, Wolfner MF, Harrington LC. Duration and dose-dependency of female sexual receptivity responses to seminal fluid proteins in *Aedes albopictus* and *Ae. aegypti* mosquitoes. *J Insect Physiol* (2012) 58(10):1307-13. doi: 10.1016/j.jinsphys.2012.07.003

Hickin ML, Kakumanu ML, Schal C. Effects of *Wolbachia* elimination and B-vitamin supplementation on bed bug development and reproduction. *Sci Rep* (2022) 12(1):10270. doi: https://doi.org/10.1038/s41598-022-14505-2

Hill CA, Meyer JM, Ejendal KF, Echeverry DF, Lang EG, Avramova LV, Conley JM, Watts VJ. Re-invigorating the insecticide discovery pipeline for vector control: GPCRs as targets

for the identification of next gen insecticides. *Pestic Biochem and Physiol* (2013) 106(3):141-148. doi:10.1016/j.pestbp.2013.02.008

Hirota B, Okude G, Anbutsu H, Futahashi R, Moriyama M, Meng XY, Nikoh N, Koga R, Fukatsu T. A novel, extremely elongated, and endocellular bacterial symbiont supports cuticle formation of a grain pest beetle. *mBio* (2017) 8(5):e01482-17. doi: 10.1128/mBio.01482-17

Hiss EA, Fuchs MS. The Effect of matrone on oviposition in the mosquito, *Aedes aegypti*. *J Insect Physiol* (1972) 18:2217–2227.

Holze H, Schrader L, Buellesbach J. Advances in deciphering the genetic basis of insect cuticular hydrocarbon biosynthesis and variation. *Heredity* (2021) 126(2):219-234. doi: 10.1038/s41437-020-00380-y

Hosokawa T, Koga R, Kikuchi Y, Meng XY, Fukatsu T. *Wolbachia* as a bacteriocyte-associated nutritional mutualist. *Proc Natl Acad Sci* (2010) 107(2):769-74. doi: 10.1073/pnas.0911476107

Jaskowska E, Butler C, Preston G, Kelly S. Phytomonas: trypanosomatids adapted to plant environments. *PLoS Pathog* (2015) 11(1):e1004484. doi: 10.1371/journal.ppat.1004484

Jaspers MH, Pflanz R, Riedel D, Kawelke S, Feussner I, Schuh R. The fatty acyl-CoA reductase Waterproof mediates airway clearance in *Drosophila*. *Dev Biol* (2014) 385(1):23-31. doi: 10.1016/j.ydbio.2013.10.022

Jones JC, Pilitt DR. Blood-feeding behavior of adult *Aedes aegypti* mosquitoes. *Biol Bull* (1973) 145(1):127-39. doi: 10.2307/1540353

Jung SH, Lee JH, Chae HS, Seong JY, Park Y, Park ZY, Kim YJ. Identification of a novel insect neuropeptide, CNMa and its receptor. *FEBS Lett* (2014) 588(12):2037-41.

doi: 10.1016/j.febslet.2014.04.028

Kamps AR, Pruitt MM, Herriges JC, Coffman CR. An evolutionarily conserved arginine is essential for tre1 G protein-coupled receptor function during germ cell migration in *Drosophila melanogaster*. *PLoS One* (2010) 5(7):e11839. doi:10.1371/journal.pone.0011839

Kastner KW, Shoue DA, Estiu GL, Wolford J, Fuerst MF, Markley LD, Izaguirre JA, McDowell MA. Characterization of the *Anopheles gambiae* octopamine receptor and discovery of potential agonists and antagonists using a combined computational-experimental approach. *Malar J* (2014) 13:434. doi: 10.1186/1475-2875-13-434

Katoh, K, Misawa K, Kuma KI; Miyata T. MAFFT: A novel method for rapid multiple sequence alignment based on fast fourier transform. *Nucleic Acids Res* (2002) 30:3059–3066. doi: 10.1093/nar/gkf436

Keyes-Scott NI, Lajevardi A, Swade KR, Brown MR, Paluzzi JP, Vogel KJ. The peptide hormone CNMa influences egg production in the mosquito *Aedes aegypti*. *Insects* (2022) 13(3):230. doi:10.3390/insects13030230

Kiefer JST, Batsukh S, Bauer E, Hirota B, Weiss B, Wierz JC, Fukatsu T, Kaltenpoth M, Engl T. Inhibition of a nutritional endosymbiont by glyphosate abolishes mutualistic benefit on cuticle synthesis in *Oryzaephilus surinamensis*. *Commun Biol* (2021) 4(1):554. doi: 10.1038/s42003-021-02057-6

Kiefer JST, Bauer E, Okude G, Fukatsu T, Kaltenpoth M, Engl T. Cuticle supplementation and nitrogen recycling by a dual bacterial symbiosis in a family of xylophagous beetles. *ISME J* (2023) 17(7):1029-1039. doi: 10.1038/s41396-023-01415-y

Kim B, Kanai MI, Oh Y, Kyung M, Kim EK, Jang IH, Lee JH, Kim SG, Suh GSB, Lee WJ. Response of the microbiome-gut-brain axis in *Drosophila* to amino acid deficit. *Nature* (2021) 593(7860):570-574. doi: 10.1038/s41586-021-03522-2

Klowden MJ, Chambers GM. Male accessory gland substances activate egg development in nutritionally stressed *Aedes aegypti* mosquitoes. *J Insect Physiol* (1991) 37(10). doi: https://doi.org/10.1016/0022-1910(91)90105-9

Klowden MJ. *Physiological Systems in Insects*. Elsevier. (2013) 3rd ed.

Kotaki T, Shinada T, Kaihara K, Ohfune Y, Numata H. Structure determination of a new juvenile hormone from a heteropteran insect. *Org Lett* (2009) 11(22):5234-7. doi: 10.1021/ol902161x

Kohyama-Koganeya A, Kim YJ, Miura M, Hirabayashi Y. A *Drosophila* orphan G protein-coupled receptor BOSS functions as a glucose-responding receptor: Loss of boss causes abnormal energy metabolism. *Proc Natl Acad Sci* (2008) 105(40):15328-15333. doi:10.1073/pnas.0807833105

Kramer KJ, Hopkins TL. Tyrosine metabolism for insect cuticle tanning. *Arch Insect Biochem Physiol* (1987) 6:279-301. doi: https://doi.org/10.1002/arch.940060406

Kriventseva EV, Kuznetsov D, Tegenfeldt F, Manni M, Dias R, Simão FA, Zdobnov EM. OrthoDB v10: sampling the diversity of animal, plant, fungal, protist, bacterial and viral genomes for evolutionary and functional annotations of orthologs. *Nucleic Acids Res* (2019) 47(D1):D807-D811. doi: 10.1093/nar/gky1053

Krupp JJ, Nayal K, Wong A, Millar JG, Levine JD. Desiccation resistance is an adaptive life-history trait dependent upon cuticular hydrocarbons, and influenced by mating status and temperature *in D. melanogaster*. *J Insect Physiol* (2020) 121:103990.

doi: 10.1016/j.jinsphys.2019.103990

Kunwar PS, Sano H, Renault AD, Barbosa V, Fuse N, Lehmann R. Tre1 GPCR initiates germ cell transepithelial migration by regulating *Drosophila melanogaster* E-cadherin. *J Cell Biol* (2008) 183(1):157-168. doi:10.1083/jcb.200807049

Kunwar PS, Starz-Gaiano M, Bainton RJ, Heberlein U, Lehmann R. Tre1, a G protein-coupled receptor, directs transepithelial migration of *Drosophila* germ cells. *PLoS Biol* (2003) 1(3):e80. doi:10.1371/journal.pbio.0000080

Kuznetsov D, Tegenfeldt F, Manni M, Seppey M, Berkeley M, Kriventseva EV, Zdobnov EM. OrthoDB v11: annotation of orthologs in the widest sampling of organismal diversity. *Nucleic Acids Res* (2023) 51(D1):D445-D451. doi: 10.1093/nar/gkac998

Lake P, Friend WG. The use of artificial diets to determine some of the effects of *Nocardia rhodnii* on the development of *Rhodnius prolixus*. *J Insect Physiol* (1968) 14(4):543-62. doi: 10.1016/0022-1910(68)90070-x

Lane NJ, Harrison JB. An unusual cell surface modification: a double plasma membrane. *J Cell Sci* (1979) 39:355-72. doi: 10.1242/jcs.39.1.355

LeBlanc MG, Lehmann R. Domain-specific control of germ cell polarity and migration by multifunction Tre1 GPCR. *J Cell Biol* (2017) 216(9):2945-2958. doi:10.1083/jcb.201612053

Lee CK, Cheong HK, Ryu KS, Lee JI, Lee W, Jeon YH, Cheong C. Biotinoyl domain of human acetyl-CoA carboxylase: Structural insights into the carboxyl transfer mechanism. *Proteins* (2008) 72(2):613-24. doi: 10.1002/prot.21952

Lehane M. *The Biology of Blood-Sucking in Insects*. Cambridge University Press (2005) 2nd ed.

Leyria J, El-Mawed H, Orchard I, Lange AB. Regulation of a trehalose-specific facilitated transporter (TRET) by insulin and adipokinetic hormone in *Rhodnius prolixus*, a vector of Chagas disease. *Front Physiol* (2021) 12:624165. doi: 10.3389/fphys.2021.624165

Li DT, Dai YT, Chen X, Wang XQ, Li ZD, Moussian B, Zhang CX. Ten fatty acyl-CoA reductase family genes were essential for the survival of the destructive rice pest, *Nilaparvata lugens*. *Pest Manag Sci* (2020) 76(7):2304-2315. doi: 10.1002/ps.5765

Liu D, Xiao Y, Evans BS, Zhang F. Negative feedback regulation of fatty acid production based on a malonyl-CoA sensor-actuator. *ACS Synth Biol* (2015) 4(2):132-40. doi: 10.1021/sb400158w

Locke M. Secretion of wax through the cuticle of insects. *Nature* (1959) 184(4703):1967–1967. doi: https://doi.org/10.1038/1841967a0.

Lockey KH, Lipids of the insect cuticle: origin, composition and function. *Comp Biochem Physiol B Biochem Mol Biol* (1988) 89(4):595-645. doi: https://doi.org/10.1016/0305-0491(88)90305-7

Luu P, Zaki SA, Tran DH, French RL. A novel gene controlling the timing of courtship initiation in *Drosophila melanogaster*. *Genetics* (2016) 202(3):1043-1053. doi:10.1534/genetics.115.183061

Lynch SA, Mullen AM, O'Neill EE, García CÁ. Harnessing the potential of blood proteins as functional ingredients: A review of the state of the art in blood processing. *Compr Rev Food Sci Food Saf* (2017) 16(2):330-344. doi: 10.1111/1541-4337.12254

Ma T, Matsuoka S, Drummond-Barbosa D. RNAi-based screens uncover a potential new role for the orphan neuropeptide receptor Moody in *Drosophila* female germline stem cell maintenance. *PLoS One* (2020) 15(12):e0243756. doi:10.1371/journal.pone.0243756

MacLean M, Nadeau J, Gurnea T, Tittiger C, Blomquist GJ. Mountain pine beetle (*Dendroctonus ponderosae*) CYP4Gs convert long and short chain alcohols and aldehydes to hydrocarbons. *Insect Biochem Mol Biol* (2018) 102:11-20. doi: 10.1016/j.ibmb.2018.09.005

Maguire SE, Potter CJ. Diet drugs trick mosquitoes into feeling full. *Trends Pharmacol Sci* (2019) 40(7):449-451. doi: 10.1016/j.tips.2019.04.016

Majerowicz D, Calderón-Fernández GM, Alves-Bezerra M, De Paula IF, Cardoso LS, Juárez MP, Atella GC, Gondim KC. Lipid metabolism in *Rhodnius prolixus*: Lessons from the genome. *Gene* (2017) 596:27-44. doi: 10.1016/j.gene.2016.09.045

Mane-Padros D, Cruz J, Cheng A, Raikhel AS. A critical role of the nuclear receptor HR3 in regulation of gonadotrophic cycles of the mosquito *Aedes aegypti*. *PLoS One* (2012) 7(9):e45019. doi: 10.1371/journal.pone.0045019

Martelli C, Pech U, Kobbenbring S, Pauls D, Bahl B, Sommer MV, Pooryasin A, Barth J, Arias CWP, Vassiliou C, Luna AJF, Poppinga H, Richter FG, Wegener C, Fiala A, Riemensperger T. SIFamide translates hunger signals into appetitive and feeding behavior in *Drosophila*. *Cell Rep* (2017) 20(2):464-478. doi: 10.1016/j.celrep.2017.06.043. PMID: 28700946

Marchal E, Vandersmissen HP, Badisco L, Van de Velde S, Verlinden H, Iga M, Van Wielendaele P, Huybrechts R, Simonet G, Smagghe G, Vanden Broeck J. Control of ecdysteroidogenesis in prothoracic glands of insects: a review. *Peptides* (2010) 31(3):506-19. doi: 10.1016/j.peptides.2009.08.020

Martini SV, Nascimento SB, Morales MM. Rhodnius prolixus Malpighian tubules and control of diuresis by neurohormones. *An Acad Bras Cienc* (2007) 79(1):87-95. doi: 10.1590/s0001-37652007000100011

Matsumoto S, Brown MR, Suzuki A, Lea AO. Isolation and characterization of ovarian ecdysteroidogenic hormones from the mosquito, *Aedes aegypti*. *Insect Biochem* (1989) 19(7):651-656. doi:10.1016/0020-1790(89)90100-5

McBride CS, Baier F, Omondi AB, Spitzer SA, Lutomiah J, Sang R, Ignell R, Vosshall LB. Evolution of mosquito preference for humans linked to an odorant receptor. *Nature* (2014) 515(7526):222-7. doi: 10.1038/nature13964

Meyer JM, Ejendal KF, Avramova LV, Garland-Kuntz EE, Giraldo-Calderón GI, Brust TF, Watts VJ, Hill CA. A "genome-to-lead" approach for insecticide discovery: pharmacological characterization and screening of *Aedes aegypti* D(1)-like dopamine receptors. *PLoS Negl Trop Dis* (2012) 6(1):e1478. doi: 10.1371/journal.pntd.0001478

Meylaers K, Clynen E, Daloze D, DeLoof A, Schoofs L. Identification of 1-lysophosphatidylethanolamine (C(16:1)) as an antimicrobial compound in the housefly, *Musca domestica*. *Insect Biochem Mol Biol* (2004) 34(1):43-9. doi: 10.1016/j.ibmb.2003.09.001

Millar JG, Chaney JD, Mulla MS. Identification of oviposition attractants for *Culex quinquefasciatus* from fermented Bermuda grass infusions. *J Am Mosq Control Assoc* (1992) 8(1):11-7.

Moore RF Jr, Taft HM. Differences in percentages of fatty acids in triglycerides and phospholipids larvae of the bollworm and the tobacco budworm as possible factors in their tolerance to insecticides. *J Econ Entomol* (1971) 64(5):1060-5.

doi: 10.1093/jee/64.5.1060

Moraes B, Braz V, Santos-Araujo S, Oliveira IA, Bomfim L, Ramos I, Gondim KC. Deficiency of acetyl-CoA carboxylase impairs digestion, lipid synthesis, and reproduction in the kissing bug *Rhodnius prolixus*. *Front Physiol* (2022) 13:934667. doi: 10.3389/fphys.2022.934667

Moriconi DE, Dulbecco AB, Juárez MP, Calderón-Fernández GM. A fatty acid synthase gene (FASN3) from the integument tissue of *Rhodnius prolixus* contributes to cuticle water loss regulation. *Insect Mol Biol* (2019) 28(6):850-861. doi: 10.1111/imb.12600

Moto K, Yoshiga T, Yamamoto M, Takahashi S, Okano K, Ando T, Nakata T, Matsumoto S. Pheromone gland-specific fatty-acyl reductase of the silkmoth, *Bombyx mori*. *Proc Natl Acad Sci* (2003) 100(16):9156-61. doi: 10.1073/pnas.1531993100

Mulla MS. The future of insect growth regulators in vector control. *J Am Mosq Control Assoc* (1995) 11(2 Pt 2):269-73.

Municio AM, Odriozola JM, Pérez-Albarsanz MA. Biochemistry of development in insects. Incorporation of fatty acids into different lipid classes. *Eur J Biochem* (1975) 60(1):123-8. doi: 10.1111/j.1432-1033.1975.tb20983.x

Munoz S, Guerrero FD, Kellogg A, Heekin AM, Leung MY. Bioinformatic prediction of G protein-coupled receptor encoding sequences from the transcriptome of the foreleg, including the Haller's organ, of the cattle tick, *Rhipicephalus australis*. *PLoS One* (2017) 12(2):e0172326. doi: 10.1371/journal.pone.0172326

Mwingira V, Mboera LEG, Dicke M, Takken W. Exploiting the chemical ecology of mosquito oviposition behavior in mosquito surveillance and control: a review. *J Vector Ecol* (2020) 45(2):155-179. doi: 10.1111/jvec.12387

Nabert A. Die Corpora Allata Der Insekten. *Zeit f Wiss Zool* (1913) 104 (1).

Naccarati C, Audsley N, Keen JN, Kim JH, Howell GJ, Kim YJ, Isaac RE. The host-seeking inhibitory peptide, Aea-HP-1, is made in the male accessory gland and transferred to the female during copulation. *Peptides* (2012) 34(1):150-7. doi: 10.1016/j.peptides.2011.10.027

Nässel DR, Broeck JV. Insulin/IGF signaling in *Drosophila* and other insects: factors that regulate production, release and post-release action of the insulin-like peptides. *Cell Mol Life Sci* (2016) 73(2). doi:10.1007/s00018-015-2063-3

Nation JL. *Encyclopedia of Entomology*. Integument: Structure and Function. Springer (2008) doi: https://doi.org/10.1007/978-1-4020-6359-6_1557

Neafsey DE, Waterhouse RM, Abai MR, Aganezov SS, Alekseyev MA, Allen JE, Amon J, Arcà B, Arensburger P, Artemov G, Assour LA, Basseri H, Berlin A, Birren BW, Blandin SA, Brockman AI, Burkot TR, Burt A, Chan CS... Besansky NJ. Mosquito genomics. Highly evolvable malaria vectors: the genomes of 16 *Anopheles* mosquitoes. *Science* (2015) 347(6217):1258522. doi: 10.1126/science.1258522

Nuss AB, Brown MR. Isolation of an insulin-like peptide from the Asian malaria mosquito, *Anopheles stephensi*, that acts as a steroidogenic gonadotropin across diverse mosquito taxa. *Gen Comp Endocrinol* (2018) 258:140-148. doi: 10.1016/j.ygcen.2017.05.007

Nyirady SA. The germfree culture of three species of Triatominae: *Triatoma protracta* (Uhler), *Triatoma rubida* (Uhler) and *Rhodnius prolixus* Stål. *J Med Entomol* (1973) 10(5):417-48. doi: 10.1093/jmedent/10.5.417

Oliveira MF, Gandara ACP, Braga CMS, Silva JR, Mury FB, Dansa-Petretski M, Menezes D, Vannier-Santos MA, Oliveira PL. Heme crystallization in the midgut of triatomine insects. *Comp Biochem Physiol C Toxicol Pharmacol* (2007) 146(1-2):168-174. doi: 10.1016/j.cbpc.2006.12.007

Oliveira MF, Kycia SW, Gomez A, Kosar AJ, Bohle DS, Hempelmann E, Menezes D, Vannier-Santos MA, Oliveira PL, Ferreira ST. Structural and morphological characterization of hemozoin produced by *Schistosoma mansoni* and *Rhodnius prolixus*. *FEBS Lett* (2005) 579(27):6010-6. doi: 10.1016/j.febslet.2005.09.035

Oliveira MF, Silva JR, Dansa-Petretski M, de Souza W, Lins U, Braga CM, Masuda H, Oliveira PL. Haem detoxification by an insect. *Nature* (1999) 400(6744):517-8. doi: 10.1038/22910.

Oliveira MF, Silva JR, Dansa-Petretski M, de Souza W, Braga CM, Masuda H, Oliveira PL. Haemozoin formation in the midgut of the blood-sucking insect *Rhodnius prolixus*. *FEBS Lett* (2000) 477(1-2):95-8. doi: 10.1016/s0014-5793(00)01786-5

Oryan A, Wahedi A, Paluzzi JV. Functional characterization and quantitative expression analysis of two GnRH-related peptide receptors in the mosquito, *Aedes aegypti*. *Biochem Biophys Res Commun* (2018) 497(2):550-557. doi: 10.1016/j.bbrc.2018.02.088

Otálora-Luna F, Pérez-Sánchez AJ, Sandoval C, Aldana E. Evolution of hematophagous habit in Triatominae (Heteroptera: Reduviidae). *RCHN* (2015) 88(1):4. doi: https://doi.org/10.1186/s40693-014-0032-0.

Palatini U, Masri RA, Cosme LV, Koren S, Thibaud-Nissen F, Biedler JK, Krsticevic F, Johnston JS, Halbach R, Crawford JE, Antoshechkin I, Failloux AB, Pischedda E, Marconcini M, Ghurye J, Rhie A, Sharma A, Karagodin DA, Jenrette J…Bonizzoni M.

Improved reference genome of the arboviral vector *Aedes albopictus*. *Genome Biol* (2020) 21(1):215. doi: 10.1186/s13059-020-02141-w

Paluzzi JP, O'Donnell MJ. Identification, spatial expression analysis and functional characterization of a pyrokinin-1 receptor in the Chagas' disease vector, *Rhodnius prolixus*. *Mol Cell Endocrinol* (2012) 363(1-2):36-45. doi: 10.1016/j.mce.2012.07.007

Parvy JP, Napal L, Rubin T, Poidevin M, Perrin L, Wicker-Thomas C, Montagne J. *Drosophila melanogaster* acetyl-CoA-carboxylase sustains a fatty acid-dependent remote signal to waterproof the respiratory system. *PLoS Genet* (2012) 8(8):e1002925. doi: 10.1371/journal.pgen.1002925

Pascini TV, Ramalho-Ortigão M, Ribeiro JM, Jacobs-Lorena M, Martins GF. Transcriptional profiling and physiological roles of *Aedes aegypti* spermathecal-related genes. *BMC Genomics* (2020) 21(1):143. doi: 10.1186/s12864-020-6543-y

Peng L, Yin HY, Huang C. CNMa-CNMa receptor at microbiome-gut-brain axis: novel target to regulate feeding decision. *Signal Transduct Target Ther* (2021) 6(1):283. doi: 10.1038/s41392-021-00708-y

Petruccelli E, Lark A, Mrkvicka JA, Kitamoto T. Significance of DopEcR, a G-protein coupled dopamine/ecdysteroid receptor, in physiological and behavioral response to stressors. *J Neurogenet* (2020) 34(1):55-68. doi:10.1080/01677063.2019.1710144

Pontes EG, Leite P, Majerowicz D, Atella GC, Gondim KC. Dynamics of lipid accumulation by the fat body of *Rhodnius prolixus*: the involvement of lipophorin binding sites. *J Insect Physiol* (2008) 54(5):790-7. doi: 10.1016/j.jinsphys.2008.02.003

Predel R, Neupert S, Garczynski SF, Crim JW, Brown MR, Russell WK, Kahnt J, Russell DH, Nachman RJ. Neuropeptidomics of the mosquito *Aedes aegypti*. *J Proteome Res* (2010) 9(4):2006-15. doi: 10.1021/pr901187p

Rajpurohit S, Vrkoslav V, Hanus R, Gibbs AG, Cvačka J, Schmidt PS. Post-eclosion temperature effects on insect cuticular hydrocarbon profiles. *Ecol Evol* (2020) 11(1):352-364. doi: 10.1002/ece3.7050

Ramirez JL, Souza-Neto J, Torres Cosme R, Rovira J, Ortiz A, Pascale JM, Dimopoulos G. Reciprocal tripartite interactions between the *Aedes aegypti* midgut microbiota, innate immune system and dengue virus influences vector competence. *PLoS Negl Trop Dis* (2012) 6(3):e1561. doi: 10.1371/journal.pntd.0001561

Reyes-Villanueva F. Egg development may require multiple bloodmeals among small *Aedes aegypti* (Diptera: Culicidae) field collected in northeastern Mexico. *Fla Entomol* (2004) 87(4):630–32.

Riehle MA, Brown MR. Insulin stimulates ecdysteroid production through a conserved signaling cascade in the mosquito *Aedes aegypti*. *Insect Biochem Mol Biol* (1999) 29(10):855-60. doi: 10.1016/s0965-1748(99)00084-3

Rio RVM, Attardo GM, Weiss BL. Grandeur alliances: symbiont metabolic integration and obligate arthropod hematophagy. *Trends Parasitol* (2016) 32(9):739-749. doi: 10.1016/j.pt.2016.05.002

Rivera-Perez C, Nouzova M, Lamboglia I, Noriega FG. Metabolic analysis reveals changes in the mevalonate and juvenile hormone synthesis pathways linked to the mosquito reproductive physiology. *Insect Biochem Mol Biol* (2014) 51:1-9. doi: 10.1016/j.ibmb.2014.05.001

Rodríguez-Ruano SM, Škochová V, Rego ROM, Schmidt JO, Roachell W, Hypša V, Nováková E. Microbiomes of North American Triatominae: The grounds for Chagas disease epidemiology. *Front Microbiol* (2018) 9:1167. doi: 10.3389/fmicb.2018.01167

Roy SG, Hansen IA, Raikhel AS. Effect of insulin and 20-hydroxyecdysone in the fat body of the yellow fever mosquito, *Aedes aegypti*. *Insect Biochem Mol Biol*. (2007) 37(12):1317-1326. doi:10.1016/j.ibmb.2007.08.004

Roy SG, Raikhel AS. Nutritional and hormonal regulation of the TOR effector 4E-binding protein (4E-BP) in the mosquito *Aedes aegypti*. *FASEB J* (2012) 26(3):1334-42. doi: 10.1096/fj.11-189969

Sajadi F, Uyuklu A, Paputsis C, Lajevardi A, Wahedi A, Ber LT, Matei A, Paluzzi JV. CAPA neuropeptides and their receptor form an anti-diuretic hormone signaling system in the human disease vector, *Aedes aegypti*. *Sci Rep* (2020) 10(1):1755. doi: 10.1038/s41598-020-58731-y

Salcedo-Porras N, Umaña-Diaz C, Bitencourt ROB, Lowenberger C. The role of bacterial symbionts in Triatomines: An evolutionary perspective. *Microorganisms* (2020) 8(9):1438. doi: 10.3390/microorganisms8091438

Sandoval CM, Ortiz N, Jaimes D, Lorosa E, Galvão C, Rodriguez O, Scorza JV, Gutiérrez R. Feeding behaviour of *Belminus ferroae* (Hemiptera: Reduviidae), a predaceous Triatominae colonizing rural houses in Norte de Santander, Colombia. *Med Vet Entomol* (2010) 24(2):124-31. doi: 10.1111/j.1365-2915.2010.00868.x

Santos VSV, Limongi JE, Pereira BB. Association of low concentrations of pyriproxyfen and spinosad as an environment-friendly strategy to rationalize *Aedes aegypti* control programs. *Chemosphere* (2020) 247:125795. doi:10.1016/j.chemosphere.2019.125795

Saraiva FB, Alves-Bezerra M, Majerowicz D, Paes-Vieira L, Braz V, Almeida MGMD, Meyer-Fernandes JR, Gondim KC. Blood meal drives de novo lipogenesis in the fat body of *Rhodnius prolixus*. *Insect Biochem Mol Biol* (2021) 133:103511. doi: 10.1016/j.ibmb.2020.103511

Scott TW, Takken W. Feeding strategies of anthropophilic mosquitoes result in increased risk of pathogen transmission. *Trends Parasitol* (2012) 28(3):114-21. doi: 10.1016/j.pt.2012.01.001

Sellami A, Veenstra JA. SIFamide acts on fruitless neurons to modulate sexual behavior in *Drosophila melanogaster*. *Peptides* (2015) 74:50-56. doi:10.1016/j.peptides.2015.10.003

Shin SC, Kim SH, You H, Kim B, Kim AC, Lee KA, Yoon JH, Ryu JH, Lee WJ. *Drosophila* microbiome modulates host developmental and metabolic homeostasis via insulin signaling. *Science* (2011) 334(6056):670-4. doi: 10.1126/science.1212782

Shutt B, Stables L, Aboagye-Antwi F, Moran J, Tripet F. Male accessory gland proteins induce female monogamy in anopheline mosquitoes. *Med Vet Entomol* (2010) 24(1):91-4. doi: 10.1111/j.1365-2915.2009.00849.x

Siddall JB. Insect growth regulators and insect control: a critical appraisal. *Environ Health Perspect* (1976) 14:119-26. doi: 10.1289/ehp.7614119

Sieglaff DH, Duncan KA, Brown MR. Expression of genes encoding proteins involved in ecdysteroidogenesis in the female mosquito, *Aedes aegypti*. *Insect Biochem Mol Biol* (2005) 35(5):471-90. doi: 10.1016/j.ibmb.2005.01.011

Siju KP, Reifenrath A, Scheiblich H, Neupert S, Predel R, Hansson BS, Schachtner J, Ignell R. Neuropeptides in the antennal lobe of the yellow fever mosquito, *Aedes aegypti*. *J Comp Neurol* (2014) 522(3):592-608. doi: 10.1002/cne.23434

Silva JR, Mury FB, Oliveira MF, Oliveira PL, Silva CP, Dansa-Petretski M. Perimicrovillar membranes promote hemozoin formation into *Rhodnius prolixus* midgut. *Insect Biochem Mol Biol* (2007) 37(6):523-31. doi: 10.1016/j.ibmb.2007.01.001

Silva JR, Gomes-Silva L, Lins UC, Nogueira NF, Dansa-Petretski M. The haemoxisome: a haem-iron containing structure in the *Rhodnius prolixus* midgut cells. *J Insect Physiol* (2006) 52(6):542-50. doi: 10.1016/j.jinsphys.2006.01.004

Silva-Oliveira G, De Paula IF, Medina JM, Alves-Bezerra M, Gondim KC. Insulin receptor deficiency reduces lipid synthesis and reproductive function in the insect *Rhodnius prolixus*. *Biochim Biophys Acta Mol Cell Biol Lipids* (2021) 1866(2):158851. doi: 10.1016/j.bbalip.2020.158851

Sivagnaname N, Amalraj DD, Kalyanasundaram M, Das PK. Oviposition attractancy of an infusion from a wood inhabiting fungus for vector mosquitoes. *Indian J Med Res* (2001) 114:18-24.

Slater GS, Birney E. Automated generation of heuristics for biological sequence comparison. *BMC Bioinformatics* (2005) 6:31. doi: 10.1186/1471-2105-6-31

Smallegange RC, Qiu YT, van Loon JJ, Takken W. Synergism between ammonia, lactic acid and carboxylic acids as kairomones in the host-seeking behaviour of the malaria mosquito *Anopheles gambiae* sensu stricto (Diptera: Culicidae). *Chem Senses* (2005) 30(2):145-52. doi: 10.1093/chemse/bji010

Sorapukdee S, Narunatsopanon S. Comparative study on compositions and functional properties of porcine, chicken and duck blood. *Korean J Food Sci Anim Resour* (2017) 37(2):228-241. doi: 10.5851/kosfa.2017.37.2.228

Souza RS, Virginio F, Riback TIS, Suesdek L, Barufi JB, Genta FA. Microorganism-based larval diets affect mosquito development, size and nutritional reserves in the Yellow Fever mosquito *Aedes aegypti* (Diptera: Culicidae). *Front Physiol* (2019) 10:152. doi: 10.3389/fphys.2019.00152

Stamatakis A. RAxML Version 8: A tool for phylogenetic analysis and post-analysis of large phylogenies. *Bioinformatics* (2014) 30:1312–1313. doi: 10.1093/bioinformatics/btu033

Steel CGH, Bollenbacher WE, Smith SL, Gilbert LI. Haemolymph ecdysteroid titres during larval-adult development in *Rhodnius prolixus*: Correlations with moulting hormone action and brain neurosecretory cell activity. *J Insect Physiol* (1982) 28(6). doi: https://doi.org/10.1016/0022-1910(82)90032-4

Sterkel M, Oliveira PL, Urlaub H, Hernandez-Martinez S, Rivera-Pomar R, Ons S. OKB, a novel family of brain-gut neuropeptides from insects. *Insect Biochem Mol Biol* (2012) 42(7):466-473. doi:10.1016/j.ibmb.2012.03.003

Subramanian S, Shankarganesh K. *Ecofriendly Pest Management for Food Security*. Insect Hormones (as Pesticides). Elsevier (2016) 613-650. doi:10.1016/B978-0-12-803265-7.00020-8

Tallon AK, Hill SR, Ignell R. Sex and age modulate antennal chemosensory-related genes linked to the onset of host seeking in the yellow-fever mosquito, *Aedes aegypti*. *Sci Rep* (2019) 9(1):43. doi: 10.1038/s41598-018-36550-6

Te Brugge V, Paluzzi JP, Schooley DA, Orchard I. Identification of the elusive peptidergic diuretic hormone in the blood-feeding bug *Rhodnius prolixus*: a CRF-related peptide. *J Exp Biol* (2011) 214(3):371-381. doi:10.1242/jeb.046292

Tedrow RE, Rakotomanga T, Nepomichene T, Howes RE, Ratovonjato J, Ratsimbasoa AC, Svenson GJ, Zimmerman PA. *Anopheles* mosquito surveillance in Madagascar reveals multiple blood feeding behavior and *Plasmodium* infection. *PLoS Negl Trop Dis* (2019) 13(7):e0007176. doi: 10.1371/journal.pntd.0007176

Teerawanichpan P, Robertson AJ, Qiu X. A fatty acyl-CoA reductase highly expressed in the head of honeybee (*Apis mellifera*) involves biosynthesis of a wide range of aliphatic fatty alcohols. *Insect Biochem Mol Biol* (2010) 40(9):641-9. doi: 10.1016/j.ibmb.2010.06.004

Terhzaz S, Rosay P, Goodwin SF, Veenstra JA. The neuropeptide SIFamide modulates sexual behavior in *Drosophila*. *Biochem Biophys Res Commun* (2007) 352(2):305-10. doi: 10.1016/j.bbrc.2006.11.030

Thuma L, Carter D, Weavers H, Martin P. *Drosophila* immune cells extravasate from vessels to wounds using Tre1 GPCR and Rho signaling. *J Cell Biol* (2018) 217(9):3045-3056. doi:10.1083/jcb.201801013

Tobias NJ, Eberhard FE, Guarneri AA. Enzymatic biosynthesis of B-complex vitamins is supplied by diverse microbiota in the *Rhodnius prolixus* anterior midgut following *Trypanosoma cruzi* infection. *Comput Struct Biotechnol J* (2020) 18:3395-3401. doi: 10.1016/j.csbj.2020.10.031

Ulmer CZ, Koelmel JP, Ragland JM, Garrett TJ, Bowden JA. LipidPioneer: A comprehensive user-generated exact mass template for lipidomics. *J Am Soc Mass Spectrom* (2017) 28(3):562-565. doi: 10.1007/s13361-016-1579-6

USDA - Arthropod-borne Animal Diseases Research: Manhattan, KS. 2024. https://www.ars.usda.gov/research/project/?accnNo=436363&fy=2021. 9 April 2024

Vafopoulou X, Steel CGH. Circadian regulation of synthesis of ecdysteroids by prothoracic glands of the insect *Rhodnius prolixus*: evidence of a dual oscillator system. *Gen Comp Endocrinol* (1991) 83(1):27-34. doi: 10.1016/0016-6480(91)90102-c

Vafopoulou X, Steel CGH. Prothoracicotropic hormone of *Rhodnius prolixus*: partial characterization and rhythmic release of neuropeptides related to *Bombyx* PTTH and bombyxin. *Invert Reprod Dev* (2002) 42:111–120 10.1080/07924259.2002.9652767

Vallejo GA, Guhl F, Schaub GA. Triatominae-*Trypanosoma cruzi*/*T. rangeli*: Vector-parasite interactions. *Acta Trop* (2009) 110(2-3):137-47. doi: 10.1016/j.actatropica.2008.10.001

Valzania L, Coon KL, Vogel KJ, Brown MR, Strand MR. Hypoxia-induced transcription factor signaling is essential for larval growth of the mosquito *Aedes aegypti*. *Proc Natl Acad Sci* (2018a) 115(3):457-465. doi: 10.1073/pnas.1719063115

Valzania L, Martinson VG, Harrison RE, Boyd BM, Coon KL, Brown MR, Strand MR. Both living bacteria and eukaryotes in the mosquito gut promote growth of larvae. *PLoS Negl Trop Dis* (2018b) 12(7):e0006638. doi: 10.1371/journal.pntd.0006638

Valzania L, Mattee MT, Strand MR, Brown MR. Blood feeding activates the vitellogenic stage of oogenesis in the mosquito *Aedes aegypti* through inhibition of glycogen synthase kinase 3 by the insulin and TOR pathways. *Dev Biol* (2019) 454(1):85-95. doi: 10.1016/j.ydbio.2019.05.011

Van Rensburg CE, Jooné GK, O'Sullivan JF, Anderson R. Antimicrobial activities of clofazimine and B669 are mediated by lysophospholipids. *Antimicrob Agents Chemother* (1992) 36(12):2729-35. doi: 10.1128/AAC.36.12.2729

Veenstra JA. The neuropeptide SMYamide, a SIFamide paralog, is expressed by salivary gland innervating neurons in the American cockroach and likely functions as a hormone. *Peptides* (2021) 136:170466. doi:10.1016/j.peptides.2020.170466

Vigneron A, Masson F, Vallier A, Balmand S, Rey M, Vincent-Monégat C, Aksoy E, Aubailly-Giraud E, Zaidman-Rémy A, Heddi A. Insects recycle endosymbionts when the benefit is over. *Curr Biol* (2014) 24(19):2267-73. doi: 10.1016/j.cub.2014.07.065

Villalobos-Sambucaro MJ, Nouzova M, Ramirez CE, Eugenia Alzugaray M, Fernandez-Lima F, Ronderos JR, Noriega FG. The juvenile hormone described in *Rhodnius prolixus* by Wigglesworth is juvenile hormone III skipped bisepoxide. *Sci Rep* (2020) 10(1):3091. doi: 10.1038/s41598-020-59495-1

Villarreal SM, Pitcher S, Helinski MEH, Johnson L, Wolfner MF, Harrington LC. Male contributions during mating increase female survival in the disease vector mosquito *Aedes aegypti*. *J Insect Physiol* (2018) 108:1-9. doi: 10.1016/j.jinsphys.2018.05.001

Vogel KJ, Brown MR, Strand MR. Phylogenetic investigation of peptide hormone and growth factor receptors in five dipteran genomes. *Front Endocrinol* (2013) 4. doi:10.3389/fendo.2013.00193

Vogel KJ, Brown MR, Strand MR. Ovary ecdysteroidogenic hormone requires a receptor tyrosine kinase to activate egg formation in the mosquito *Aedes aegypti*. *Proc Natl Acad Sci* (2015) 112(16). doi:10.1073/pnas.1501814112

Vogel KJ, Valzania L, Coon KL, Brown MR, Strand MR. Transcriptome sequencing reveals large-scale changes in axenic *Aedes aegypti* larvae. *PLoS Negl Trop Dis* (2017) (1):e0005273. doi: 10.1371/journal.pntd.0005273

Vonesh JR, Blaustein L. Predator-induced shifts in mosquito oviposition site selection: A meta-analysis and implications for vector control. *Israel J Ecol Evol* (2010) 56:263–279. doi: 10.1560/IJEE.56.3-4.263

Wahedi A, Paluzzi JP. Molecular identification, transcript expression, and functional deorphanization of the adipokinetic hormone/corazonin-related peptide receptor in the disease vector, *Aedes aegypti*. *Sci Rep* (2018) 8(1):2146. doi: 10.1038/s41598-018-20517-8

Wang JL, Saha TT, Zhang Y, Zhang C, Raikhel AS. Juvenile hormone and its receptor methoprene-tolerant promote ribosomal biogenesis and vitellogenesis in the *Aedes aegypti* mosquito. *J Biol Chem* (2017) 292(24):10306-10315. doi: 10.1074/jbc.M116.761387

Wang Y, Yu W, Li S, Guo D, He J, Wang Y. Acetyl-CoA carboxylases and diseases. *Front Oncol* (2022) 12:836058. doi: 10.3389/fonc.2022.836058

Wang Z, Receveur JP, Pu J, Cong H, Richards C, Liang M, Chung H. Desiccation resistance differences in *Drosophila* species can be largely explained by variations in cuticular hydrocarbons. *Elife* (2022) 11:e80859. doi: 10.7554/eLife.80859

Waniek PJ, Pacheco Costa JE, Jansen AM, Costa J, Araújo CA. Cathepsin L of *Triatoma brasiliensis* (Reduviidae, Triatominae): sequence characterization, expression pattern and zymography. *J Insect Physiol* (2012) 58(1):178-87. doi: 10.1016/j.jinsphys.2011.11.008

Wigglesworth VB. Memoirs: The physiology of the cuticle and of ecdysis in *Rhodnius prolixus* (Triatomidae, Hemiptera); with special reference to the function of the oenocytes and of the dermal glands. *J Cell Sci* (1933) s2-76(302):269–318. doi: https://doi.org/10.1242/jcs.s2-76.302.269

Wigglesworth VB. The physiology of ecdysis in *Rhodnius prolixus* (Hemiptera). II. Factors controlling moulting and metamorphosis. *J Cell Sci* (1934) 2(77):191–222.

Wigglesworth VB. Symbiotic bacteria in a blood-sucking insect, *Rhodnius Prolixus* Stål. (Hemiptera, Triatomidae). *Parasitology* (1936) 28(2):284–89. doi: https://doi.org/10.1017/S0031182000022459.

Wigglesworth VB. The thoracic gland in *Rhodnius Prolixus* (Hemiptera) and its role in moulting. *J Exp Biol* (1952) 29(4):561–570. doi: https://doi.org/10.1242/jeb.29.4.561

Wigglesworth VB. Structural lipids in the insect cuticle and the function of the oenocytes. *Tissue Cell* (1970) 2(1):155-79. doi: 10.1016/s0040-8166(70)80013-1

Wigglesworth VB. Incorporation of lipid into the epicuticle of *Rhodnius* (Hemiptera). *J Cell Sci* (1975) 19(3)459-485.

Wigglesworth VB. Sclerotin and lipid in the waterproofing of the insect cuticle. *Tissue Cell* (1985a) 17 (2):227-248.

Wigglesworth VB. The transfer of lipid in insects from the epidermal cells to the cuticle. *Tissue Cell* (1985b) 17(2):249-65. doi: 10.1016/0040-8166(85)90092-8

Wigglesworth VB. Temperature and the transpiration of water through the insect cuticle. *Tissue Cell* (1986) 18(1):99–115. doi: https://doi.org/10.1016/0040-8166(86)90010-8

Wigglesworth VB. The source of lipids and polyphenols for the insect cuticle: The role of fat body, oenocytes and oenocytoids. *Tissue Cell* (1988) 20(6):919-32.

Wishart DS, Tzur D, Knox C, Eisner R, Guo AC, Young N, Cheng D, Jewell K, Arndt D, Sawhney S, Fung C, Nikolai L, Lewis M, Coutouly MA, Forsythe I, Tang P, Shrivastava S, Jeroncic K, Stothard P… Querengesser L. HMDB: the Human Metabolome Database. *Nucleic Acids Res* (2007) 35(Database issue):D521-6. doi: 10.1093/nar/gkl923

Wishart DS, Knox C, Guo AC, Eisner R, Young N, Gautam B, Hau DD, Psychogios N, Dong E, Bouatra S, Mandal R, Sinelnikov I, Xia J, Jia L, Cruz JA, Lim E, Sobsey CA, Shrivastava S, Huang P…Forsythe I. HMDB: a knowledgebase for the human metabolome. *Nucleic Acids Res* (2009) 37(Database issue):D603-10. doi: 10.1093/nar/gkn810

Wishart DS, Jewison T, Guo AC, Wilson M, Knox C, Liu Y, Djoumbou Y, Mandal R, Aziat F, Dong E, Bouatra S, Sinelnikov I, Arndt D, Xia J, Liu P, Yallou F, Bjorndahl T, Perez-Pineiro R, Eisner R… Scalbert A. HMDB 3.0--The Human Metabolome Database in 2013. *Nucleic Acids Res* (2013) 41(Database issue):D801-7. doi: 10.1093/nar/gks1065

Wishart DS, Feunang YD, Marcu A, Guo AC, Liang K, Vázquez-Fresno R, Sajed T, Johnson D, Li C, Karu N, Sayeeda Z, Lo E, Assempour N, Berjanskii M, Singhal S, Arndt D, Liang Y, Badran H, Grant J… Scalbert A. HMDB 4.0: the human metabolome database for 2018. *Nucleic Acids Res* (2018) 46(D1):D608-D617. doi: 10.1093/nar/gkx1089

Wishart DS, Guo A, Oler E, Wang F, Anjum A, Peters H, Dizon R, Sayeeda Z, Tian S, Lee BL, Berjanskii M, Mah R, Yamamoto M, Jovel J, Torres-Calzada C, Hiebert-Giesbrecht M, Lui VW, Varshavi D, Varshavi D… Gautam V. HMDB 5.0: the Human Metabolome Database for 2022. *Nucleic Acids Res* (2022) 50(D1):D622-D631. doi: 10.1093/nar/gkab1062

Wrońska AK, Kaczmarek A, Boguś MI, Kuna A. Lipids as a key element of insect defense systems. *Front Genet* (2023) 14:1183659. doi: 10.3389/fgene.2023.1183659

Wu Q, Brown MR. Signaling and function of insulin-like peptides in insects. *Annu Rev Entomol* (2006) 51:1-24. doi: 10.1146/annurev.ento.51.110104.151011

Wu K, Li S, Wang J, Ni Y, Huang W, Liu Q, Ling E. Peptide hormones in the insect midgut. *Front Physiol* (2020) 11:191. doi: 10.3389/fphys.2020.00191

Wulff JP, Sierra I, Sterkel M, Holtof M, Van Wielendaele P, Francini F, Broeck JV, Ons S. Orcokinin neuropeptides regulate ecdysis in the hemimetabolous insect *Rhodnius prolixus*. *Insect Biochem Mol Biol* (2017) 81:91-102. doi: 10.1016/j.ibmb.2017.01.003

Yamamoto Y, Sakurai T, Chen Z, Inoue N, Chiba H, Hui SP. Lysophosphatidylethanolamine affects lipid accumulation and metabolism in a human liver-derived cell line. *Nutrients* (2022) 14(3):579. doi: 10.3390/nu14030579

Yamanaka N, Roller L, Zitňan D, Satake H, Mizoguchi A, Kataoka H, Tanaka Y. Bombyx orcokinins are brain-gut peptides involved in the neuronal regulation of ecdysteroidogenesis. *J Comp Neurol* (2011) 519(2):238-46. doi: 10.1002/cne.22517

Zandawala M, Hamoudi Z, Lange AB, Orchard I. Adipokinetic hormone signalling system in the Chagas disease vector, *Rhodnius prolixus*. *Insect Mol Biol* (2015) 24(2):264-276. doi:10.1111/imb.12157

Zhou X, Ling X, Guo H, Zhu-Salzman K, Ge F, Sun Y. *Serratia symbiotica* enhances fatty acid metabolism of pea aphid to promote host development. *Int J Mol Sci* (2021) 22(11):5951. doi: 10.3390/ijms22115951